

BULLETIN OF RUSSIAN STATE MEDICAL UNIVERSITY

BIOMEDICAL JOURNAL OF PIROGOV RUSSIAN NATIONAL RESEARCH MEDICAL UNIVERSITY

EDITOR-IN-CHIEF Denis Rebrikov, DSc, professor

DEPUTY EDITOR-IN-CHIEF Alexander Oettinger, DSc, professor

EDITORS Valentina Geidebrekht, PhD; Nadezda Tikhomirova

TECHNICAL EDITOR Evgeny Lukyanov

TRANSLATORS Nadezda Tikhomirova, Vyacheslav Vityuk

DESIGN AND LAYOUT Marina Doronina

EDITORIAL BOARD

Averin VI, DSc, professor (Minsk, Belarus)
Alipov NN, DSc, professor (Moscow, Russia)
Belousov VV, DSc, professor (Moscow, Russia)
Bogomilskiy MR, corr. member of RAS, DSc, professor (Moscow, Russia)
Bozhenko VK, DSc, CSc, professor (Moscow, Russia)
Bylova NA, CSc, docent (Moscow, Russia)
Gainetdinov RR, CSc (Saint-Petersburg, Russia)
Gendlin GYe, DSc, professor (Moscow, Russia)
Ginter EK, member of RAS, DSc (Moscow, Russia)
Gorbacheva LR, DSc, professor (Moscow, Russia)
Gordeev IG, DSc, professor (Moscow, Russia)
Gudkov AV, PhD, DSc (Buffalo, USA)
Gulyaeva NV, DSc, professor (Moscow, Russia)
Gusev EI, member of RAS, DSc, professor (Moscow, Russia)
Danilenko VN, DSc, professor (Moscow, Russia)
Zarubina TV, DSc, professor (Moscow, Russia)
Zatevakhin II, member of RAS, DSc, professor (Moscow, Russia)
Kagan VE, professor (Pittsburgh, USA)
Kzyzhkowska YuG, DSc, professor (Heidelberg, Germany)
Kobrinskii BA, DSc, professor (Moscow, Russia)
Kozlov AV, MD PhD (Vienna, Austria)
Kotelevtsev YuV, CSc (Moscow, Russia)
Lebedev MA, PhD (Darem, USA)
Manturova NE, DSc (Moscow, Russia)
Milushkina OYu, DSc, professor (Moscow, Russia)
Mitupov ZB, DSc, professor (Moscow, Russia)
Moshkovskii SA, DSc, professor (Moscow, Russia)
Munblit DB, MSc, PhD (London, Great Britain)

Negrebetsky VV, DSc, professor (Moscow, Russia)
Novikov AA, DSc (Moscow, Russia)
Pivovarov YuP, member of RAS, DSc, professor (Moscow, Russia)
Polunina NV, corr. member of RAS, DSc, professor (Moscow, Russia)
Poryadin GV, corr. member of RAS, DSc, professor (Moscow, Russia)
Razumovskii AYU, corr. member of RAS, DSc, professor (Moscow, Russia)
Rebrova OYu, DSc (Moscow, Russia)
Rudoy AS, DSc, professor (Minsk, Belarus)
Rylova AK, DSc, professor (Moscow, Russia)
Savelieva GM, member of RAS, DSc, professor (Moscow, Russia)
Semiglazov VF, corr. member of RAS, DSc, professor (Saint-Petersburg, Russia)
Skoblina NA, DSc, professor (Moscow, Russia)
Slavyanskaya TA, DSc, professor (Moscow, Russia)
Smirnov VM, DSc, professor (Moscow, Russia)
Spallone A, DSc, professor (Rome, Italy)
Starodubov VI, member of RAS, DSc, professor (Moscow, Russia)
Stepanov VA, corr. member of RAS, DSc, professor (Tomsk, Russia)
Suchkov SV, DSc, professor (Moscow, Russia)
Takhchidi KhP, member of RAS, DSc, professor (Moscow, Russia)
Trufanov GE, DSc, professor (Saint-Petersburg, Russia)
Favorova OO, DSc, professor (Moscow, Russia)
Filipenko ML, CSc, leading researcher (Novosibirsk, Russia)
Khazipov RN, DSc (Marsel, France)
Chundukova MA, DSc, professor (Moscow, Russia)
Shimanovskii NL, corr. member of RAS, DSc, professor (Moscow, Russia)
Shishkina LN, DSc, senior researcher (Novosibirsk, Russia)
Yakubovskaya RI, DSc, professor (Moscow, Russia)

SUBMISSION <http://vestnikrgmu.ru/login?lang=en>

CORRESPONDENCE editor@vestnikrgmu.ru

COLLABORATION manager@vestnikrgmu.ru

ADDRESS ul. Ostrovityanova, d. 1, Moscow, Russia, 117997

Indexed in Scopus. CiteScore 2022: 0.5

Scopus[®]

SCImago Journal & Country Rank 2020: 0.14

SJR

Scimago Journal & Country Rank

Indexed in WoS. JCR 2021: 0.5

WEB OF SCIENCE[™]

Listed in HAC 31.01.2020 (№ 507)



ВЫСШАЯ
АТТЕСТАЦИОННАЯ
КОМИССИЯ (ВАК)

Five-year h-index is 8

Google
scholar

Open access to archive

CYBERLENINKA

Issue DOI: 10.24075/brsmu.2023-02

The mass media registration certificate № 012769 issued on July 29, 1994

Founder and publisher is Pirogov Russian National Research Medical University (Moscow, Russia)

The journal is distributed under the terms of Creative Commons Attribution 4.0 International License www.creativecommons.org



Approved for print 30.04.2023
Circulation: 100 copies. Printed by Print.Formula
www.print-formula.ru

ВЕСТНИК РОССИЙСКОГО ГОСУДАРСТВЕННОГО МЕДИЦИНСКОГО УНИВЕРСИТЕТА

НАУЧНЫЙ МЕДИЦИНСКИЙ ЖУРНАЛ РНИМУ ИМ. Н. И. ПИРОГОВА

ГЛАВНЫЙ РЕДАКТОР Денис Ребриков, д. б. н., профессор

ЗАМЕСТИТЕЛЬ ГЛАВНОГО РЕДАКТОРА Александр Эттингер, д. м. н., профессор

РЕДАКТОРЫ Валентина Гейдебрект, к. б. н.; Надежда Тихомирова

ТЕХНИЧЕСКИЙ РЕДАКТОР Евгений Лукьянов

ПЕРЕВОДЧИКИ Надежда Тихомирова, Вячеслав Виток

ДИЗАЙН И ВЕРСТКА Марины Дорониной

РЕДАКЦИОННАЯ КОЛЛЕГИЯ

В. И. Аверин, д. м. н., профессор (Минск, Белоруссия)
Н. Н. Алипов, д. м. н., профессор (Москва, Россия)
В. В. Белоусов, д. б. н., профессор (Москва, Россия)
М. Р. Богомилский, член-корр. РАН, д. м. н., профессор (Москва, Россия)
В. К. Боженко, д. м. н., к. б. н., профессор (Москва, Россия)
Н. А. Былова, к. м. н., доцент (Москва, Россия)
Р. Р. Гайнетдинов, к. м. н. (Санкт-Петербург, Россия)
Г. Е. Гендлин, д. м. н., профессор (Москва, Россия)
Е. К. Гинтер, академик РАН, д. б. н. (Москва, Россия)
Л. Р. Горбачева, д. б. н., профессор (Москва, Россия)
И. Г. Гордеев, д. м. н., профессор (Москва, Россия)
А. В. Гудков, PhD, DSc (Буффало, США)
Н. В. Гуляева, д. б. н., профессор (Москва, Россия)
Е. И. Гусев, академик РАН, д. м. н., профессор (Москва, Россия)
В. Н. Даниленко, д. б. н., профессор (Москва, Россия)
Т. В. Зарубина, д. м. н., профессор (Москва, Россия)
И. И. Затевахин, академик РАН, д. м. н., профессор (Москва, Россия)
В. Е. Каган, профессор (Питтсбург, США)
Ю. Г. Кжышковска, д. б. н., профессор (Гейдельберг, Германия)
Б. А. Кобринский, д. м. н., профессор (Москва, Россия)
А. В. Козлов, MD PhD (Вена, Австрия)
Ю. В. Котелевцев, к. х. н. (Москва, Россия)
М. А. Лебедев, PhD (Дарем, США)
Н. Е. Мантурова, д. м. н. (Москва, Россия)
О. Ю. Милушкина, д. м. н., доцент (Москва, Россия)
З. Б. Митупов, д. м. н., профессор (Москва, Россия)
С. А. Мошковский, д. б. н., профессор (Москва, Россия)
Д. Б. Мунблит, MSc, PhD (Лондон, Великобритания)

В. В. Негребский, д. х. н., профессор (Москва, Россия)
А. А. Новиков, д. б. н. (Москва, Россия)
Ю. П. Пивоваров, д. м. н., академик РАН, профессор (Москва, Россия)
Н. В. Полунина, член-корр. РАН, д. м. н., профессор (Москва, Россия)
Г. В. Порядин, член-корр. РАН, д. м. н., профессор (Москва, Россия)
А. Ю. Разумовский, член-корр., профессор (Москва, Россия)
О. Ю. Реброва, д. м. н. (Москва, Россия)
А. С. Рудой, д. м. н., профессор (Минск, Белоруссия)
А. К. Рылова, д. м. н., профессор (Москва, Россия)
Г. М. Савельева, академик РАН, д. м. н., профессор (Москва, Россия)
В. Ф. Семиглазов, член-корр. РАН, д. м. н., профессор (Санкт-Петербург, Россия)
Н. А. Скоблина, д. м. н., профессор (Москва, Россия)
Т. А. Славянская, д. м. н., профессор (Москва, Россия)
В. М. Смирнов, д. б. н., профессор (Москва, Россия)
А. Спаллоне, д. м. н., профессор (Рим, Италия)
В. И. Стародубов, академик РАН, д. м. н., профессор (Москва, Россия)
В. А. Степанов, член-корр. РАН, д. б. н., профессор (Томск, Россия)
С. В. Сучков, д. м. н., профессор (Москва, Россия)
Х. П. Тахчиди, академик РАН, д. м. н., профессор (Москва, Россия)
Г. Е. Труфанов, д. м. н., профессор (Санкт-Петербург, Россия)
О. О. Фаворова, д. б. н., профессор (Москва, Россия)
М. Л. Филипенко, к. б. н. (Новосибирск, Россия)
Р. Н. Хазипов, д. м. н. (Марсель, Франция)
М. А. Чундокова, д. м. н., профессор (Москва, Россия)
Н. Л. Шимановский, член-корр. РАН, д. м. н., профессор (Москва, Россия)
Л. Н. Шишкина, д. б. н. (Новосибирск, Россия)
Р. И. Якубовская, д. б. н., профессор (Москва, Россия)

ПОДАЧА РУКОПИСЕЙ <http://vestnikrgmu.ru/login>

ПЕРЕПИСКА С РЕДАКЦИЕЙ editor@vestnikrgmu.ru

СОТРУДНИЧЕСТВО manager@vestnikrgmu.ru

АДРЕС РЕДАКЦИИ ул. Островитянова, д. 1, г. Москва, 117997

Журнал включен в Scopus. CiteScore 2022: 0,5

Журнал включен в WoS. JCR 2021: 0,5

Индекс Хирша (h²) журнала по оценке Google Scholar: 8

Scopus®

WEB OF SCIENCE™

Google
scholar

Scimago Journal & Country Rank 2020: 0,14

Журнал включен в Перечень 31.01.2020 (№ 507)

Здесь находится открытый архив журнала

SJR
Scimago Journal & Country Rank



ВЫСШАЯ
АТТЕСТАЦИОННАЯ
КОМИССИЯ (ВАК)

CYBERLENINKA

DOI выпуска: 10.24075/vrgmu.2023-02

Свидетельство о регистрации средства массовой информации № 012769 от 29 июля 1994 г.

Учредитель и издатель — Российский национальный исследовательский медицинский университет имени Н. И. Пирогова (Москва, Россия)

Журнал распространяется по лицензии Creative Commons Attribution 4.0 International www.creativecommons.org



Подписано в печать 30.04.2023
Тираж 100 экз. Отпечатано в типографии Print.Formula
www.print-formula.ru

ORIGINAL RESEARCH

4

Comparison of the oncolytic activity of recombinant vaccinia virus strains LVP-RFP and MVA-RFP against solid tumors

Shakiba Y, Naberezhnaya ER, Kochetkov DV, Yusubalieva GM, Vorobyev PO, Chumakov PM, Baklaushev VP, Lipatova AV

Сравнение онколитической активности рекомбинантных штаммов вируса осповакцины LVP-RFP и MVA-RFP в отношении солидных опухолей

Я. Шакиба, Е. Р. Набережная, Д. В. Кочетков, Г. М. Юсубалиева, П. О. Воробьев, П. М. Чумаков, В. П. Баклаушев, А. В. Липатова

ORIGINAL RESEARCH

12

Predicting the blastocyst development rate during assisted reproductive technologies based on semen microbiota

Panacheva EA, Kudryavtseva EV, Zornikov DL, Plotko EE, Petrov VM, Voroshilina ES

Прогнозирование эффективности эмбриологического этапа вспомогательных репродуктивных технологий по микробному составу эякулята

Е. А. Паначева, Е. В. Кудрявцева, Д. Л. Зорников, Е. Э. Плотко, В. М. Петров, Е. С. Ворошилина

ORIGINAL RESEARCH

19

Genetic characterization of *Aerococcus* sp. 1KP-2016 strain isolated from a patient with bloodstream infection

Chaplin AV, Chagina IA, Pimenova AS, Gadua NT, Kargaltseva NM, Borisova OYu, Donskikh EE, Kafarskaya LI

Генетическая характеристика штамма *Aerococcus* sp. 1KP-2016, выделенного от пациента с инфекцией кровотока

А. В. Чаплин, И. А. Чагина, А. С. Пименова, Н. Т. Гадуа, Н. М. Каргальцева, О. Ю. Борисова, Е. Е. Донских, Л. И. Кафарская

ORIGINAL RESEARCH

24

Features of reactivity of the EEG mu rhythm in children with autism spectrum disorders in helping behavior situations

Pavlenko VB, Kaida AI, Klinkov VN, Mikhailova AA, Orekhova LS, Portugalskaya AA

Особенности реактивности μ -ритма ЭЭГ у детей с расстройствами аутистического спектра в ситуациях помогающего поведения

В. Б. Павленко, А. И. Кайда, В. Н. Клинов, А. А. Михайлова, Л. С. Орехова, А. А. Португальская

ORIGINAL RESEARCH

31

Effects of the metaplasticity-based theta-burst transcranial stimulation protocols on working memory performance

Bakulin IS, Zabirowa AH, Poydasheva AG, Sinitsyn DO, Lagoda DYU, Suponeva NA, Piradov MA

Эффект основанных на метапластичности протоколов транскраниальной стимуляции тета-вспышками на показатели рабочей памяти

И. С. Бакулин, А. Х. Забиrowa, А. Г. Пойдашева, Д. О. Синицын, Д. Ю. Лагода, Н. А. Супонева, М. А. Пирадов

ORIGINAL RESEARCH

40

Sources and impact of human brain potential variability in the brain-computer interface

Ganin IP, Vasilyev AN, Glazova TD, Kaplan AY

Источники и значимость вариативности потенциалов мозга человека в интерфейсе мозг-компьютер

И. П. Ганин, А. Н. Васильев, Т. Д. Глазова, А. Я. Каплан

CLINICAL CASE

48

Single-stage endovitreous surgery of retinal detachment complicated by macular hole involving the short-term perfluorocarbon tamponade

Takhchidi KhP, Takhchidi NKH, Mahno NA

Одномоментное эндовитреальное лечение отслойки сетчатки, осложненной макулярным разрывом с кратковременной тампонадой перфторорганическим соединением

Х. П. Тахчиди, Н. Х. Тахчиди, Н. А. Махно

OPINION

53

Metabolic engineering is a promising way to generate highly effective producers of bioactive substances

Blokhina AE, Palkina KA, Shakhova ES, Malyshevskaya AK, Osipova ZM, Myshkina NM

Метаболическая инженерия — перспективный путь получения высокоэффективных продуцентов биологически активных веществ

А. Е. Блохина, К. А. Палкина, Е. С. Шахова, А. К. Малышевская, З. М. Осипова, Н. М. Мышкина

COMPARISON OF THE ONCOLYTIC ACTIVITY OF RECOMBINANT VACCINIA VIRUS STRAINS LVP-RFP AND MVA-RFP AGAINST SOLID TUMORS

Shakiba Y^{1,2}, Naberezhnaya ER^{1,2}, Kochetkov DV¹, Yusubalieva GM^{1,3}, Vorobyev PO¹, Chumakov PM¹, Baklaushev VP^{1,3}, Lipatova AV¹✉

¹ Engelhardt Institute of Molecular Biology, Russian Academy of Sciences, Moscow, Russia

² Moscow Institute of Physics and Technology, Dolgoprudny, Russia

³ Federal Research and Clinical Center for Specialized Types of Medical Care and Medical Technologies FMBA of Russia, Moscow, Russia

Among oncolytic viruses, modified vaccinia virus Ankara (MVA), a highly attenuated vaccinia virus (VV) is a well-studied variant with promising results in preclinical and clinical trials. The Lister VV strain from the Moscow Institute of Viral Preparations (LVP) has been studied to a lesser extent than MVA and has a different oncolytic property from MVA. The aim of this work was to compare the oncolytic efficacy of LVP and MVA strains against solid tumors. We developed recombinant variants LVP-RFP and MVA-RFP; to enhance onco-selectivity thymidine kinase (TK) gene was inactivated by insertion of red fluorescent protein (RFP) gene to the TK locus. The replication kinetics and oncolytic activity of the obtained recombinant strains were evaluated *in vitro* and *in vivo* on tumor cell lines and mouse syngeneic tumor models of metastatic mouse 4T1 mammary adenocarcinoma, CT26 colon adenocarcinoma, and B16 melanoma. Both MVA-RFP and LVP-RFP showed high replication efficiency in tumor cells and pronounced oncolytic activity against B16 melanoma and 4T1 breast adenocarcinoma allografts. In relation to 4T1, which is a model of triple negative human breast cancer, LVP-RFP showed more than 50% increased cytotoxicity in *in vitro* tests compared to MVA-RFP, as well as a significant slowdown in the progression of 4T1 allografts and an increase in animal survival in experiments *in vivo*. Thus, the LVP strain may be more promising than MVA as a platform for the development of recombinant oncolytic viruses for the breast cancer treatment.

Keywords: vaccinia virus, LVP, MVA, viral oncolytic therapy, breast cancer, colon carcinoma, melanoma

Funding: the development of oncolytic viruses and *in vitro* experiments were supported by the Russian Science Foundation (Russian Science Foundation grant № 20-75-10157); *in vivo* experiments were also supported by the Russian Science Foundation (Russian Science Foundation grant № 22-64-00057).

Author contribution: Ya Shakiba — literature analysis, pre-analytical work, *in vitro* and *in vivo* experiments, analysis and interpretation of data, preparation of figures and graphs; ER Naberezhnaya — *in vitro* experiments, data analysis and interpretation; DV Kochetkov — animal care, data interpretation; GM Yusubalieva — data visualization, manuscript editing; PO Vorobyev — production of preparative quantities of the virus for *in vivo* studies; VP Baklaushev — study planning, preanalytical stage of work, data analysis; AV Lipatova, PM Chumakov — research management, design development of recombinant strains, data interpretation, editing the manuscript.

Compliance with ethical standards: the study was approved by the ethics committee of the EIMB RAS (protocol № 3 dated October 27, 2022). Experiments carried out in accordance with Directive 2010/63/EU of the European Parliament and of the Council of Europe on the protection of animals used for research.

✉ **Correspondence should be addressed:** Anastasia V. Lipatova
Vavilova, 32, Moscow, 119991, Russia; lipatovaanv@gmail.com

Received: 20.02.2023 **Accepted:** 02.04.2023 **Published online:** 28.04.2023

DOI: 10.24075/brsmu.2023.010

СРАВНЕНИЕ ОНКОЛИТИЧЕСКОЙ АКТИВНОСТИ РЕКОМБИНАНТНЫХ ШТАММОВ ВИРУСА ОСПОВАКЦИНЫ LVP-RFP И MVA-RFP В ОТНОШЕНИИ СОЛИДНЫХ ОПУХОЛЕЙ

Я. Шакиба^{1,2}, Е. Р. Набережная^{1,2}, Д. В. Кочетков¹, Г. М. Юсубалиева^{1,3}, П. О. Воробьев¹, П. М. Чумаков¹, В. П. Баклаушев^{1,3}, А. В. Липатова¹✉

¹ Институт молекулярной биологии имени Энгельгардта Российской академии наук, Москва, Россия

² Московский физико-технический институт, Долгопрудный, Россия

³ Федеральный научно-клинический центр специализированных видов медицинской помощи и медицинских технологий Федерального медико-биологического агентства, Москва, Россия

Среди онколитических вирусов одним из наиболее изученных является вирус осповакцины (V), штамма модифицированного высокоаттенуированного вируса Анкара (MVA), показавшего многообещающие результаты в доклинических и клинических испытаниях. Штамм Lister VV из Московского Института вирусных препаратов (LVP) исследован в меньшей степени, чем MVA и имеет отличный от MVA тропизм. Целью работы было сравнить онколитическую эффективность штаммов LVP и MVA в отношении солидных опухолей. Для повышения селективности LVP и MVA к опухолевым клеткам нами были получены рекомбинантные варианты с инактивацией гена тимидинкиназы (TK), MVA-RFP и LVP-RFP, экспрессирующие красный флуоресцентный белок. Кинетику репликации и онколитическую активность полученных рекомбинантных штаммов оценивали *in vitro* и *in vivo* на линиях опухолевых клеток и аллотрансплантатах мышинных сингенных моделей метастатической аденокарциномы молочной железы мыши 4T1, аденокарциномы толстой кишки CT26 и меланомы B16. Как MVA-RFP, так и LVP-RFP показали высокую эффективность репликации в опухолевых клетках и выраженную онколитическую активность в отношении аллотрансплантатов меланомы B16 и аденокарциномы молочной железы 4T1. В отношении 4T1, являющейся моделью тройного негативного рака молочной железы человека, LVP-RFP по сравнению с MVA-RFP показал более чем на 50% повышенную цитотоксичность в тестах *in vitro*, а также достоверное замедление прогрессирования аллотрансплантатов 4T1 и повышение выживаемости животных в экспериментах *in vivo*. Применение штамма LVP в качестве платформы при разработке рекомбинантных онколитических вирусов для терапии рака молочной железы может быть более перспективным, чем применение штамма MVA.

Ключевые слова: вирус осповакцины, LVP, MVA, вирусная онколитическая терапия, рак молочной железы, карцинома толстой кишки, меланома

Финансирование: разработка онколитических вирусов и эксперименты *in vitro* были выполнены при поддержке Российского научного фонда (грант РНФ № 20-75-10157); эксперименты *in vivo* также выполнены при поддержке Российского научного фонда (грант РНФ № 22-64-00057).

Вклад авторов: Я. Шакиба — анализ литературы, выполнение преаналитического этапа работы, проведение экспериментов *in vitro* и *in vivo*, анализ и интерпретация данных, подготовка рисунков и графиков; Е. Р. Набережная — проведение экспериментов *in vitro*, анализ и интерпретация данных; Д. В. Кочетков — уход за животными, интерпретация данных; Г. М. Юсубалиева — визуализация данных, редактирование рукописи; П. О. Воробьев — наработка препаративных количеств вируса для *in vivo* исследований; В. П. Баклаушев — планирование исследования, выполнение преаналитического этапа работы, анализ данных; А. В. Липатова, П. М. Чумаков — руководство исследованием, разработка дизайна, создание рекомбинантных штаммов, интерпретация данных, редактирование рукописи.

Соблюдение этических стандартов: исследование одобрено этическим комитетом ИМБ РАН (протокол № 3 от 27 октября 2022 г.). Эксперименты проводили в соответствии с директивой Европейского парламента и Совета Европейского союза 2010/63/ЕС о защите животных, используемых для исследований.

✉ **Для корреспонденции:** Анастасия Валерьевна Липатова
ул. Вавилова, д. 32, г. Москва, 119991, Россия; lipatovaanv@gmail.com

Статья получена: 20.02.2023 **Статья принята к печати:** 02.04.2023 **Опубликована онлайн:** 28.04.2023

DOI: 10.24075/vrgmu.2023.010

Oncolytic viruses represent a new class of drugs for the treatment of malignant neoplasms that are resistant to classical approaches of anticancer therapy. Oncolytic viruses selectively infect tumor cells, causing a direct cytopathic effect and indirect activation of cytotoxic cells, which ultimately leads to tumor regression [1]. The vaccinia virus (VV) is an oncolytic vector with excellent characteristics, including high tropism and cytolytic activity against tumor cells, rapid replication without integration into the host cell genome, resistance to the hypoxic tumor microenvironment, and a well-characterized safety profile [2, 3].

The LVP strain demonstrated significant cytotoxic activity against tumors of various histological affiliations (colorectal cancer, gastric cancer, malignant mesothelioma, lung cancer, thyroid and breast cancer) [4, 5]. The biodistribution of the LVP strain was also studied - the virus selectively infects tumor cells without being detected in the ovaries, spleen, or brain tissues after intravenous injection [6, 7]. The vaccinia virus expresses several immunomodulatory proteins to evade the body's immune response, such as interferon decoy receptors or inhibitors of innate immune regulatory pathways such as toll-like receptors or NF- κ B signaling [8]. The Lister strain has been reported to encode more genes involved in immune evasion, such as A53R, the soluble tumor necrosis factor receptor, or T1/35kDa, an inhibitor of CC chemokines, which are absent in other strains such as MVA or WR (Western Reserve), resulting in less adverse inflammatory side effects after introduction to the host's body [9, 10]. LVP is an attenuated sub variant of the English Lister strain obtained by adaptation to calf skin [11]. This strain was partly used in the smallpox eradication program after 1971 and is reported to have oncolytic properties and significantly less virulence compared to other Lister strain sub variants [12, 13]. This strain has not been studied in a number of preclinical or clinical trials [14–19].

Modified vaccinia virus Ankara (MVA) is one of the most widely studied VV strains with a promising potential in oncolytic viral therapy. MVA is a highly attenuated strain that does not replicate well in human cells, and its ability to reproduce is mainly limited to avian embryonic cells, making it quite safe [20]. In addition, MVA is a potent type I interferon inducer and elicits a strong humoral and cellular immune response. These properties of MVA make it an important candidate for the development of antitumor therapy [20]. MVA has been approved by the US Food and Drug Administration (FDA) as a safe smallpox vaccine [21]. In addition, the recombinant version MVA-BN vaccine vector has been approved by the European Medicines Agency (EMA) as part of the Ebola vaccine and is actively used in clinical trials of infectious diseases and tumor immunotherapy [22].

In this study, we obtained recombinant strains MVA-RFP and LVP-RFP with inactivation of the viral thymidine kinase (TK) gene to increase specificity for tumor cells [23] by inserting the reporter gene tagRFP (red fluorescent protein) into the TK gene locus. Inactivation of the TK gene makes virus replication dependent on cellular TK, which is expressed only during the S-phase of the cell cycle, while transformed cells constantly express it. For example, recombinant viruses with a defective TK gene selectively replicate in rapidly dividing tumor cells that constantly express cellular thymidine kinase [24].

The aim of this work was to compare the oncolytic efficacy of MVA-RFP and LVP-RFP in solid tumors of mouse syngeneic models of 4T1 mammary adenocarcinoma, B16 melanoma, and CT26 colon carcinoma.

METHODS

Cell cultures

Hamster kidney BHK-21 (ATCC # CCL-10), CT26 colon carcinoma (ATCC # CRL-2639), 4T1 mammary adenocarcinoma (ATCC # CRL-3406), B16 melanoma (ATCC # CRL-6475) and HEK293T (ATCC # CRL-3216) cell lines were purchased from the American Culture Collection (ATCC; USA). Rat fibroblasts deficient in TK (Rat2 TK-/-) were taken from the collection of the Cell Proliferation Laboratory of the IMB RAS (Moscow, Russia). All cells were cultured in DMEM supplemented with glutamine (Gibco; USA) and 10% fetal bovine serum (FBS) (Gibco; USA) and incubated at 37 °C under 5% CO₂.

Viruses

The vaccinia virus strain LVP was obtained from the collection of the Cell Proliferation Laboratory of the IMB RAS (Moscow, Russia). Modified vaccinia virus Ankara (MVA) (ATCC № VR-1508) was purchased from ATCC.

A shuttle plasmid carrying the tagRFP gene was cloned to construct the MVA-RFP and LVP-RFP strains. The tagRFP gene sequence was amplified by PCR from the pTagRFP-C plasmid construct (Evrogen; Russia) using primers 5-AGA GAGCCTGGATGGTGTCTAAGGGCGAAGAG and 5-AGAG AGGGATCCTTAATTAAGTTTGTGCCCCAGTTTG (Evrogen; Russia). tagRFP was expressed under the control of the 7.5k promoter. The frame was flanked by the TK gene region; the initial plasmid construct for recombination was created at the Cell Proliferation Laboratory of the IMB RAS (Moscow, Russia) [6]. Recombinant strains were obtained by lipofection of HEK293T cells with Lipofectamine 3000 (Thermo Fischer; USA) and subsequent infection with a wild-type vaccinia strain. After 48 h, a cryolysate of infected cells was prepared and viral particles were selected on Rat-2 TK-/- cells treated with bromodeoxyuridine at a concentration of 25 µg/mL [24]. After several rounds of selection, the virus was cloned by the plaque method to dissociate the wild strain. The resulting recombinant strains were grown in BHK-21 cells and purified by centrifugation in a sucrose density gradient [25]. The correctness of the inserts in the recombinant variants was confirmed by Sanger sequencing of the corresponding genome region. DNA sequencing was performed using the ABI PRISM® BigDye™ Terminator v. 3.1 (Thermo Fischer; USA) followed by analysis of the reaction products on an Applied Biosystems 3730 DNA Analyzer automatic sequencer (Thermo Fischer; USA) at the Genome Shared Use Center of the IMB RAS.

Titration of the virus

BHK-21 cells were seeded at 10,000 cells per well in a 96-well plate, the next day the medium was removed and the cells were infected with 10-fold dilutions of the viruses and incubated in DMED medium supplemented with 2% FBS. After 48 hours, when the cytopathic effect developed, the 50% infectious dose of tissue culture (TCID₅₀) was evaluated according to the Reed and Muench method [26].

Assessment of cytotoxic activity of viruses

4T1, B16, CT26, and BHK-21 cells were seeded at 10,000 cells/well in 96-well plates, then infected at 1 and 10 MOI (multiplicity of infection) of the MVA-RFP or LVP-RFP strains. Cytotoxic activity was assessed using the MTT test 24, 48,

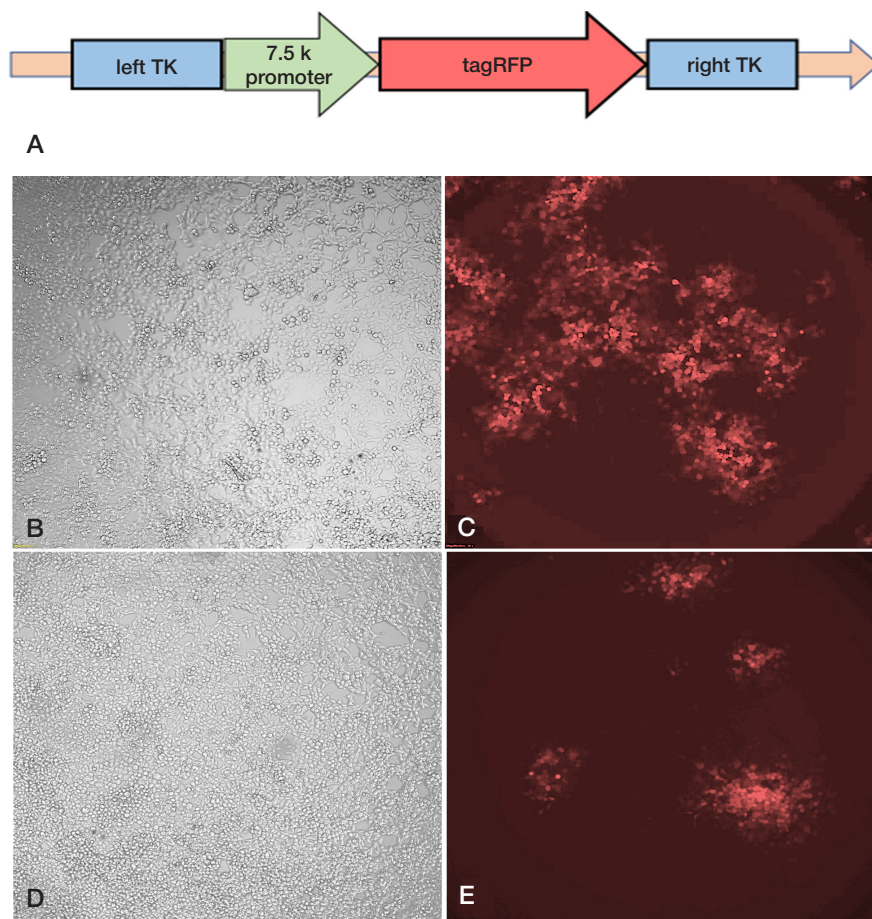


Fig. 1. Characterization of recombinant LVP-RFP and MVA-RFP strains *in vitro*. **A.** Schematic of the plasmid vector used in the development of the LVP-RFP and MVA-RFP strains. **B, C.** Fluorescence microscopy of HEK293T cells infected with the recombinant LVP-RFP strain. **D, E.** Fluorescence microscopy of HEK293T infected with MVA-RFP ($\times 100$ magnification)

and 72 h after infection. The percentage of viable cells was calculated as the ratio of cell viability in infected wells to cell viability in uninfected control wells multiplied by 100 [27].

Estimation of virus replication rate by flow cytometry

The level of RFP expression in infected cells correlates with the level of viral replication. 4T1, B16, CT26, and BHK-21 cells were seeded at 100,000 cells per well in 24-well plates, infected with MVA-RFP or LVP-RFP strains with MOIs of 1 and 10. 24 and 48 h after infection, cells removed from the surface with trypsin and resuspended in phosphate-buffered saline (PBS) (PanEco, Russia) with the addition of 2% FBS. The number of the brightly fluorescent cells in the RFP range was measured using a BD LSRFortessa Cell Analyzer (Beckman Dickinson; USA). Analysis was performed using Flowing Software 2.0 (Perttu Terho; Finland). The results are based on three independent experiments with three repetitions, and at least 10,000 events per sample.

Assessment of oncolytic activity of viruses *in vivo*

Six-week-old female BALB/c and C57BL/6 mice were used in the experiments. Mice had free access to food and water and were kept in standard conditions with controlled temperature (21–23 °C) and air ventilation, as well as a 12/12 light regimen. For tumor formation, 10^6 CT26 colon carcinoma or 4T1 breast cancer cells were implanted subcutaneously in the right flank of BALB/c mice, and 10^6 B16 melanoma cells were implanted in the right flank of C57BL/6 mice. Prior to virotherapy, mice

with verified tumor allografts of CT26 ($n = 15$), 4T1 ($n = 15$), and B16 ($n = 15$) mice were divided into three subgroups ($n = 5$ each). 5×10^7 PFU of the viruses in 50 μ l of PBS were injected intratumorally on the 7th and 9th days after tumor implantation. Control groups received intratumoral injections of PBS. Tumor volume was measured using a modified ellipsoidal formula: $V = \frac{1}{2} (\text{length} \times \text{width}^2)$ [28] every two days until the tumor volume reached 2000 mm³. After reaching the maximum allowed volume, mice were euthanized and based on these data, survival curves were built.

Statistical analysis

All data are presented as mean \pm standard deviation. Statistical analysis was performed using unpaired t-tests and two-way analysis of variance, differences were considered significant at $p < 0.05$. GraphPad Prism 8.0.2 (GraphPad Software, Inc.; USA) was used to prepare all graphs and perform statistical analysis.

RESULTS

Construction of recombinant viruses

TK inactivated LVP-RFP and MVA-RFP strains containing an insertion of red fluorescent protein (tagRFP) were generated by recombination of the viral genome with a plasmid construct. Fluorescence microscopy of HEK293T cells infected with recombinant strains of LVP-RFP and MVA-RFP showed that the viruses replicate and produce functionally active RFP (Fig. 1).

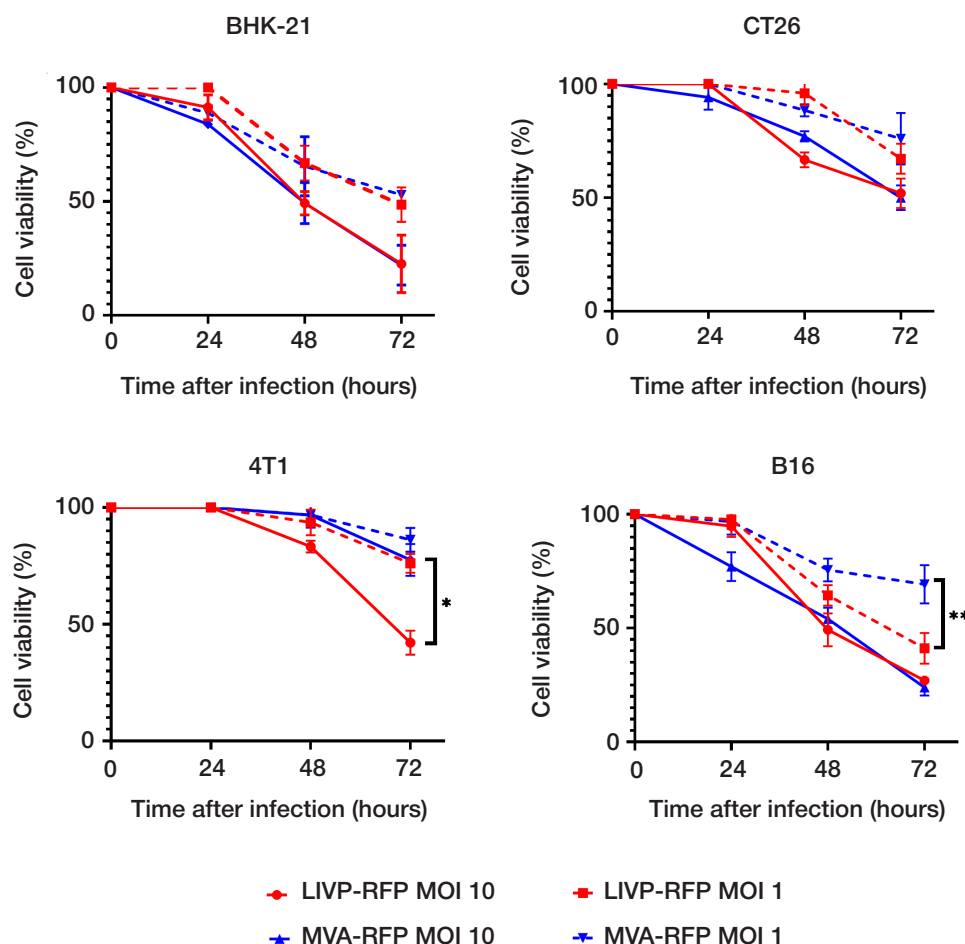


Fig. 2. Cytotoxicity of recombinant LVP-RFP and MVA-RFP strains in various tumor cell cultures. BHK-21, B16, CT26 and 4T1 cells were infected with MOI 1 and 10 of LVP-RFP and MVA-RFP viruses and cell viability was assessed using the MTT assay at 24, 48 and 72 hours post-infection. Statistical analysis was performed using a *t*-test; * — $p < 0.05$ and ** — $p < 0.01$ indicate significance.

Cytotoxic activity of LVP-RFP and MVA-RFP strains against mouse tumor cells

The cytotoxic activity of recombinant vaccinia virus strains LVP-RFP and MVA-RFP was assessed for 72 h using the MTT assay in mouse B16 melanoma, CT26 colon carcinoma, and 4T1 mammary adenocarcinoma cell cultures, as well as in the VV-sensitive BHK-21 cell line, which we used as a positive control. In BHK-21 culture, LVP-RFP and MVA-RFP strains caused more than 75% cell death at MOI 10 and more than 50% death at MOI 1 (MOI 1) after 72 h (Fig. 2). B16 melanoma was the most sensitive of the studied metastatic tumor lines, in culture of which 50% cell death was observed 72 h after infection with MOI 10 LVP-RFP or MVA-RFP (Fig. 2B; solid lines). Upon infection with B16 MOI 1, the recombinant LVP-RFP strain showed significantly higher cytotoxicity after 72 h compared to MVA-RFP (Fig. 2; dotted lines). The most resistant to oncolytic virotherapy was CT26 colorectal carcinoma line, in culture of which less than 50% cell death was observed at a multiplicity of infection of 10 LVP-RFP or MVA-RFP (Fig. 2). In 4T1 mammary adenocarcinoma, a cytopathic effect was detected only in infection with a multiplicity of 10. At the same time, a significantly higher cytotoxicity ($> 50\%$) was noted for the LVP-RFP strain compared to MVA-RFP (Fig. 2).

Assessment of viral replication by flow cytometry

The replication efficiency of viral strains in the studied cell lines was assessed by the number of fluorescent RFP-positive cells,

which was determined using flow cytometry. It was found that the level of infection of the control line BHK-21 approaches 100% already after 24 h and does not change significantly after 48 h (Fig. 3). In the B16 melanoma cell line, an increase in the number of RFP-positive cells was observed, and the MVA-RFP strain, which infected more than 60% of the cells within 48 hours, showed a significantly higher replication efficiency. The 4T1 breast adenocarcinoma line, on the contrary, was characterized by the lowest replication efficiency of vaccinia virus, with the highest level of infection was observed when infected with the LVP-RFP strain and it reached almost 30% after 48 hours. The efficiency of the viral replication in CT26 cell culture (about 40% for MOI 10) did not differ between LVP-RFP and MVA-RFP.

Evaluation of the antitumor activity of LVP-RFP and MVA-RFP strains in experiments *in vivo*

The oncolytic activity of the recombinant LVP-RFP and MVA-RFP strains was studied in BALB/c mice with allografts of 4T1 breast or CT26 colon carcinomas, as well as in C57BL/6 mice with allografts of B16 melanoma. Double intratumoral injection of oncolytic viruses on days 7 and 9 after tumor inoculation resulted in a slowdown in tumor growth (Fig. 4) and an increase in animal survival (Fig. 5) in all groups treated with both LVP-RFP and MVA-RFP compared to control groups that were injected with PBS. The most noticeable slowdown in tumor growth was found in the treatment of B16 melanoma allografts with the intratumoral injection of MVA-RFP, as well

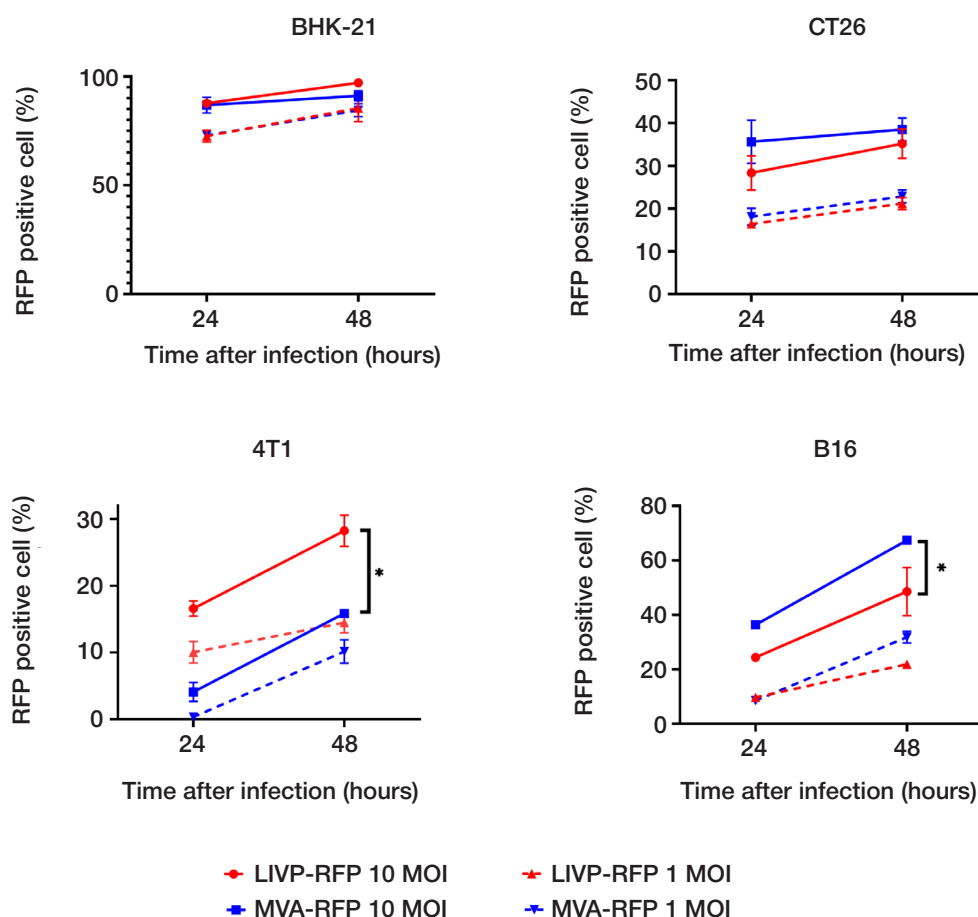


Fig. 3. Replication efficiency of viral strains in cell lines BHK-21, B16, CT26, 4T1 infected with MOI 1 and 10 LVP-RFP and MVA-RFP based on the results of flow cytometry after 24 and 48 h. The y-axis shows the number of cells in percent expressing RFP. Statistical analysis was performed using a *t*-test; * — $p < 0.05$ indicate significant

as 4T1 carcinoma allografts with the introduction of LVP-RFP, which fully corresponded to the results obtained *in vitro*. Survival in the 4T1 and B16 subgroups (after virotherapy) was significantly higher compared to the control, while the animals treated with LVP-RFP had a longer life expectancy than in the MVA-RFP subgroups (Fig. 5). Progression of CT26 carcinoma was not altered in any way by both LVP-RFP and MVA-RFP therapy (Fig. 4), although both experimental subgroups showed an increase in survival of animals injected with recombinant viruses (Fig. 5).

Thus, data obtained from both *in vitro* and *in vivo* experiments confirm the superior oncolytic activity of the recombinant LVP-RFP strain against the 4T1 breast adenocarcinoma model.

DISCUSSION

In this comparative study, we evaluated the cytotoxicity and replication capacity *in vitro*, and *in vivo* therapeutic potential against solid mouse tumors of recombinant LVP-RFP and MVA-RFP strains derived from vaccinia virus strains LVP and MVA, respectively, containing an insert of red fluorescent protein gene in the structural part of the viral thymidine kinase gene.

The effectiveness of the therapy with oncolytic viruses consists of two main components: the activation of the immune system in response to the introduction of viruses and the direct cytotoxic effect of viruses on tumor cells [29]. Activation of immunocompetent cytotoxic CD8⁺ lymphocytes, CD56⁺ NK cells, and tissue macrophages is of critical importance due to the fact that the most resistant and malignant tumors are characterized by the most pronounced immunosuppressive

effect on the tumor microenvironment [30]. Therefore, systemic or intratumoral administration of viral particles that infect tumor cells and activate antigen-presenting cells is accompanied by increased production of inflammatory cytokines and recruitment of cytotoxic immune cells, which ultimately can slow down tumor progression. Antitumor immune responses are supplemented by a direct cytopathic effect of oncolytic viruses on tumor cells due to increased proliferation rate, inhibition of apoptosis, and other oncogenic mechanisms [30].

One of the key difficulties in the use of oncolytic viruses for therapy is a pronounced host immune response to the viral infection, which causes adverse side effects and reduces the effectiveness of the virotherapy. Poxviruses are unique in their ability to evade the host's immune response, making them generally safe for use in therapy, in particular, the Lister strain has proven to be highly safe in humans as it has been used during the worldwide smallpox eradication program [7, 31]. This strain has been shown to induce less pro-inflammatory cytokines such as IL8, IL6 and IFN γ in the host and induce higher levels of anti-inflammatory cytokines such as IL10 compared to other strains such as WR [5, 32].

Increasing the onco-selectivity of the virus limits viral infection at the site of the tumor and prevents infection of other organs, resulting in fewer inflammatory side effects. One of the strategies for increasing tumor selectivity and reducing the vaccinia virus virulence is deletion of the viral thymidine kinase gene [33].

In our study, we have shown that LVP-RFP replicates and lyses 4T1 cells more efficiently than the MVA-RFP strain. In subsequent *in vivo* experiments, we were able to demonstrate the relationship between the ability of the virus to replicate in

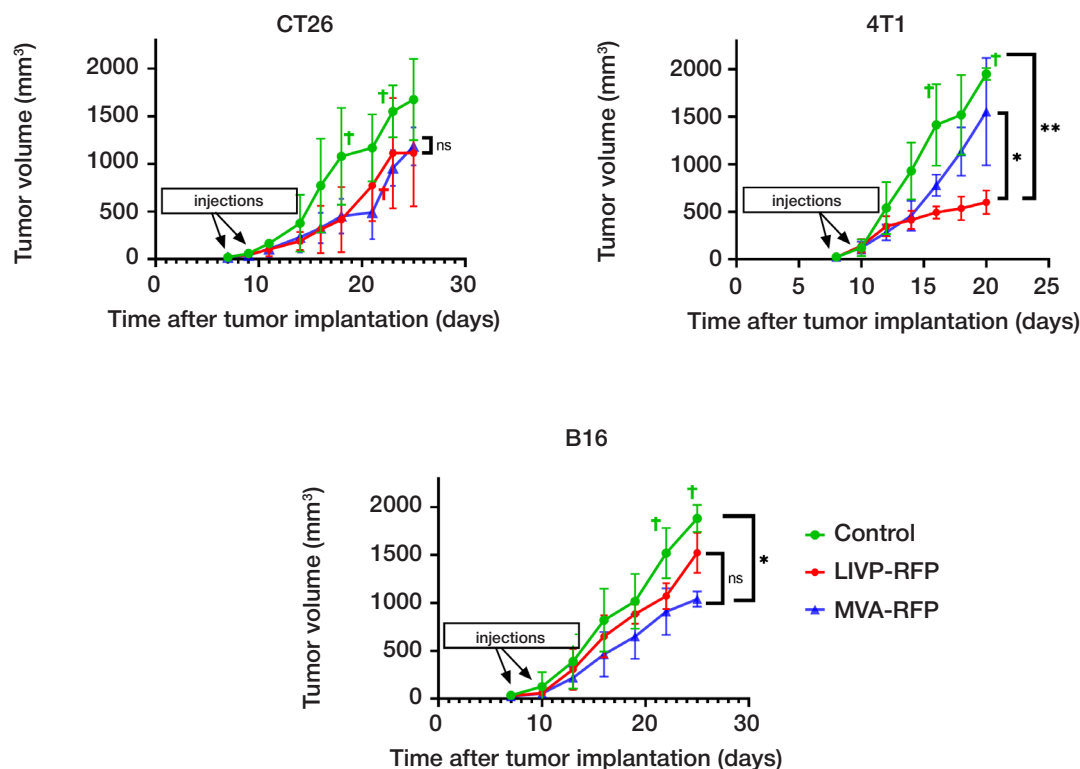


Fig. 4. Dynamics of changes in tumor volume in mice with allografts of colon carcinoma CT26, breast carcinoma 4T1, and melanoma B16 after treatment with recombinant strains of LVP-RFP or MVA-RFP. Tumor measurements were taken every two days after treatment. The symbol † indicates the euthanasia of the animal. Statistical analysis was performed using a t-test; * — $p < 0.05$; ns — no statistically significant differences

tumor cells *in vitro* and its ability to slow tumor progression *in vivo*. A significantly smaller volume of tumor allografts of 4T1 adenocarcinoma and an increase in the survival of animals after LVP-RFP therapy compared to MVA-RFP indicate a more pronounced oncolytic activity of LVP-RFP in relation to 4T1 adenocarcinoma.

The 4T1 breast cancer cell line is a highly invasive and metastatic cell model of triple negative breast cancer (TNBC) [34]. TNBC is considered the most aggressive form of breast cancer with the worst prognosis and the absence of targeted treatment options [35]. Our results indicate that the LVP strain has greater potential for the treatment of TNBC compared to MVA.

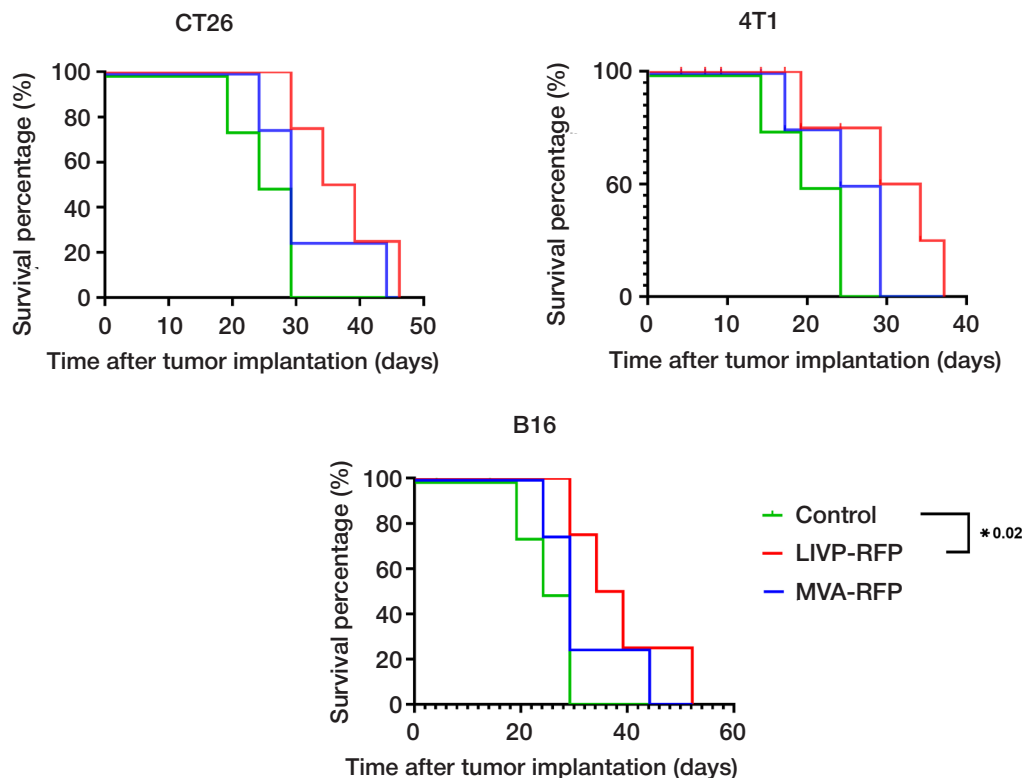


Fig. 5. Kaplan-Meier survival curves in experimental subgroups of mice with allografts of adenocarcinoma CT26, 4T1, and melanoma B16 after two intratumoral injections of recombinant LVP-RFP or MVA-RFP viruses

CONCLUSIONS

A comparative study of the oncolytic properties of LVP-RFP and MVA-RFP strains with an inactivated thymidine kinase gene showed that the LVP-RFP strain is more effective for

oncolytic virotherapy of 4T1 breast cancer. The use of the LVP strain as a platform for the development of recombinant oncolytic viruses for the treatment of triple-negative breast cancer may be more promising than the use of the MVA strain.

References

1. Thorne SH, Hwang TH, Kirn DH. Vaccinia virus and oncolytic virotherapy of cancer. *Curr Opin Mol Ther*. 2005; 7 (4): 359–65.
2. Ho TY, et al. Deletion of immunomodulatory genes as a novel approach to oncolytic vaccinia virus development. *Mol Ther Oncolytics*. 2021; 22: 85–97.
3. Kirn DH, et al. Enhancing poxvirus oncolytic effects through increased spread and immune evasion. *Cancer Res*. 2008; 68 (7): 2071–5.
4. Haddad D, et al. A novel genetically modified oncolytic vaccinia virus in experimental models is effective against a wide range of human cancers. *Ann Surg Oncol*. 2012; 19: 665–74.
5. Hughes J, et al. Lister strain vaccinia virus with thymidine kinase gene deletion is a tractable platform for development of a new generation of oncolytic virus. *Gene Ther*. 2015; 22 (6): 476–84.
6. Shakiba Y, et al. Oncolytic efficacy of a recombinant vaccinia virus strain expressing bacterial flagellin in solid tumor models. *Viruses*. 2023; 15 (4): 828. DOI: 10.3390/v15040828.
7. Tysome JR, et al. Lister vaccine strain of vaccinia virus armed with the endostatin–angiostatin fusion gene: an oncolytic virus superior to dl 1520 (ONYX-015) for human head and neck cancer. *Hum Gene Ther*. 2011; 22 (9): 1101–8.
8. Smith GL. Vaccinia virus immune evasion. *Immunol Lett*. 1999; 65 (1–2): 55–62.
9. Bahar MW, et al. How vaccinia virus has evolved to subvert the host immune response. *J Struct Biol*. 2011; 175 (2): 127–34.
10. Smith GL, et al. Vaccinia virus immune evasion: mechanisms, virulence and immunogenicity. *J Gen Virol*. 2013; 94 (11): 2367–92.
11. Shvalov AN, et al. Complete genome sequence of vaccinia virus strain L-IVP. *Genome Announc*. 2016; 4 (3): e00372–16.
12. Gentshev I, et al. Preclinical evaluation of oncolytic vaccinia virus for therapy of canine soft tissue sarcoma. 2012; 7 (5): e37239.
13. Shchelkunov SN, et al. Enhancing the protective immune response to administration of a LVP-GFP live attenuated vaccinia virus to mice. *PLoS One*. 2021; 10 (3): 377.
14. Kochneva G, et al. Engineering of double recombinant vaccinia virus with enhanced oncolytic potential for solid tumor virotherapy. *Oncotarget*. 2016; 7 (45): 74171.
15. Zonov E, et al. Features of the antitumor effect of vaccinia virus lister strain. *Viruses*. 2016; 8 (1): 20.
16. Koval O, et al. Recombinant vaccinia viruses coding transgenes of apoptosis-inducing proteins enhance apoptosis but not immunogenicity of infected tumor cells. *Biomed Res Int*. 2017; 2017: 3620510. DOI: 10.1155/2017/3620510.
17. Tkacheva A, et al. Targeted therapy of human glioblastoma combining the oncolytic properties of parvovirus H-1 and attenuated strains of the vaccinia virus. *Molecular Genetics, Microbiology and Virology*. 2019; 37 (2): 83–91.
18. Gholami S, et al. Vaccinia virus GLV-1h153 is a novel agent for detection and effective local control of positive surgical margins for breast cancer. *Breast Cancer Res*. 2013; 15 (2): R26.
19. Holloway R, et al. 837P Phase II trial of oncolytic vaccinia virus primed immunochemotherapy in platinum-resistant/refractory ovarian cancer (PRROC)(NCT02759588). *Annals of Oncology*. 2020; 31: 628.
20. Suter M, et al. Modified vaccinia Ankara strains with identical coding sequences actually represent complex mixtures of viruses that determine the biological properties of each strain. *Vaccine*. 2009; 27 (52): 7442–50.
21. Pittman PR, et al. Phase 3 efficacy trial of modified vaccinia Ankara as a vaccine against smallpox. *N Engl J Med*. 2019; 381 (20): 1897–908.
22. Gatti-Mays ME, et al. A phase I dose-escalation trial of BN-CV301, a recombinant poxviral vaccine targeting MUC1 and CEA with costimulatory molecules. *Clin Cancer Res*. 2019; 25 (16): 4933–44.
23. Parato KA, et al. The oncolytic poxvirus JX-594 selectively replicates in and destroys cancer cells driven by genetic pathways commonly activated in cancers. *Mol Ther*. 2012; 20 (4): 749–58.
24. Byrd CM, et al. Construction of recombinant vaccinia virus: cloning into the thymidine kinase locus. *Methods Mol Biol*. 2004: 31–40.
25. Cotter CA, et al. Preparation of cell cultures and vaccinia virus stocks. *Curr Protoc Mol Biol*. 2017; 117 (1): 16.16.1–16.16.18.
26. Ramakrishnan MAJ. Determination of 50% endpoint titer using a simple formula. *World J Virol*. 2016; 5 (2): 85.
27. Morgan DM. Tetrazolium (MTT) assay for cellular viability and activity. *Methods Mol Biol*. 1998: 179–84.
28. Tomayko MM, Reynolds CP. Determination of subcutaneous tumor size in athymic (nude) mice. *Cancer Chemother Pharmacol*. 1989; 24: 148–54.
29. Cottingham MG, Carroll MW. Recombinant MVA vaccines: dispelling the myths. *Vaccine*. 2013; 31 (39): 4247–51.
30. Zitvogel L, Tesniere A, Kroemer G. Cancer despite immunosurveillance: immunoselection and immunosubversion. *Nat Rev Immunol*. 2006; 6 (10): 715–27.
31. Thorne SH. Immunotherapeutic potential of oncolytic vaccinia virus. *Immunol Res*. 2011; 50: 286–93.
32. Matsuda T, et al. A comparative safety profile assessment of oncolytic virus therapy based on clinical trials. *Ther Innov Regul Sci*. 2018; 52 (4): 430–7.
33. Buller RML, et al. Decreased virulence of recombinant vaccinia virus expression vectors is associated with a thymidine kinase-negative phenotype. *Nature*. 1985; 317 (6040): 813–5.
34. Schrörs B, et al. Multi-omics characterization of the 4T1 murine mammary gland tumor model. *Front Oncol*. 2020; 10: 1195.
35. Li Z, et al. Immunotherapeutic interventions of triple negative breast cancer. *J Transl Med*. 2018; 16 (1): 147.

Литература

1. Thorne SH, Hwang TH, Kirn DH. Vaccinia virus and oncolytic virotherapy of cancer. *Curr Opin Mol Ther*. 2005; 7 (4): 359–65.
2. Ho TY, et al. Deletion of immunomodulatory genes as a novel approach to oncolytic vaccinia virus development. *Mol Ther Oncolytics*. 2021; 22: 85–97.
3. Kirn DH, et al. Enhancing poxvirus oncolytic effects through increased spread and immune evasion. *Cancer Res*. 2008; 68 (7): 2071–5.
4. Haddad D, et al. A novel genetically modified oncolytic vaccinia virus in experimental models is effective against a wide range of human cancers. *Ann Surg Oncol*. 2012; 19: 665–74.
5. Hughes J, et al. Lister strain vaccinia virus with thymidine kinase gene deletion is a tractable platform for development of a new generation of oncolytic virus. *Gene Ther*. 2015; 22 (6): 476–84.
6. Shakiba Y, et al. Oncolytic efficacy of a recombinant vaccinia virus strain expressing bacterial flagellin in solid tumor models. *Viruses*. 2023; 15 (4): 828. DOI: 10.3390/v15040828.
7. Tysome JR, et al. Lister vaccine strain of vaccinia virus armed

- with the endostatin-angiostatin fusion gene: an oncolytic virus superior to dl 1520 (ONYX-015) for human head and neck cancer. *Hum Gene Ther*. 2011; 22 (9): 1101–8.
8. Smith GL. Vaccinia virus immune evasion. *Immunol Lett*. 1999; 65 (1–2): 55–62.
 9. Bahar MW, et al. How vaccinia virus has evolved to subvert the host immune response. *J Struct Biol*. 2011; 175 (2): 127–34.
 10. Smith GL, et al. Vaccinia virus immune evasion: mechanisms, virulence and immunogenicity. *J Gen Virol*. 2013; 94 (11): 2367–92.
 11. Shvalov AN, et al. Complete genome sequence of vaccinia virus strain L-IVP. *Genome Announc*. 2016; 4 (3): e00372–16.
 12. Gentshev I, et al. Preclinical evaluation of oncolytic vaccinia virus for therapy of canine soft tissue sarcoma. 2012; 7 (5): e37239.
 13. Shchelkunov SN, et al. Enhancing the protective immune response to administration of a LVP-GFP live attenuated vaccinia virus to mice. *PLoS One*. 2021; 10 (3): 377.
 14. Kochneva G, et al. Engineering of double recombinant vaccinia virus with enhanced oncolytic potential for solid tumor virotherapy. *Oncotarget*. 2016; 7 (45): 74171.
 15. Zonov E, et al. Features of the antitumor effect of vaccinia virus lister strain. *Viruses*. 2016; 8 (1): 20.
 16. Koval O, et al. Recombinant vaccinia viruses coding transgenes of apoptosis-inducing proteins enhance apoptosis but not immunogenicity of infected tumor cells. *Biomed Res Int*. 2017; 2017: 3620510. DOI: 10.1155/2017/3620510.
 17. Tkacheva A, et al. Targeted therapy of human glioblastoma combining the oncolytic properties of parvovirus H-1 and attenuated strains of the vaccinia virus. *Molecular Genetics, Microbiology and Virology*. 2019; 37 (2): 83–91.
 18. Gholami S, et al. Vaccinia virus GLV-1h153 is a novel agent for detection and effective local control of positive surgical margins for breast cancer. *Breast Cancer Res*. 2013; 15 (2): R26.
 19. Holloway R, et al. 837P Phase II trial of oncolytic vaccinia virus primed immunochemotherapy in platinum-resistant/refractory ovarian cancer (PRROC)(NCT02759588). *Annals of Oncology*. 2020; 31: 628.
 20. Suter M, et al. Modified vaccinia Ankara strains with identical coding sequences actually represent complex mixtures of viruses that determine the biological properties of each strain. *Vaccine*. 2009; 27 (52): 7442–50.
 21. Pittman PR, et al. Phase 3 efficacy trial of modified vaccinia Ankara as a vaccine against smallpox. *N Engl J Med*. 2019; 381 (20): 1897–908.
 22. Gatti-Mays ME, et al. A phase I dose-escalation trial of BN-CV301, a recombinant poxviral vaccine targeting MUC1 and CEA with costimulatory molecules. *Clin Cancer Res*. 2019; 25 (16): 4933–44.
 23. Parato KA, et al. The oncolytic poxvirus JX-594 selectively replicates in and destroys cancer cells driven by genetic pathways commonly activated in cancers. *Mol Ther*. 2012; 20 (4): 749–58.
 24. Byrd CM, et al. Construction of recombinant vaccinia virus: cloning into the thymidine kinase locus. *Methods Mol Biol*. 2004: 31–40.
 25. Cotter CA, et al. Preparation of cell cultures and vaccinia virus stocks. *Curr Protoc Mol Biol*. 2017; 117 (1): 16.16.1–16.16.18.
 26. Ramakrishnan MAJ. Determination of 50% endpoint titer using a simple formula. *World J Virol*. 2016; 5 (2): 85.
 27. Morgan DM. Tetrazolium (MTT) assay for cellular viability and activity. *Methods Mol Biol*. 1998: 179–84.
 28. Tomayko MM, Reynolds CP. Determination of subcutaneous tumor size in athymic (nude) mice. *Cancer Chemother Pharmacol*. 1989; 24: 148–54.
 29. Cottingham MG, Carroll MW. Recombinant MVA vaccines: dispelling the myths. *Vaccine*. 2013; 31 (39): 4247–51.
 30. Zitvogel L, Tesniere A, Kroemer G. Cancer despite immunosurveillance: immunoselection and immunosubversion. *Nat Rev Immunol*. 2006; 6 (10): 715–27.
 31. Thorne SH. Immunotherapeutic potential of oncolytic vaccinia virus. *Immunol Res*. 2011; 50: 286–93.
 32. Matsuda T, et al. A comparative safety profile assessment of oncolytic virus therapy based on clinical trials. *Ther Innov Regul Sci*. 2018; 52 (4): 430–7.
 33. Buller RML, et al. Decreased virulence of recombinant vaccinia virus expression vectors is associated with a thymidine kinase-negative phenotype. *Nature*. 1985; 317 (6040): 813–5.
 34. Schrörs B, et al. Multi-omics characterization of the 4T1 murine mammary gland tumor model. *Front Oncol*. 2020; 10: 1195.
 35. Li Z, et al. Immunotherapeutic interventions of triple negative breast cancer. *J Transl Med*. 2018; 16 (1): 147.

PREDICTING THE BLASTOCYST DEVELOPMENT RATE DURING ASSISTED REPRODUCTIVE TECHNOLOGIES BASED ON SEMEN MICROBIOTA

Panacheva EA², Kudryavtseva EV¹, Zornikov DL¹, Plotko EE², Petrov VM¹, Voroshilina ES^{1,2} ✉

¹ Ural State Medical University of the Ministry of Health of Russian Federation, Yekaterinburg, Russia

² Medical Center "Garmonia", Yekaterinburg, Russia

Obtaining enough good and excellent quality embryos is one of the key factors for achieving pregnancy using assisted reproductive technologies. This work was aimed at developing a mathematical model for predicting good and excellent quality embryos based on semen microbiota assessment in normozoospermia. The study included 127 men whose semen was used for in vitro fertilization (IVF). Patients were divided into 2 groups depending on the proportion of good-quality blastocyst developed on the 5th day of culturing (good-quality blastocyst development rate, GBDR). The 1st group included 57 patients with GBDR \geq 40%, the 2nd group included 70 patients with GBDR < 40%. All patients' semen was assessed at the day of fertilization. Semen parameters were evaluated in accordance with the WHO standards and semen microbiota composition was determined by means of real-time PCR. Discriminant analysis was used for development of the prognostic model. We developed a method for predicting efficiency of the embryological IVF stage in normozoospermia: EGO-Pro-N prognostic index (Embryos of GOod and Excellent quality Prognosis in Normozoospermia). If the EGO-Pro-N value is greater than 0.212, the probability of receiving GBDR \geq 40% is low. Conversely, if the EGO-Pro-N value is less than or equal to 0.212, the probability is high. Sensitivity and specificity of the method were 71.9% and 70.0% respectively, accuracy was 70.9%. The developed model allows us to predict good and excellent quality embryos based on comprehensive semen microbiota assessment in normozoospermia before IVF.

Keywords: semen microbiota composition, prognosis, ART effectiveness, IVF, real-time PCR, discriminant analysis

Acknowledgments: the authors would like to thank VN Khayutin, director of "Garmonia" Medical Center, for allowing them to conduct the study in the clinic's laboratory department.

Author contribution: Panacheva EA — organization of the study, data analysis, conducting PCR tests, article authoring, Kudryavtseva EV, Zornikov DL — statistical processing, data analysis, article authoring; Plotko EE, Petrov VM — data analysis, article authoring; Voroshilina ES — organization of the study, conducting PCR tests, data analysis, article authoring.

Compliance with ethical standards: the study was approved by the Ethics Committee of Ural State Medical University, Federal State Budget Educational Institution of Higher Education under the Ministry of Health of the Russian Federation (Protocol № 7 of September 20, 2019). All patients signed the informed written consent to participation in the study.

✉ **Correspondence should be addressed:** Ekaterina S. Voroshilina
Tveritina, 16, Yekaterinburg, 620100, Russia; voroshilina@gmail.com

Received: 23.03.2023 **Accepted:** 14.04.2023 **Published online:** 26.04.2023

DOI: 10.24075/brsmu.2023.015

ПРОГНОЗИРОВАНИЕ ЭФФЕКТИВНОСТИ ЭМБРИОЛОГИЧЕСКОГО ЭТАПА ВСПОМОГАТЕЛЬНЫХ РЕПРОДУКТИВНЫХ ТЕХНОЛОГИЙ ПО МИКРОБНОМУ СОСТАВУ ЭЯКУЛЯТА

Е. А. Паначева², Е. В. Кудрявцева¹, Д. Л. Зорников¹, Е. Э. Плотко², В. М. Петров¹, Е. С. Ворошилина^{1,2} ✉

¹ Уральский государственный медицинский университет Минздрава России, Екатеринбург, Россия

² Медицинский центр «Гармония», Екатеринбург, Россия

Один из ключевых факторов наступления беременности при использовании вспомогательных репродуктивных технологий (ВРТ) — получение достаточного количества эмбрионов хорошего и отличного качества. Целью работы было разработать математическую модель для прогнозирования качества получаемых эмбрионов на основании результатов оценки микробного состава эякулята, используемого для оплодотворения в программах ВРТ при нормозооспермии. Эякулят 127 мужчин использовали в процедуре экстракорпорального оплодотворения (ЭКО). В зависимости от доли blastocyst хорошего и отличного качества, сформировавшихся на 5-й день культивирования (good-quality blastocyst development rate, GBDR), пациенты были разделены на две группы. В первую включены 57 пациентов с GBDR \geq 40%, во вторую — 70 пациентов с GBDR < 40%. Всем пациентам в день оплодотворения проведено исследование параметров спермограммы по стандарту ВОЗ и определен состав микробиоты эякулята методом количественной ПЦР в реальном времени. С помощью дискриминантного анализа разработан способ прогнозирования эффективности эмбриологического этапа ВРТ у пар, планирующих процедуру ЭКО, при показателях эякулята, соответствующих критериям нормозооспермии, с расчетом прогностического индекса «Эмбрионы хорошего и отличного качества. Прогноз нормозооспермии» (ЭХО-Про-Н). Если значение ЭХО-Про-Н > 0,212, вероятность получения GBDR \geq 40% низкая, если ЭХО-Про-Н \leq 0,212, вероятность высокая. Показатели чувствительности и специфичности составили соответственно 71,9% и 70,0%, эффективность способа — 70,9%. Разработанная прогностическая модель дает возможность прогнозирования получения GBDR \geq 40% на основании комплексной оценки микробиоты эякулята.

Ключевые слова: микробиота эякулята, прогнозирование, эффективность ВРТ, ЭКО, ПЦР в реальном времени, дискриминантный анализ

Благодарности: авторы благодарят директора Медицинского центра «Гармония» (г. Екатеринбург) В. Н. Хаютина за возможность выполнения исследования на базе центра.

Вклад авторов: Е. А. Паначева — организация исследования, отбор пациентов, выполнение ПЦР-РВ, анализ полученных данных, написание статьи; Е. В. Кудрявцева, Д. Л. Зорников — статистическая обработка, анализ полученных данных, написание статьи; Е. Э. Плотко, В. М. Петров — анализ полученных данных, написание статьи; Е. С. Ворошилина — организация исследования, выполнение ПЦР-РВ, анализ полученных данных, написание статьи.

Соблюдение этических стандартов: исследование одобрено этическим комитетом ФГБОУ ВО УГМУ Минздрава России (протокол № 7 от 20 сентября 2019 г.). Все участники подписали добровольное информированное согласие на участие. Исследование проведено в соответствии с требованиями Хельсинкской декларации Всемирной ассоциации «Этические принципы проведения научных медицинских исследований с участием человека» от июня 1964 г.

✉ **Для корреспонденции:** Екатерина Сергеевна Ворошилина
ул. Тверитина, д. 16, г. Екатеринбург, 620100, Россия; voroshilina@gmail.com

Статья получена: 23.03.2023 **Статья принята к печати:** 14.04.2023 **Опубликована онлайн:** 26.04.2023

DOI: 10.24075/vrgmu.2023.015

The demand in assisted reproductive technologies (ART) is continuously growing. At the same time, according to the National Registry of the Russian Association of Human Reproduction, the effectiveness of *in-vitro* fertilization (IVF) treatment programs does not exceed 34.8% in terms of embryo transfer rate [1]. Obtaining the sufficient amount of good and excellent quality embryos is one of the key factors for achieving pregnancy using ART [2]. Predicting the amount of good-quality embryos would allow us to optimize patient preparation and select the best management option for the embryological stage. Currently specialists are actively searching for embryo quality markers based on various data. This data includes metabolomic, proteomic, transcriptomic semen parameters, follicular fluid, and embryo culture medium [3]. At the same time, the impact of semen microbiota on the ART results, as well as on the quality of obtained embryos, requires further study.

IVF is performed in non-sterile conditions [4]. Despite meticulously following aseptic measures, at most we are able to decrease the level of microbial contamination in IVF labs and in embryo cultures. Gametes (semen and oocytes) used for culturing embryos usually come from sources containing bacteria in most cases [5]. According to molecular genetic analyses, semen microbiota can be represented by complex microbial communities. These communities are made up of different bacterial genera and phyla, including obligate and facultative anaerobic bacteria, even in patients without inflammation and with normal semen parameters [6–8]. There is a correlation between detecting specific groups of opportunistic microorganisms (OMs) in semen samples and the decrease of semen parameters [9, 10].

Excluding pathogens causing sexually transmitted infections (STIs) in urethral or semen samples is currently the only stage of preparing male patients for the ART programs [11]. Presence of other microorganisms, which could be both, the cause of subclinical inflammation in the urogenital tract (UGT) and the cause of ART protocol failures, is not tested.

Bacterial contamination during embryo culture is a serious problem faced in all IVF laboratories [12, 13]. According to previous reports, the frequency of bacterial contamination is less than 1%, however, its occurrence could lead to bad quality embryos, as well as to embryonic demise, thus to the ART treatment failure.

Semen microbiota is considered one of the main sources of bacterial contamination for culture media [12]. Despite meticulous processing, the obtained semen sample still contains microorganisms that could lead to contamination of the embryo culture medium. In classic IVF, oocytes are co-cultured with the processed semen for 16–20 hours in a CO₂ incubator at a temperature of 37 °C. Such conditions are favorable for the development of microorganisms, primarily for obligate anaerobes. As a result, media may contain toxic bacterial metabolites. Negative effects of bacterial toxins can cause embryo cell fragmentation and embryonic death [13].

The effect of semen microbiota on the development of embryos should be evaluated more carefully in order to develop adequate measures to prevent unsuccessful outcomes of the embryological stage of ART.

The aim of this study was to develop a mathematical model for predicting the quality of the obtained embryos based on the results of the semen microbiota assessment in normozoospermia.

METHODS

Research design

A single-center cohort retrospective study included an assessment of the semen parameters and semen microbiota

of 127 men who entered into the ART programs at «Garmonia» Medical Center (Yekaterinburg, Russia) from 2020 to 2021. The embryology key performance indicators were evaluated: fertilization rate, blastocyst development rate, and good and excellent quality blastocyst (with maximum potential for implantation) development rate.

Inclusion and exclusion criteria

Inclusion criteria: patient age 19–51 years; semen parameters meet the criteria of the normozoospermia; fertilization of eggs by classic IVF; consent to participate in the study; age of women 22–40 years; absence of genetic diseases in patients and their relatives. The study included programs with fresh oocytes using classic IVF. Exclusion criteria: use of unfrozen oocytes for fertilization; oocyte fertilization by intracytoplasmic semen injection (ICSI); clinical manifestations of UGT infectious and inflammatory diseases; STIs; intake of hormonal, antibacterial drugs during the last three months, genetic diseases in patients or their relatives; semen volume less than 2 ml; refusal of patients to participate in the study.

ART embryological stage

Oocyte-cumulus complexes were placed in the Flushing medium (Origio; Denmark). Sequential Fert medium (Origio; Denmark) was used for oocyte fertilization. After fertilization evaluation, the zygotes were placed in the SAGE 1-Step medium (Origio; Denmark), in which the embryos were cultured until day 5.

To prepare semen samples, SupraSperm (Origio; Denmark) density gradient sedimentation method was used, then the spermatozoa were washed twice in the SpermPrep buffer (Origio; Denmark), after which the "swim-up" method was used.

Assessment of embryo morphology

The quality of developing zygotes and embryos was individually assessed under a microscope approximately 18, 72 and 96 hours after fertilization. Embryo morphological evaluation was performed on the 5th day of development from the moment of fertilization.

Embryos of excellent and good quality on the 5th day of cultivation had the following morphological characteristics: adequate amount of densely packed cells in the intracellular mass, the trophectoderm contains many cells that have formed a dense epithelium; the blastocoele occupies more than 80% of the embryo volume. The efficiency of the ART embryological stage was considered acceptable when at least 40% of blastocysts of good and excellent quality (good-quality blastocyst development rate — GBDR) from the total number of fertilized eggs were obtained: GBDR ≥ 40% [14].

Depending on the proportion of blastocysts of good and excellent quality formed at the embryological stage, patients were divided into two groups: the first included 57 patients with GBDR ≥ 40%, the second had 70 patients (GBDR < 40%).

Research methods

In both groups controlled ovarian hyperstimulation was initiated according to a short protocol using antagonists of recombinant and/or urinary gonadotropins at a daily dose of 150–300 IU. Human chorionic gonadotropin was used as an ovulation trigger 34–36 hours before the puncture. Follicle aspiration was performed under intravenous anesthesia.

Table 1. The detection rate of specific groups of microorganisms quantities exceeding the threshold value*

Groups of microorganisms	Detection rate				Significance <i>p</i>
	Group 1 (<i>n</i> = 57)		Group 2 (<i>n</i> = 70)		
	<i>n</i>	%	<i>n</i>	%	
<i>Lactobacillus</i> spp.	17	29.8	11	15.7	0.084
Gram-positive facultative anaerobes	24	42.1	23	32.9	0.356
<i>Staphylococcus</i> spp.	6	10.5	3	4.3	0.297
<i>Streptococcus</i> spp.	7	12.3	13	18.6	0.463
<i>Corynebacterium</i> spp.	21	36.8	16	22.9	0.116
Gram-negative facultative anaerobes	0	0	11	15.7	0.001
<i>Haemophilus</i> spp.	0	0	10	14.3	0.002
<i>Pseudomonas aeruginosa</i> / <i>Ralstonia</i> spp. / <i>Burkholderia</i> spp.	0	0	1	1.4	1
Obligate anaerobes	35	61.4	41	58.6	0.856
<i>G.vaginalis</i>	8	14	17	24.3	0.181
<i>Megasphaera</i> spp. / <i>Veillonella</i> spp. / <i>Dialister</i> spp.	10	17.5	18	25.7	0.291
<i>Sneathia</i> spp. / <i>Leptotrichia</i> spp. / <i>Fusobacterium</i> spp.	4	7	5	7.1	1
<i>Bacteroides</i> spp. / <i>Porphyromonas</i> spp. / <i>Prevotella</i> spp.	14	24.6	24	34.3	0.25
<i>Peptostreptococcus</i> spp. / <i>Parvimonas</i> spp.	8	14	11	15.7	1
<i>Anaerococcus</i> spp.	17	29.8	14	20	0.219
<i>Eubacterium</i> spp.	30	52.6	29	41.4	0.217
<i>A.cluster</i>	4	7	7	10	0.753
<i>Enterobacteriaceae</i> spp. / <i>Enterococcus</i> spp.	8	14	6	8.6	0.398
Mycoplasma	10	17.5	11	15.7	0.814
<i>U. urealyticum</i>	2	3.5	4	5.7	0.69
<i>U. parvum</i>	7	12.3	7	10	0.779
<i>M. hominis</i>	2	3.5	2	2.9	1

Note: * — for *U. urealyticum*, *U. parvum*, *M. hominis* groups, threshold values are > 0, for other groups of microorganisms $\geq 10^3$ GE/ml.

Patient preparation and semen sampling were carried out in accordance with WHO recommendations on the collection of semen for microbiological studies (paragraph 2.2.4 of the WHO Guidelines) [15]. Ejaculatory abstinence for the period of 3–4 days was mandatory. Prior to semen collection, patients urinated and washed their external genitalia. Semen was collected through masturbation into a sterile container. Native semen was used for the study. The analysis of semen concentration and motility was carried out using the Biola AFS-500 analyzer ("Biola"; Russia). The morphology of spermatozoa was evaluated in stained preparations with a 1000x microscope magnification using an immersion lens. The LeucoScreen test (FertiPro; Belgium) was used to count peroxidase-positive leukocytes. The normozoospermia criteria were met by samples with semen volume of at least 1.5 ml, spermatozoa concentration of at least 15 million/ml, a total mobility of at least 40% or progressive mobility of at least 32%, normal spermatozoa morphology of at least 4%, a leukocyte count of no more than 1 million/ml, and the absence of increased viscosity. Semen microbial composition was determined using a quantitative real-time PCR (qPCR) using the Androflor real-time PCR detection kit (DNA Technology; Russia) and the DTprime detection thermal cycler (DNA-Technology; Russia).

The material for the study (0.5 ml of native semen) was collected on the day of oocyte fertilization in an Eppendorf tube containing 1 ml of buffer solution (PREP-PK kit; DNA Technology;

Russia). DNA was isolated using PREP-NA extraction kit ("DNA Technology"; Russia). qPCR was performed according to the manufacturer's instructions.

Once the amplification is over, the special software (DNA Technology; Russia) automatically calculates the quantities (expressed in genome equivalents per 1 ml (GE/ml)) of the total bacterial load (TBL) and each of the detected OM in a given sample. Positive signals for the target microorganisms were detected before the 35th amplification cycle, which is equivalent to the microbial load of at least 10^3 GE/ml and more. The proportions of individual species and groups of bacteria were calculated relative to the sum of all bacteria detected in the sample. The Androflor real-time PCR detection kit is designed to determine TBL and the level of 19 OM groups (*Lactobacillus* spp., *Staphylococcus* spp., *Streptococcus* spp., *Corynebacterium* spp., *Haemophilus* spp., *Pseudomonas aeruginosa* / *Ralstonia* spp. / *Burkholderia* spp., *Enterobacteriaceae* / *Enterococcus* spp., *Gardnerella vaginalis* (*G. vaginalis*), *Eubacterium* spp., *Sneathia* spp. / *Leptotrichia* spp. / *Fusobacterium* spp., *Megasphaera* spp. / *Veillonella* spp. / *Dialister* spp., *Bacteroides* spp. / *Porphyromonas* spp. / *Prevotella* spp., *Anaerococcus* spp., *Peptostreptococcus* spp., *Atopobium cluster* (*A. cluster*), *Mycoplasma hominis* (*M. hominis*), *Ureaplasma urealyticum* (*U. urealyticum*), *Ureaplasma parvum* (*U. parvum*), *Candida* spp.), the presence of obligate pathogens (*Neisseria gonorrhoeae*, *Chlamydia*

Table 2. The average quantities of *Haemophilus spp.* and GNFA in groups 1 and 2 and the accuracy of these indicators in predicting a favorable outcome of the ART embryological stage

Microorganism group	Median (5 th and 95 th percentile)		<i>p</i>	The AUC value (95% CI)
	Group 1	Group 2		
<i>Haemophilus spp.</i> , GE/ml	0 (0–0)	0 (0–103.8)	0.003	0.571 (0.472–0.671)
GNFA, GE/ml	0 (0–0)	0 (0–103.8)	0.002	0.579 (0.479–0.678)

trachomatis, *Mycoplasma genitalium* and *Trichomonas vaginalis*); and the level of human genomic DNA (as a control of taking biological material).

Methods of statistical analysis

Statistical data processing was carried out using R-version 4.2.2 (build 2022-10-31) and StatPlus:mac 8.0.3 (AnalystSoft; USA). The normality of the distribution for tested parameters was checked by the Shapiro–Wilk test. The median with 5th and 95th percentiles was indicated to describe the distribution of variables. The Mann–Whitney U test was applied to compare the medians between groups 1 and 2, whereas the two-tailed Fisher's exact test was used to compare the frequencies between the groups. All differences were considered statistically significant at $p < 0.05$.

To develop the regression equation, which formed the basis of the prognostic model for obtaining at least 40% of embryos of good and excellent quality, the method of discriminant analysis with the calculation of canonical discriminant function coefficients (CDFC) was used. ROC analysis was performed to evaluate the accuracy of the proposed predictive model. The optimal cutoff value was determined by the Youden's index.

RESULTS

Clinical characteristics of the patients

Initially, the groups were compared by age, height, weight and patient's medical history. The groups were comparable by age of men (35.0 (28.8–43.2) vs. 34.0 (28.5–45.0) years old in group 1 and 2, respectively; $p = 0.664$) and age of women (34.0 (26.0–40.0) vs. 34.0 (28.0–40.0) years old in group 1 and 2, respectively; $p = 0.507$). In terms of body mass index, the differences were not significant ($p > 0.05$). There was no significant difference in medical history (cardiovascular pathology, diseases of the urinary or respiratory tract, or nervous system, endocrinopathies, pathology of the gastrointestinal tract and autoimmune diseases) between the two groups ($p > 0.05$). Thus, the groups were clinically comparable.

Embryological stage data

The number of MII mature oocytes was 559 and 606 in group 1 and group 2, respectively. At the same time, the average number of oocytes obtained during puncture in patients of groups 1 and 2 did not differ (medians were 9 and 8, $p = 0.250$). As a result of IVF, 458 zygotes were obtained in group 1 and 442 in group 2, the average number of zygotes obtained did not differ between groups (medians were 6 and 5.5 for groups 1 and 2, respectively; $p = 0.207$). The fertilization rate, the blastulation rate and the GBDR were calculated for each patient. The fertilization rate did not differ in group 1 and group 2 patients (medians were 85.7% and 80.0%, respectively; $p = 0.471$), while significant differences were found in the blastulation rate and GBDR. The blastulation rate was 75.0% in group 1 and 37.5% in group 2 ($p < 0.001$); the GBDR was 72.7% in group 1 and 27.7% in group 2 ($p < 0.001$).

Analysis of semen microbial composition

Bacterial DNA (TBL) was absent or detected in an amount of less than 10^3 GE/ml in 5 (8.8%) of 57 samples of group 1 and 5 (7.1%) of 70 samples of group 2 ($p = 0.752$). In positive samples, from 1 to 13 groups of microorganisms were simultaneously detected in above the threshold values. The detection rate of specific groups of bacteria in above the threshold values is shown in Table 1.

Haemophilus spp. and, as a result, the group of gram-negative facultative anaerobes (GNFA) to which these bacteria belong, were detected less frequently in the group 1 samples. Detection rate of other groups of OMs did not significantly differ between groups 1 and 2. Taking into account statistically significant differences in the detection rates of *Haemophilus spp.* and GNFA between groups 1 and 2, we tried to assess quantitative differences for these microorganism groups and their accuracy in predicting a favorable outcome of the ART embryological stage, but received the unsatisfactory results (Table 2).

None of the individual semen microbiota parameters of demonstrated acceptable accuracy in predicting a favorable outcome of the ART embryological stage. Due to the variety of combinations in which the individual groups of OMs were found, it was decided to apply discriminant analysis to calculate a prognostic index that takes into account all significant parameters of semen microbiota.

Discriminant analysis

To predict GBDR $\geq 40\%$ for patients whose semen parameters met the criteria of normozoospermia, we developed a prognostic index EGO-Pro-N (Embryos of GOod and Excellent quality Prognosis in Normozoospermia)

To develop a prognostic index a discriminant analysis was carried out in the obtained matrices of laboratory parameters for patients of the analyzed groups.

To determine the contribution of each individual microorganism to forming the probability of obtaining GBDR $\geq 40\%$ and to develop a prognostic index, we ranked the parameters using the calculation of the CDFC.

The EGO-Pro-N index was calculated using the following formula:

$$\text{EGO-Pro-N} = 0.22 \times X_1 - 0.26 \times X_2 - 0.59 \times X_3 + 0.25 \times X_4 + 0.26 \times X_5 + 0.21 \times X_6 - 0.4 \times X_7 + 0.15 \times X_8 + 0.09 \times X_9 + 0.15 \times X_{10} - 0.25 \times X_{11} - 0.33 \times X_{12} - 0.17 \times X_{13} + 0.51 \times X_{14} + 0.9 \times X_{15} - 0.28 \times X_{16} - 0.47, \text{ where}$$

X_1 — total bacterial load (TBL),

X_2 — *Lactobacillus spp.*,

X_3 — *Staphylococcus spp.*,

X_4 — *G. vaginalis*,

X_5 — *Megasphaera spp.* / *Veillonella spp.* / *Dialister spp.*,

X_6 — *Sneathia spp.* / *Leptotrichia spp.* / *Fusobacterium spp.*,

X_7 — *U. urealyticum*,

X_8 — *U. parvum*,

X_9 — *A. cluster*,

X_{10} — *Bacteroides spp.* / *Porphyromonas spp.* / *Prevotella spp.*,

X11 — *Anaerococcus* spp.,
 X12 — *Peptostreptococcus* spp. / *Parvimonas* spp.,
 X13 — *Eubacterium* spp.,
 X14 — *Haemophilus* spp.,
 X15 — *P. aeruginosa* / *Ralstonia* spp. / *Burkholderia* spp.,
 X16 — *Enterobacteriaceae* spp. / *Enterococcus* spp.

If the EGO-Pro-N value is > 0.212 , it can be predicted that the probability of $\text{GBDR} \geq 40\%$ is low, if $\text{EGO-Pro-N} \leq 0.212$, it is high.

The average value of EGO-Pro-N in groups 1 and 2 was -0.470 (-2.430 ; -0.580) and 0.365 (-0.933 ; -2.260), respectively. The differences are statistically significant ($p < 0.001$). Graphically, the EGO-Pro-N index value is shown in Fig. 1.

The ROC curve for the EGO-Pro-N index is shown in Fig. 2. The area under the curve (AUC) value is 0.777 (95% CI: 0.670 – 0.856), which is considered as acceptable discrimination in predicting models.

The optimal cutoff value for the EGO-Pro-N index was 0.212 . This threshold made it possible to predict the production of $\text{GBDR} \geq 40\%$ with a sensitivity of 71.9% and a specificity of 70.0% with 70.9% overall accuracy (Table 3).

DISCUSSION

The present study included couples who participated in ART protocols, and whose semen parameters met the criteria of normozoospermia. According to current clinical guidelines, the presence of STI pathogens was excluded in both partners at the stage of preconception care [11]. Such semen samples are considered ideal for IVF, and in routine clinical practice, an extended study of semen microbiota is not carried out. Our study showed that most of the used semen samples contained bacterial DNA in an amount of at least 10^3 GE/ml. Up to 13 groups of microorganisms in various combinations were simultaneously identified in positive samples. The presence of bacteria in semen has been shown previously in numerous studies [4, 6, 8, 10, 16], our observations once again confirm this fact.

We were interested in semen microbiota in terms of its potentially negative impact on the outcome of the ART embryological stage. In this study we were able to demonstrate the difference in semen microbiota composition between the samples with acceptable proportion of good quality blastocysts on the 5th day ($\text{GBDR} \geq 40\%$) and those with insufficient number of embryos. The latter group was characterized by the presence of GNFA (mainly *Haemophilus* spp.). At the same time, in cases where the efficacy of the embryological stage was satisfactory, there was a tendency to more frequent detection of *Lactobacillus* spp. and *Corynebacterium* spp., but the difference was not significant.

Given these observations, we made an attempt to develop prognostic model based on the semen microbiota parameters, which could be used to assess its quality even at the stage of preconception care. Attempts to predict the effectiveness of the embryological stage of ART have been carried out repeatedly using data from proteomic, transcriptomic and metabolomic analyses of semen, follicular fluid and culture media [2, 3]. According to some data, 93 types of semen proteins can be functionally associated with the formation of a zygote and the next stages of embryo development at the embryological stage of ART [16]. Potential protein markers in semen have been identified that could predict the outcome of in vitro ART in couples with idiopathic infertility [17]. The presence of Alphaproteobacteria in semen samples with normozoospermia reduced the likelihood of obtaining good and excellent quality

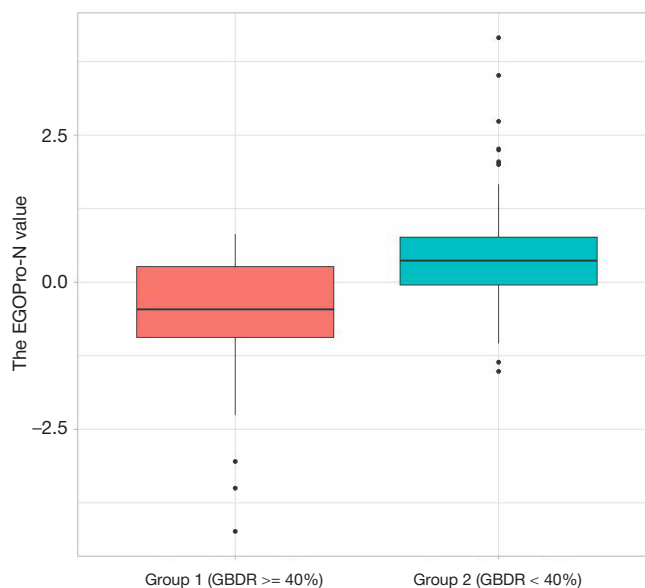


Fig. 1. The EGO-Pro-N index values in groups 1 and 2

embryos [4]. However, these observations did not lead to the development appropriate predictive models.

The developed mathematical model with the calculation of the prognostic index EGO-Pro-N can be used at the stage of preconception care before the ART procedure, especially in cases when the expected number of oocytes is low, and each embryo of good and excellent quality is of great value.

It is important to clarify that bacterial contamination of culture media with embryos was registered only in cases of oocyte fertilization using classic IVF. In ICSI programs, when a single spermatozoon is injected into an oocyte using micro-tools, such cases have not been registered [18]. This is probably due to the fact that in the case of ICSI, fewer viable bacteria may be introduced into the culture medium. Thus, in order to increase the effectiveness of the IVF program, in case of a negative prognosis for obtaining a sufficient number of good-quality embryos, ICSI may be recommended.

CONCLUSIONS

The developed prognostic model makes it possible to predict the acceptable GBDR based on semen microbiota investigation in semen samples used for IVF. The semen microbiota evaluation in patients planning to undergo the ART procedure

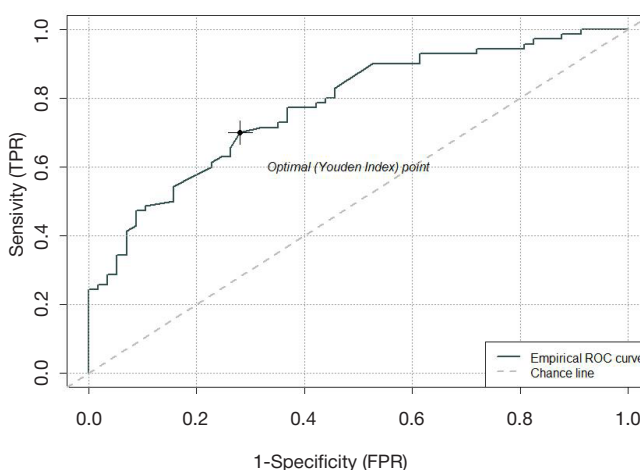


Fig. 2. ROC curve for the EGO-Pro-N index

Table 3. Sensitivity and specificity of the EGO-Pro-N index (classification matrix)

Group/ Prognosis	1	2	Total	The number of correct prognoses, %
1	41	16	57	71.9
2	21	49	70	70
Total	62	65	127	70.9

can be performed at the stage of preconception care, including the cases when the semen parameters meet the criteria of normozoospermia. The use of the proposed EGO-Pro-N index justifies the development of an individual treatment plan for

the ART patients to obtain the optimal number of high-quality embryos. The proposed method can be used in routine clinical practice, it does not require significant material costs and organizational efforts.

References

- Korsak VS, Smirnova AA, Shurygina OV. Registr VRT Obshherossiyskoj obshhestvennoj organizacii «Rossijskaya associaciya reprodukcii cheloveka». Otchet za 2020 god. Problemy reprodukcii. 2022; 28 (6): 12–27. Russian.
- Irina AA, Kalinina II, Troshina TG, Ilin KA, Boltovskaya MN, Stepanova II, i dr. Follikulyarnaya zhidkost' kak sreda, opredelyayushchaya kachestvo oocita i ishod programm VRT (obzor literatury). Problemy reprodukcii. 2008; 14 (4): 27–39. Russian.
- Valiaxmetova EhZ, Kulakova EV, Skibina YuS, Gryaznov AYU, Syssoeva AP, Makarova NP, i dr. Neinvazivnoe testirovanie preimplantacionnyx ehmbriionov cheloveka in vitro kak sposob prognozirovaniya ishodov programm. Russian. ehkstrakorporal'nogo oplodotvoreniya. Akusherstvo i ginekologiya. 2021; 5: 5–16.
- Štšepetova J, Baranova J, Simm J, Parm Ü, Rööp T, Sokmann S, et al. The complex microbiome from native semen to embryo culture environment in human in vitro fertilization procedure. Reproductive Biology and Endocrinology. 2020; 18: 1–13.
- Franasiak JM, Scott Jr RT. Reproductive tract microbiome in assisted reproductive technologies. Fertility and sterility. 2015; 104 (6): 1364–71.
- Voroshilina ES, Zornikov DL, Ivanov AV, Pochernnikov DG, Panacheva EA. Semen microbiota: cluster analysis of real-time PCR data. Bulletin of RSMU. 2020; (5): 62–9. DOI: 10.24075/brsmu.2020.064.
- Hou D, Zhou X, Zhong X, Settles ML, Herring, Wang SL, et al. Microbiota of the seminal fluid from healthy and infertile men. Fertility and sterility. 2013; 100 (5): 1261–9.
- Weng SL, Chiu CM, Lin FM, Huang WC, Liang C, Yang T, et al. Bacterial communities in semen from men of infertile couples: metagenomic sequencing reveals relationships of seminal microbiota to semen quality. PloS one. 2014; 9 (10): e110152.
- Pagliuca C, Cariati F, Bagnulo F, Scaglione E, Carotenuto C, Farina F et al. Microbiological evaluation and sperm DNA fragmentation in semen samples of patients undergoing fertility investigation. Genes. 2021; 12 (5): 654.
- Baud D, Pattaroni C, Vulliamoz N, Castella V, Marsland BJ, Stojanov M. Sperm microbiota and its impact on semen parameters. Frontiers in microbiology. 2019; 10: 234.
- Prikaz Ministerstva zdravooxraneniya RF ot 31 iyulya 2020 g. N 803n «O poryadke ispol'zovaniya vspomogatel'nyx reproduktivnyx tekhnologij, protivopokazaniyax i ogranicheniyax k ix primeneniyu». Russian.
- Lin LL, Guu HF, Yi YC, Kung HF, Chang JC, Chen YF, et al. Contamination of ART culture Media—The role of semen and strategies for prevention. Taiwanese Journal of Obstetrics and Gynecology. 2021; 60 (3): 523–5.
- Li R, Du F, Ou S, Ouyang N, Wang W. A new method to rescue embryos contaminated by bacteria. F&S Reports. 2022; 3 (2): 168–71.
- The Vienna consensus: report of an expert meeting on the development of ART laboratory performance indicators. Reproductive BioMedicine Online. 2017; 35 (5): 494–510.
- WHO. WHO Laboratory Manual for the Examination and Processing of Human Semen, 5th ed.; WHO Press, World Health Organization: Geneva, Switzerland. 2010.
- Jodar M, Attardo-Parrinello C, Soler-Ventura A et al. Sperm proteomic changes associated with early embryo quality after ICSI. Reprod Biomed Online. 2020; 40 (5): 700–10.
- Castillo J, Jodar M, Oliva R. The contribution of human sperm proteins to the development and epigenome of the preimplantation embryo. Human Reproduction Update. 2018; 24 (5): 535–55.
- Peter MM Kastrop, Lia AM de Graaf-Miltburg, Dagmar R Gutknecht, Sjerp M Weima. Microbial contamination of embryo cultures in an ART laboratory: sources and management. Human Reproduction. 2007; 22 (8): 2243–48.

Литература

- Корсак В. С., Смирнова А. А., Шурьгина О. В. Регистр ВРТ Общероссийской общественной организации «Российская ассоциация репродукции человека». Отчет за 2020 год. Проблемы репродукции. 2022; 28 (6): 12–27.
- Ильина А. А., Калинина И. И., Трошина Т. Г., Ильин К. А., Болтовская М. Н., Степанова И. И. и др. Фолликулярная жидкость как среда, определяющая качество ооцита и исход программ ВРТ (обзор литературы). Проблемы репродукции. 2008; 14 (4): 27–39.
- Валиахметова Э. З., Кулакова Е. В., Скибина Ю. С., Грязнов А. Ю., Сысоева А. П., Макарова Н. П. и др. Неинвазивное тестирование преимплантационных эмбрионов человека in vitro как способ прогнозирования исходов программ экстракорпорального оплодотворения. Акушерство и гинекология. 2021; 5: 5–16.
- Štšepetova J, Baranova J, Simm J, Parm Ü, Rööp T, Sokmann S, et al. The complex microbiome from native semen to embryo culture environment in human in vitro fertilization procedure. Reproductive Biology and Endocrinology. 2020; 18: 1–13.
- Franasiak JM, Scott Jr RT. Reproductive tract microbiome in assisted reproductive technologies. Fertility and sterility. 2015; 104 (6): 1364–71.
- Ворошилина Е. С., Зорников Д. Л., Иванов А. В., Почерников Д. Г., Паначева Е. А. Микробиота эякулята: кластерный анализ результатов, полученных при исследовании методом ПЦР-РВ. Вестник Российского государственного медицинского университета. 2020; (5): 66–73.
- Hou D, Zhou X, Zhong X, Settles ML, Herring, Wang SL, et al. Microbiota of the seminal fluid from healthy and infertile men. Fertility and sterility. 2013; 100 (5): 1261–9.
- Weng SL, Chiu CM, Lin FM, Huang WC, Liang C, Yang T, et al. Bacterial communities in semen from men of infertile couples: metagenomic sequencing reveals relationships of seminal microbiota to semen quality. PloS one. 2014; 9 (10): e110152.

9. Pagliuca C, Cariatì F, Bagnulo F, Scaglione E, Carotenuto C, Farina F et al. Microbiological evaluation and sperm DNA fragmentation in semen samples of patients undergoing fertility investigation. *Genes*. 2021; 12 (5): 654.
10. Baud D, Pattaroni C, Vulliemoz N, Castella V, Marsland BJ, Stojanov M. Sperm microbiota and its impact on semen parameters. *Frontiers in microbiology*. 2019; 10: 234.
11. Приказ Министерства здравоохранения РФ от 31 июля 2020 г. N 803н «О порядке использования вспомогательных репродуктивных технологий, противопоказаниях и ограничениях к их применению».
12. Lin LL, Guu HF, Yi YC, Kung HF, Chang JC, Chen YF, et al. Contamination of ART culture Media—The role of semen and strategies for prevention. *Taiwanese Journal of Obstetrics and Gynecology*. 2021; 60 (3): 523–5.
13. Li R, Du F, Ou S, Ouyang N, Wang W. A new method to rescue embryos contaminated by bacteria. *F&S Reports*. 2022; 3 (2): 168–71.
14. The Vienna consensus: report of an expert meeting on the development of ART laboratory performance indicators. *Reproductive BioMedicine Online*. 2017; 35 (5): 494–510.
15. Руководство ВОЗ по исследованию и обработке эякулята человека, пятое издание. Москва, 2012.
16. Jodar M, Attardo-Parrinello C, Soler-Ventura A et al. Sperm proteomic changes associated with early embryo quality after ICSI. *Reprod Biomed Online*. 2020; 40 (5): 700–10.
17. Castillo J, Jodar M, Oliva R. The contribution of human sperm proteins to the development and epigenome of the preimplantation embryo. *Human Reproduction Update*. 2018; 24 (5): 535–55.
18. Peter MM Kastrop, Lia AM de Graaf-Miltenburg, Dagmar R Gutknecht, Sjerp M Weima. Microbial contamination of embryo cultures in an ART laboratory: sources and management. *Human Reproduction*. 2007; 22 (8): 2243–48.

GENETIC CHARACTERIZATION OF *AEROCOCCUS* SP. 1KP-2016 STRAIN ISOLATED FROM A PATIENT WITH BLOODSTREAM INFECTION

Chaplin AV^{1,2}✉, Chagina IA¹, Pimenova AS¹, Gadua NT¹, Kargaltseva NM¹, Borisova OYu^{1,2}, Donskikh EE², Kafarskaya LI²

¹ Gabrichevsky Research Institute for Epidemiology and Microbiology, Moscow, Russia

² Pirogov Russian National Research Medical University, Moscow, Russia

Aerococcus genus bacteria are often associated with human urinary tract and bloodstream infections. The *Aerococcus* sp. 1KP-2016 strain isolated from the buffy coat had the 16S rRNA sequence that was a 98.7% (and less) match with the previously described members of this genus. The purpose of this study was to perform whole genome sequencing of *Aerococcus* 1KP-2016 followed by phylogenetic reconstruction. We have shown that *Aerococcus* 1KP-2016 belongs to the new species of the *Aerococcus* genus that is closest to *Aerococcus viridans* and *Aerococcus urinaeequi*. The genomic sequence, which consists of 2.042 million bps with GC content at 38.5%, was deposited in the DBJ/EMBL/GenBank under identifier NEEY000000000.

Keywords: *Aerococcus*, bloodstream infection, buffy coat (blood leukocyte layer), whole genome sequencing, phylogenetic analysis

Author contribution: AV Chaplin — phylogenetic analysis, data analysis, manuscript authoring; IA Chagina, AS Pimenova, NT Gadua — microbiological studies, manuscript authoring; NM Kargaltseva, LI Kafarskaya — literature analysis, manuscript authoring; OYu Borisova — molecular genetic studies, data analysis, literature analysis, manuscript authoring; EE Donskikh — data analysis, literature analysis, manuscript authoring.

Compliance with ethical standards: the study was approved by the Ethics Committee of the Gabrichevsky Research Institute for Epidemiology and Microbiology (Minutes #28 of November 18, 2014); the patient signed a voluntary consent to participation in the study.

✉ **Correspondence should be addressed:** Andrey Viktorovich Chaplin
10 Admiral Makarov str., Moscow, 125212, Russia; okolomedik@gmail.co

Received: 22.03.2023 **Accepted:** 16.04.2023 **Published online:** 25.04.2023

DOI: 10.24075/brsmu.2023.012

ГЕНЕТИЧЕСКАЯ ХАРАКТЕРИСТИКА ШТАММА *AEROCOCCUS* SP. 1KP-2016, ВЫДЕЛЕННОГО ОТ ПАЦИЕНТА С ИНФЕКЦИЕЙ КРОВотоКА

А. В. Чаплин^{1,2}✉, И. А. Чагина¹, А. С. Пименова¹, Н. Т. Гадуа¹, Н. М. Каргальцева¹, О. Ю. Борисова^{1,2}, Е. Е. Донских², Л. И. Кафарская²

¹ Московский научно-исследовательский институт эпидемиологии и микробиологии имени Г. Н. Габричевского, Москва, Россия

² Российский национальный исследовательский медицинский университет имени Н. И. Пирогова, Москва, Россия

Бактерии рода *Aerococcus* часто ассоциированы с инфекциями мочевыводящих путей и кровотока у человека. Штамм *Aerococcus* sp. 1KP-2016, выделенный из лейкоцитарного слоя крови, обладал последовательностью 16S рРНК, совпадающей на 98,7% и менее с ранее описанными представителями данного рода. Целью работы было провести полногеномное секвенирование *Aerococcus* 1KP-2016 с последующей филогенетической реконструкцией. Показано, что *Aerococcus* 1KP-2016 является представителем нового вида рода *Aerococcus*, наиболее близкого к *Aerococcus viridans* и *Aerococcus urinaeequi*. Геномная последовательность, имеющая длину 2,042 млн п.н. и GC-состав 38,5%, депонирована в DBJ/EMBL/GenBank под идентификатором NEEY000000000.

Ключевые слова: *Aerococcus*, инфекция кровотока, лейкоцитарный слой крови, полногеномное секвенирование, филогенетический анализ

Вклад авторов: А. В. Чаплин — филогенетический анализ, анализ данных, подготовка рукописи; И. А. Чагина, А. С. Пименова, Н. Т. Гадуа — микробиологические исследования, подготовка рукописи; Н. М. Каргальцева, Л. И. Кафарская — анализ литературы, подготовка рукописи; О. Ю. Борисова — молекулярно-генетические исследования, анализ данных, анализ литературы, подготовка рукописи; Е. Е. Донских — анализ данных, анализ литературы, подготовка рукописи.

Соблюдение этических стандартов: исследование одобрено этическим комитетом ФБУН МНИИЭМ им. Г. Н. Габричевского Роспотребнадзора (протокол № 28 от 18 ноября 2014 г.); от пациента получено добровольное письменное согласие на участие в исследовании.

✉ **Для корреспонденции:** Андрей Викторович Чаплин
ул. Адмирала Макарова, д. 10, г. Москва, 125212, Россия; okolomedik@gmail.com

Статья получена: 22.03.2023 **Статья принята к печати:** 16.04.2023 **Опубликована онлайн:** 25.04.2023

DOI: 10.24075/vrgmu.2023.012

The *Aerococcus* genus was first described in 1953, with the first studied representative thereof being *Aerococcus viridans* isolated from the air and street dust [1]. Currently, we know of eight species comprising the *Aerococcus* genus: *A. viridans*, *A. urinae*, *A. sanguinicola*, *A. christensenii*, *A. urinaehominis*, *A. urinaeequi*, *A. suis*, *A. vaginalis* [2].

Aerococcus bacteria are commonly associated with the urinary tract infection and urosepsis [3]. At the same time, within the last 10 years there were many reports of complications caused by the representatives of this genus, such complications manifesting as bloodstream infection and infective endocarditis, the etiology of which is most often linked to *A. urinae* and *A. sanguinicola* [2, 3]. Moreover, it was established that aerococci can cause invasive infections, such as osteomyelitis, meningitis, septic arthritis, peritonitis, and soft tissue infections,

with isolated *Aerococcus*-like microorganisms and *A. urinae* often assumed to be behind the etiology thereof [2]. Since 1987, 17 cases of bacteremia/septicemia caused by *Aerococcus*-like microorganisms (pure culture isolated from the blood) have been reported in Denmark, with 6 of them being endocarditis cases and 11 — septicemia cases; despite adequate antimicrobial therapy, 7 patients died [4]. Other authors, considering diseases of the urinary system, took isolation of *Aerococcus* in blood culture as an etiological factor of bacteremia [5].

The virulence of *Aerococcus* species is associated with their ability to build biofilms (in particular, on heart valves *in vivo*), form aggregation of platelets, and adhere to surfaces using capsular polysaccharide the presence of which was confirmed by comparative genomic analysis that revealed a wide intraspecific diversity of loci synthesizing it [2, 6, 7].

This study aimed to genetically characterize the *Aerococcus* sp. 1KP-2016 strain isolated from the blood of a patient with a bloodstream infection.

METHODS

We cultivated the *Aerococcus* sp. 1KP-2016 strain under microaerophilic conditions for 24–48 h at $37 \pm 1^\circ\text{C}$ on Columbia agar base (Conda; Spain) with 10% of sheep blood. The cultural and morphological properties of the resulting colonies were uncovered using a SterEO Discovery V12 stereoscopic microscope (Carl Zeiss; Germany) with a PlanApo S 1.0 \times FWD 60 mm lens objective and a PI 10 \times 23 Br foc eyepiece. Gram staining (ZAO ECOlab; Russia) allowed establishing stain-related properties. The stained smears were examined through an Axio Scope A1 light microscope with EC Plan-NEOFLUAR 100 \times 1.3 lens and PI 10 \times 23 Br foc eyepiece (Carl Zeiss; Germany). The biochemical properties of the bacteria were studied with the help of Micro-LA-Test STREPTOtest 16 (Lakhema, Czech Republic), a commercially available biochemical test system, and a catalase test prepared in the laboratory.

As per the guidelines by the European Committee on Antimicrobial Susceptibility Testing (EUCAST), we studied the colonies' susceptibility to antibiotics with the disk diffusion test using the commercial standardized paper disks (HiMedia Laboratories Pvt Limited; India).

The cells were boiled to release the chromosomal DNA. The 16S rRNA gene fragment was amplified as per the generally accepted protocol [8]. The PCR reaction mixture contained 1.5 mM of MgCl_2 , 10 mM of Tris-HCl (pH 8.3), 50 mM of KCl, 0.1 μM of primers 27F (5'-AGAGTTTGATCCTGGCTCAG-3') and 1492R (5'-ACGGYTACCTTGTACGACTT-3'), 200 mM of each nucleoside triphosphate and 1 unit of Taq DNA polymerase (Thermo Fisher Scientific; Lithuania). The amplification was done with 1 μl of the DNA preparation in the total volume of the reaction mixture (25 μl) using the Tertsik amplifier (DNK-Technologiya; Russia). The PCR products were purified and sequenced at ZAO Evrogen (Moscow, Russia) (<http://evrogen.ru/>). To process the results of sequencing, we used the ChromasLite software (Technelysium Pty Ltd, Australia) (for the chromatogram format); the sequences were collated with the EMBL/NCBI (<http://www.ncbi.nlm.nih.gov/nuccore>) international online database using the megablast algorithm.

The genome of the *Aerococcus* sp. 1KP-2016 strain was sequenced using the Ion Proton system (Thermo Fisher Scientific; USA) at Gabrichevsky Research Institute for Epidemiology and Microbiology. The genome was assembled de novo with the help of the SPAdes software [9]. Contest16S [10] and CheckM [11] enabled checking of the assembly for contamination. In the search for CRISPR-Cas systems we relied on CRISPRCasFinder [12], for integrated phage genomes — on PHASTER [13], for antibiotic resistance genes — ResFinder [14].

We used all publicly available genomes of the *Aerococcus* genus from the Refseq database (as of October 4, 2021) for comparative analysis, and *Abiotrophia defectiva* ATCC 49176T as an outgroup. As per the annotations given in the databases, protein-coding regions of the genomes were clustered into groups of orthologs with the help of the ProteinOrtho software (standard settings) [15]. Ultimately, we obtained a conservative part of the proteome consisting of 543 such groups, each containing a single-copy protein-coding gene from each genome. The amino acid sequences of proteins in these groups of orthologs were aligned using MUSCLE [16] and concatenated. RapidNJ algorithm [17] guided the phylogenetic reconstruction based on the resulting concatenate. To calculate the average

nucleotide identity (ANI) between genomes, we applied the ANIb approach and used the JSpeciesWS online service [18]. The ANI data are represented by two values divided by a slash in order to show the differences between mapping of fragments of the first genome onto the second one and second onto the first, respectively. As of the time of writing of this article, the release of the GTDB database, which contains an alternative taxonomy based on a purely phylogenetic approach, was 202 [19].

RESULTS

The *Aerococcus* sp. 1KP-2016 strain was isolated from the buffy coat of blood collected from a patient with a bloodstream infection (36 years old, city of Stavropol) in August 2016; the patient had subfebrile temperature for a long period of time (over a year).

Individual small smooth colonies less than 1 mm in size with uneven edges, a raised center, translucent grayish-white in color, with a small hemolysis zone formed on Columbia agar in 24–48 hours (Fig. 1). Gram-stained smear contained Gram-positive cocci forming tetrads (Fig. 2). Biochemical tests of the isolated culture returned positive for galactosidase, esculin, lactose, trehalose, and negative for catalase, hippurate, phosphatase, leucine, alpha-arginine, urease, mannitol, sorbitol, raffinose, inulin, melibiose, ribose. The culture proved to be resistant to ciprofloxacin, ofloxacin, penicillin, erythromycin, doxycycline, showed intermediate resistance to clindamycin and susceptibility only to imipenem.

The *Aerococcus* sp. 1KP-2016 strain genome assembled to the level of contigs was deposited in the DDBJ/EMBL/GenBank under identifier NEEY000000000; subsequently,

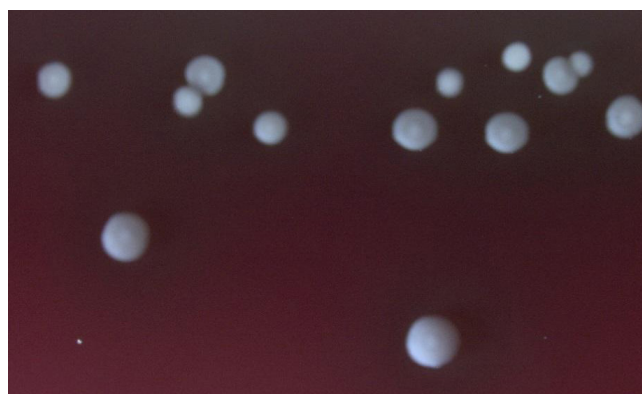


Fig. 1. *Aerococcus* sp. 1KP-2016 colonies on Columbia agar (Stereo Discovery V12 stereomicroscope (Carl Zeiss; Germany))

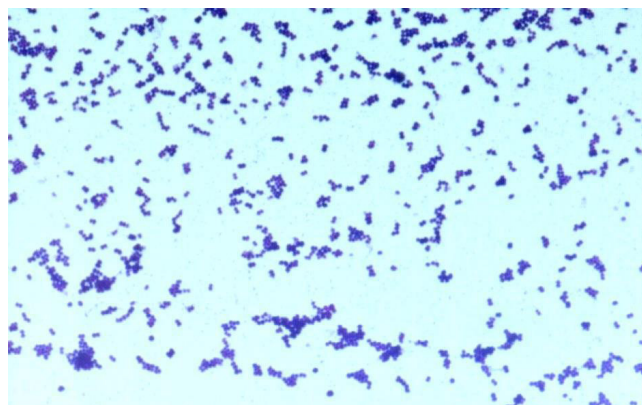


Fig. 2. Micrograph of a Gram-stained smear of *Aerococcus* sp. 1KP-2016 (Axio Scope A1 light microscope, EC Plan-NEOFLUAR 100 — 1.3 lens, PI 10 \times 23 Br foc eyepiece (Carl Zeiss; Germany))

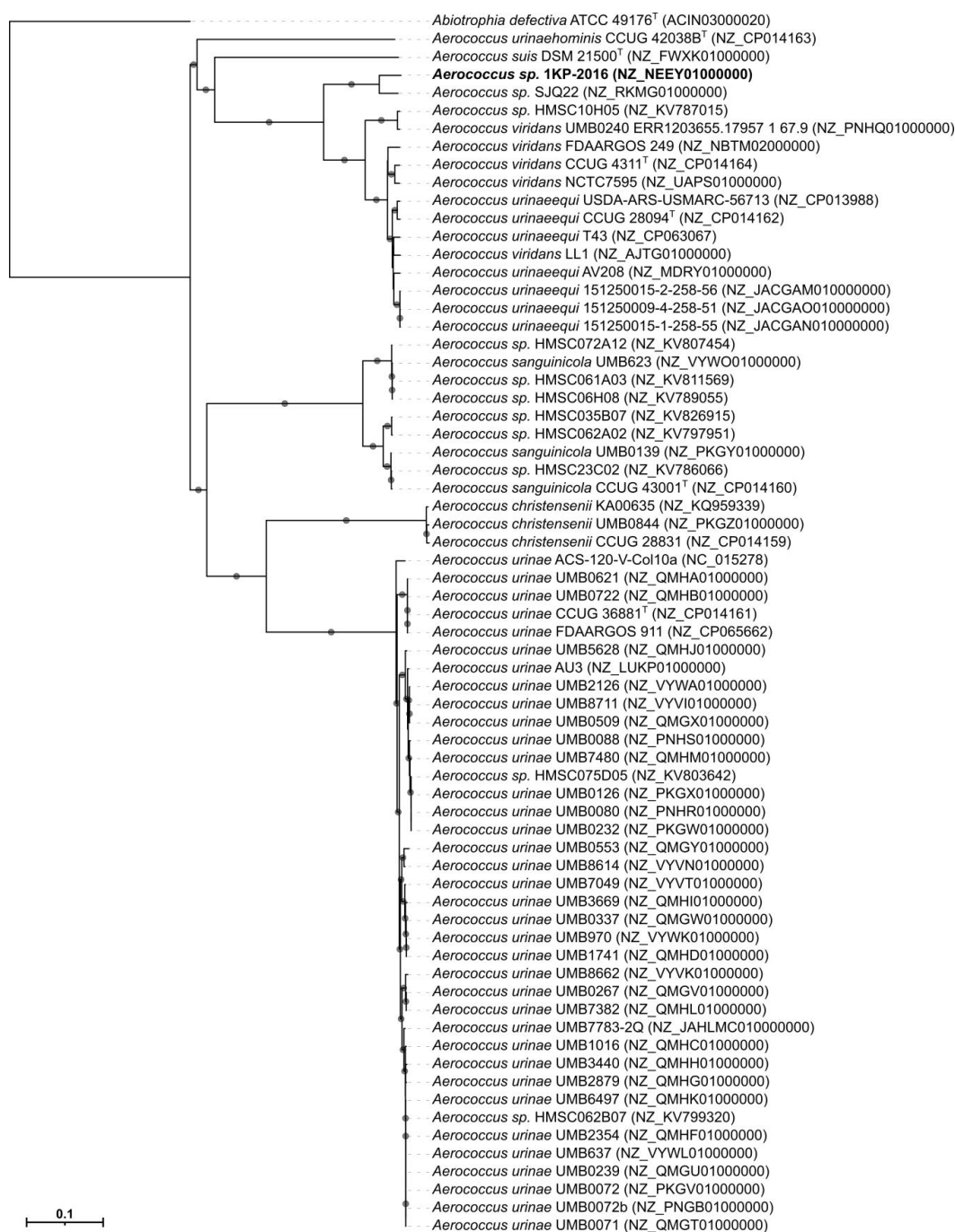


Fig. 3. Phylogenetic tree reconstructed from the sequences of 543 conserved single-copy proteins. The strain described in this work is highlighted in bold. Type strains are marked with a superscript "T". Species names are given as per the Refseq database. Clades with bootstrap level >90 are marked with circles

it was included in the NCBI Refseq as NZ_NEEY00000000. The assembly yielded 119 contigs with the mean coverage of 78x; the resulting genomic sequence consisted of 2.042 million bps, with the GC content at 38.5%. The Contest16S algorithm did not reveal any differing fragments of the 16S rRNA gene, which would have signaled of contamination. Verification of the set of conserved genes with CheckM has shown that the genome was 98.9% complete with contamination at 1.1%, which confirms high quality of the assembly. There were no CRISPR loci found in the genome. According to the PHASTER data, the genome contains two putative prophages, one of which includes intact genes of the major capsid protein (B9P78_00230), tail protein (B9P78_00200), phage terminase (B9P78_00240), and primase (B9P78_00325), which indicates its intactness. Despite the low susceptibility of the strain

to antibacterial drugs, the search for antibiotic resistance genes yielded only the gene encoding chloramphenicol-O-acetyltransferase (B9P78_09255). A region at the beginning of the NEEY01000023 contig encodes a number of enzymes participating in biosynthesis of polysaccharides (B9P78_05530-B9P78_05565) that form part of the cell wall or capsule.

The sequence of the *Aerococcus* sp. 1KP-2016 strain's 16S rRNA was 98.7% and 98.6% identical to the sequences of the type *A. viridans* and *A. urinaeequi* strains, respectively. Currently, the bacterial species differentiation threshold is accepted at 98.7% [20], which disallows relying on the 16S rRNA's similarity to make unambiguous conclusions about the taxonomic position. At the same time, the ANI between the sequenced genomic sequence and the genomes of the type strains *A. viridans* ATCC 11563 and *A. urinaeequi* DSM 20341

strains is 77.38/77.39% and 76.49/76.26%, respectively. This is significantly below the generally accepted threshold of 95–96% that allows assigning bacteria to a species [20, 21], which indicates the need to introduce a new species. The result is additionally confirmed by the GTDB, an alternative taxonomy database based on the comparison of genomes, in which the 1KP-2016 strain belongs to the separate *Aerococcus* sp002252085 species.

Reconstruction of the phylogeny (Fig. 3) of *Aerococcus* sp. 1KP-2016 strain shows that its closest relative is the *Aerococcus* sp. SJQ22 (RKM01000000) strain, which was isolated from the soil and is currently not assigned to any validated species of the *Aerococcus* genus. However, the ANI between *Aerococcus* sp. 1KP-2016 and this strain was only 87.87/88.05%, which is below the generally accepted level of similarity within the species.

DISCUSSION

Aerococcus cause sporadic urinary tract disease, endocarditis, CSF and bloodstream infections. The most commonly isolated strains are *A. urinae* (55–60%) and *A. sanguinicola* (26–46%); *A. viridians* is isolated less frequently. The prevalent strain in Europe and the US is *A. sanguinicola*, *A. viridians* is found less often. *Aerococcus* bacteria are considered as part of the normal microbiota of the urogenital tract. They are isolated from the urine in the absence of clinical symptoms of the disease. In 2010–2015, a retrospective cohort study showed the etiological role played by the *Aerococcus* bacteria in urinary tract infections and asymptomatic bacteriuria (mainly in elderly women), with a noteworthy presence of other microorganisms in 35% of the cases [5, 22]. According to a retrospective cohort study of 2005–2020, 22.4% of the involved patients had a proven clinical picture of the aerococci blood infection, and their mortality depended on the duration of the disease: at 30 days, it was 17%, and at three months — 24% [2]. For microbiologists, it is difficult to properly identify the *Aerococcus* bacteria when they

are isolated from urine or blood samples: the morphology often leads to their confusion with staphylococci, and hemolysis — with α -hemolytic streptococci. Given their low biochemical activity, biochemical tests do not yield reliable results. In this regard, it is possible to identify the species using mass spectrometry, but this method allows identification of only five species of the aerococci: *A. christensenii*, *A. sanguinicola*, *A. urinae*, *A. urinaehominis*, *A. viridians*. Therefore, sequencing of the 16S rRNA gene is used to identify strains of aerococci isolated from blood [5, 22].

This study is the first successful attempt at identification of the *Aerococcus* sp. 1KP-2016 strain isolated from the buffy coat that has a 16S rRNA sequence that matches the previously described representatives of this genus 98.7% or less. The whole genome sequencing and the subsequent phylogenetic reconstruction we undertook have shown that this strain is a representative of a new species of the *Aerococcus* genus, one closest to *A. viridians* and *A. urinaeequi*.

Consequently, aerococci are still the microorganisms the epidemiological and clinical characteristics of which have not been studied in full. There are many open fundamental questions about the pathogenetic role played by them in the invasive infectious pathologies. The complexity of identification of species within the *Aerococcus* genus requires use of the modern molecular genetic technologies that enable identification of the new types of microorganisms and expansion of the etiological spectrum of pathogens of severe invasive diseases.

CONCLUSIONS

The genotypic features of the studied strain allow attributing the 1KP-2016 strain isolated from the blood as a new species of the *Aerococcus* genus that is evolutionarily close to *A. viridians* and *A. urinaeequi* yet different from them. It is necessary to further study its phenotypic and chemotaxonomic properties while applying the polyphasic approach to bacterial taxonomy.

References

- Williams RE, Hirsch A, Cowan ST. *Aerococcus*, a new bacterial genus. J Gen Microbiol. 1953; 8: 475–80.
- Tai DBG, Go JR, Fida M, Saleh JA. Management and treatment of *Aerococcus* bacteremia and endocarditis. International J Infect Dis. 2021; 102: 584–9.
- Rasmussen M. *Aerococcus*: an increasingly acknowledged human pathogen. Clin Microbiol Infect. 2016; 22: 22–7.
- Christensen JJ, Jensen IP, Faerk J, Kristensen B, Skov R, Korner B. The Danish ALO Study Group. Bacteremia / Septicemia Due to *Aerococcus*-Like Organisms: Report of Seventeen Cases. Clin Infect Dis. 1995; 21 (4): 943–94.
- Rasmussen M. *Aerococci* and aerococcal infections. J Infection. 2013; 66: 467–74.
- Yaban B, Kikhney J, Musci M, Petrich A, Schmidt J, Hajduczenia M et al. *Aerococcus urinae* – A potent biofilm builder in endocarditis. PLoS One. 2020; 15: e0231827.
- Carkaci D, Højholt K, Nielsen XC, Dargis R, Rasmussen S, Skovgaard, O. et al. Genomic characterization, phylogenetic analysis, and identification of virulence factors in *Aerococcus sanguinicola* and *Aerococcus urinae* strains isolated from infection episodes. Microb Pathog. 2017; 112: 327–40.
- Mathieu A, Delmont TO, Vogel TM, Robe P, Nalin R, Simonet P. Life on human surfaces: skin metagenomics. PLoS One. 2013; 8 (6): e65288.
- Bankevich A, Nurk S, Antipov D, Gurevich AA, Dvorkin M, Kulikov AS. et al. SPAdes: a new genome assembly algorithm and its applications to single-cell sequencing. J Comput Biol. 2012; 19: 455–77.
- Lee I, Chalita M, Ha S-M, Na S-I, Yoon S-H, Chun J. ContEst16S: an algorithm that identifies contaminated prokaryotic genomes using 16S RNA gene sequences. Int J Syst Evol Microbiol. 2017; 67: 2053–57.
- Parks DH, Imelfort M, Skennerton CT, Hugenholtz P, Tyson GW. CheckM: assessing the quality of microbial genomes recovered from isolates, single cells, and metagenomes. Genome Res. 2015; 25: 1043–55.
- Couvin D, Bernheim A, Toffano-Nioche C, Touchon M, Michalik J, Néron B. CRISPRCasFinder, an update of CRISPRFinder, includes a portable version, enhanced performance and integrates search for Cas proteins. Nucleic Acids Res. 2018; 46: W246–51.
- Arndt D, Grant JR, Marcu A, Sajed T, Pon A, Liang Y. et al. PHASTER: a better, faster version of the PHAST phage search tool. Nucleic Acids Res. 2016; 44: W16.
- Zankari E, Hasman H, Cosentino S, Vestergaard M, Rasmussen S, Lund O, et al. Identification of acquired antimicrobial resistance genes. J Antimicrob Chemother. 2012; 67: 2640–4.
- Lechner M, Findeiß S, Steiner L, Marz M, Stadler PF, Prohaska SJ. Proteinortho: Detection of (Co-)orthologs in large-scale analysis. BMC Bioinformatics. 2011; 12.
- Edgar RC MUSCLE: multiple sequence alignment with high

- accuracy and high throughput. *Nucleic Acids Res.* 2004; 32: 1792–7.
17. Simonsen M, Mailund T, Pedersen CNS. Rapid Neighbour-Joining. In *Algorithms in Bioinformatics*; Springer Berlin Heidelberg: Berlin, Heidelberg, 2008; 113–22.
 18. Richter M, Rosselló-Móra R, Oliver Glöckner F, Peplies J. JSpeciesWS: a web server for prokaryotic species circumscription based on pairwise genome comparison. *Bioinformatics.* 2016; 32: 929–31.
 19. Parks DH, Chuvochina M, Waite DW, Rinke C, Skarshewski A, Chaumeil PA. A standardized bacterial taxonomy based on genome phylogeny substantially revises the tree of life. *Nat Biotechnol.* 2018; 36: 996.
 20. Chun J, Oren A, Ventosa A, Christensen H, Arahal DR, da Costa MS, et al. Proposed minimal standards for the use of genome data for the taxonomy of prokaryotes. *Int J Syst Evol Microbiol.* 2018; 68: 461–6.
 21. Richter M, Rosselló-Móra R. Shifting the genomic gold standard for the prokaryotic species definition. *Proc Natl Acad Sci USA.* 2009; 106: 19126–31.
 22. Narayanasamy S, King K, Dennison A, Spelman DW, Aung AK. Clinical characteristics and laboratory identification of *Aerococcus* infections: an Australian tertiary centre perspective. *Hindawi International J Microbiology.* 2017; 5684614.

Литература

1. Williams RE, Hirsch A, Cowan ST. *Aerococcus*, a new bacterial genus. *J Gen Microbiol.* 1953; 8: 475–80.
2. Tai DBG, Go JR, Fida M, Saleh JA. Management and treatment of *Aerococcus* bacteremia and endocarditis. *International J Infect Dis.* 2021; 102: 584–9.
3. Rasmussen M. *Aerococcus*: an increasingly acknowledged human pathogen. *Clin Microbiol Infect.* 2016; 22: 22–7.
4. Christensen JJ, Jensen IP, Faerk J, Kristensen B, Skov R, Korner B. The Danish ALO Study Group. Bacteremia / Septicemia Due to *Aerococcus*-Like Organisms: Report of Seventeen Cases. *Clin Infect Dis.* 1995; 21 (4): 943–94.
5. Rasmussen, M. *Aerococci* and *aerococcal* infections. *J Infection.* 2013; 66: 467–74.
6. Yaban B, Kikhney J, Musci M, Petrich A, Schmidt J, Hajduczenia M et al. *Aerococcus* *urinae* – A potent biofilm builder in endocarditis. *PLoS One.* 2020; 15: e0231827.
7. Carkaci D, Højholt K, Nielsen XC, Dargis R, Rasmussen S, Skovgaard, O. et al. Genomic characterization, phylogenetic analysis, and identification of virulence factors in *Aerococcus sanguinicola* and *Aerococcus urinae* strains isolated from infection episodes. *Microb Pathog.* 2017; 112: 327–40.
8. Mathieu A, Delmont TO, Vogel TM, Robe P, Nalin R, Simonet P. Life on human surfaces: skin metagenomics. *PLoS One.* 2013; 8 (6): e65288.
9. Bankevich A, Nurk S, Antipov D, Gurevich AA, Dvorkin M, Kulikov AS, et al. SPAdes: a new genome assembly algorithm and its applications to single-cell sequencing. *J Comput Biol.* 2012; 19: 455–77.
10. Lee I, Chalita M, Ha S-M, Na S-I, Yoon S-H, Chun J. ContEst16S: an algorithm that identifies contaminated prokaryotic genomes using 16S RNA gene sequences. *Int J Syst Evol Microbiol.* 2017; 67: 2053–57.
11. Parks DH, Imelfort M, Skennerton CT, Hugenholtz P, Tyson GW. CheckM: assessing the quality of microbial genomes recovered from isolates, single cells, and metagenomes. *Genome Res.* 2015; 25: 1043–55.
12. Couvin D, Bernheim A, Toffano-Nioche C, Touchon M, Michalik J, Néron B. CRISPRCasFinder, an update of CRISPRFinder, includes a portable version, enhanced performance and integrates search for Cas proteins. *Nucleic Acids Res.* 2018; 46: W246–51.
13. Arndt D, Grant JR, Marcu A, Sajed T, Pon A, Liang Y. et al. PHASTER: a better, faster version of the PHAST phage search tool. *Nucleic Acids Res.* 2016; 44: W16.
14. Zankari E, Hasman H, Cosentino S, Vestergaard M, Rasmussen S, Lund O, et al. Identification of acquired antimicrobial resistance genes. *J Antimicrob Chemother.* 2012; 67: 2640–4.
15. Lechner M, Findeiß S, Steiner L, Marz M, Stadler PF, Prohaska SJ. Proteinortho: Detection of (Co-)orthologs in large-scale analysis. *BMC Bioinformatics.* 2011; 12.
16. Edgar RC MUSCLE: multiple sequence alignment with high accuracy and high throughput. *Nucleic Acids Res.* 2004; 32: 1792–7.
17. Simonsen M, Mailund T, Pedersen CNS. Rapid Neighbour-Joining. In *Algorithms in Bioinformatics*; Springer Berlin Heidelberg: Berlin, Heidelberg, 2008; 113–22.
18. Richter M, Rosselló-Móra R, Oliver Glöckner F, Peplies J. JSpeciesWS: a web server for prokaryotic species circumscription based on pairwise genome comparison. *Bioinformatics.* 2016; 32: 929–31.
19. Parks DH, Chuvochina M, Waite DW, Rinke C, Skarshewski A, Chaumeil PA. A standardized bacterial taxonomy based on genome phylogeny substantially revises the tree of life. *Nat Biotechnol.* 2018; 36: 996.
20. Chun J, Oren A, Ventosa A, Christensen H, Arahal DR, da Costa MS, et al. Proposed minimal standards for the use of genome data for the taxonomy of prokaryotes. *Int J Syst Evol Microbiol.* 2018; 68: 461–6.
21. Richter M, Rosselló-Móra R. Shifting the genomic gold standard for the prokaryotic species definition. *Proc Natl Acad Sci USA.* 2009; 106: 19126–31.
22. Narayanasamy S, King K, Dennison A, Spelman DW, Aung AK. Clinical characteristics and laboratory identification of *Aerococcus* infections: an Australian tertiary centre perspective. *Hindawi International J Microbiology.* 2017; 5684614.

FEATURES OF REACTIVITY OF THE EEG MU RHYTHM IN CHILDREN WITH AUTISM SPECTRUM DISORDERS IN HELPING BEHAVIOR SITUATIONS

Pavlenko VB , Kaida AI, Klinkov VN, Mikhailova AA, Orekhova LS, Portugalskaya AA

Vernadsky Crimean Federal University, Simferopol, Russia


One of the subjects being discussed by the professional community currently is the role possibly played by the mirror neuron system (MNS) in the violation of social behavior of children with autism spectrum disorders (ASD). The MNS is known to shape the perception of emotions of others and understanding and imitation of their actions. Mu rhythm desynchronization in EEG is considered to be the indicator of the MNS activation. The purpose of this study was to identify the features of reactivity of the EEG mu rhythm within an individually determined frequency range in preschoolers with ASD in situations requiring instrumental, emotional and altruistic helping behavior (HB). The study involved children 4–7 years old with ASD ($n = 26$) and their normally developing peers without the condition ($n = 37$). Although in most cases, HB was more pronounced in the group of normally developing children, the differences between the groups are significant only for altruistic HP ($p < 0.01$), and for the situation requiring complex altruistic and emotional HP it approaches significance ($p = 0.09$). Evaluation of the mu rhythm reactivity indices showed that the tasks invoking complex altruistic and emotional HB bring this indicator down significantly in children with ASD compared to the group of normally developing participants, as shown by the central leads of the left and right hemispheres and the parietal lead of the right hemisphere (C3: $p = 0.02$; C4: $p = 0.03$; P4: $p = 0.03$). It is assumed that the detected features stem from the impaired functioning of the MNS and the downstream regulation to the MNS from prefrontal cortex and other areas of the neocortex. The data obtained can be used in development of EEG biofeedback training protocols for children with ASD.

Keywords: children, autism, EEG, μ rhythm, mirror neuron system, prosocial behavior

Funding: the work was supported by the Russian Science Foundation grant № 22-28-00720, <https://rscf.ru/project/22-28-00720/>

Author contribution: Mikhailova AA, Pavlenko VB — research plan, data processing, article authoring; Kaida AI, Klinkov VN, Orekhova LS, Portugalskaya AA — data collection, data processing, article authoring.

Compliance with ethical standards: the study was approved by the Vernadsky Crimean Federal University ethics committee (Minutes #6 of June 04, 2020). Parents of the children have agreed to their participation in the experiment in writing.

 **Correspondence should be addressed:** Vladimir B. Pavlenko
pr. Vernadskogo, 4, Simferopol, 295007, Russia; vpav55@gmail.com

Received: 19.02.2023 **Accepted:** 19.03.2023 **Published online:** 31.03.2023

DOI: 10.24075/brsmu.2023.009

ОСОБЕННОСТИ РЕАКТИВНОСТИ μ -РИТМА ЭЭГ У ДЕТЕЙ С РАССТРОЙСТВАМИ АУТИСТИЧЕСКОГО СПЕКТРА В СИТУАЦИЯХ ПОМОГАЮЩЕГО ПОВЕДЕНИЯ

В. Б. Павленко , А. И. Кайда, В. Н. Клинов, А. А. Михайлова, Л. С. Орехова, А. А. Португальская

Крымский федеральный университет имени В. И. Вернадского, Симферополь, Россия


В настоящее время обсуждается вопрос о возможной роли зеркальной системы мозга (ЗСМ), участвующей в восприятии эмоций окружающих, понимании их действий и подражании таким действиям, в нарушении социального поведения у детей с расстройствами аутистического спектра (РАС). Индикаторами активации ЗСМ считают десинхронизацию μ -ритма ЭЭГ. Целью работы было выявить особенности реактивности ЭЭГ в индивидуально определенном частотном диапазоне μ -ритма у детей с РАС дошкольного возраста в ситуациях, предполагающих проявление инструментального, эмоционального и альтруистического помогающего поведения (ПП). В исследовании приняли участие дети 4–7 лет с РАС ($n = 26$) и их типично развивающиеся сверстники ($n = 37$). Хотя в большинстве случаев нормотипичные дети демонстрировали более выраженное ПП, различия между группами статистически значимы только для альтруистического ПП ($p < 0,01$) и приближаются к значимому уровню для ситуации комплексного альтруистического и эмоционального ПП ($p = 0,09$). Оценка индексов реактивности μ -ритма показала, что при выполнении задания на комплексное альтруистическое и эмоциональное ПП этот показатель статистически значимо ниже у детей с РАС в центральных отведениях левого и правого полушарий, а также в теменном отведении правого полушария (C3: $p = 0,02$; C4: $p = 0,03$; P4: $p = 0,03$). Предполагается, что обнаруженные особенности являются следствием нарушения функционирования ЗСМ, а также нисходящей регуляции к ЗСМ со стороны префронтальной коры и других областей неокортекса. Полученные данные могут быть использованы при разработке протоколов тренингов биологической обратной связи по ЭЭГ для детей с РАС.

Ключевые слова: дети, аутизм, ЭЭГ, μ -ритм, система зеркальных нейронов, просоциальное поведение

Финансирование: работа выполнена за счет гранта Российского научного фонда № 22-28-00720, <https://rscf.ru/project/22-28-00720/>

Вклад авторов: Михайлова А. А., Павленко В. Б. — план исследований, обработка данных, написание статьи; Кайда А. И., Клинов В. Н., Орехова Л. С., Португальская А. А. — набор данных, обработка данных, написание статьи.

Соблюдение этических стандартов: исследование одобрено этическим комитетом ФГАОУ ВО «Крымский федеральный университет им. В. И. Вернадского» (протокол № 6 от 04 июня 2020 г.). Получено информированное согласие от родителей на участие детей в эксперименте.

 **Для корреспонденции:** Владимир Борисович Павленко
пр. Вернадского, д. 4, г. Симферополь, 295007, Россия; vpav55@gmail.com

Статья получена: 19.02.2023 **Статья принята к печати:** 19.03.2023 **Опубликована онлайн:** 31.03.2023

DOI: 10.24075/vrgmu.2023.009

The state of physical, spiritual and social well-being, which is part of the concept of "health", is closely related to the ability to participate, as a member of society, in pro-social behavior, help others and, in turn, receive help and support from them. The terms "prosocial" and "helping behavior" (HB) are usually

defined as voluntary actions in response to the needs of others and aimed at their benefit [1]. Autism spectrum disorders (ASD) severely handicap the ability to adequately engage in social interaction [2–4]. This manifestation of the said disorders forms one of the barriers faced by children with ASD on the way to

becoming a fully-fledged member of the society. Therefore, analysis of the underlying neurophysiological mechanisms is an urgent task. Currently, there is a number of ASD cause hypotheses being discussed. One of them points to the abnormalities in pruning of synaptic terminals peculiar to the people with ASD, which makes the number of axons and synapses atypical. As a result, the quantity of local connections within the microareas of the cerebral cortex is excessive, while functional interaction with remote regions, such as the frontal and parietal areas of the neocortex, is insufficient, which is confirmed by the EEG rhythms coherence analysis [5]. According to another hypothesis, it is the functional deficiency of the nicotinic branch of the cholinergic modulating system that disbalances excitation and inhibition, hinders attention switching and modulation of sensitivity to stimuli of various modalities in children with ASD [6]. Another hypothesis appeared about twenty years ago. It was assumed that ASD disturbs functioning of the mirror neuron system (MNS), which is involved in the perception of the emotions of others, understanding their actions and imitating them. Neocortical regions bilateral in the inferior parietal lobe and ventral premotor cortex are the core of the MNS in a human brain [7–9]. In the context of studying the features of development of prosocial behavior in children with ASD, it is especially important to investigate the last hypothesis, since helping others requires understanding of the goals of their actions, perception of emotions and evaluation of their mental states, as well as adoption of certain methods of HB [10].

According to some data, desynchronization (suppression) of the sensorimotor mu rhythm (a kind of α -activity) indicates activation of the MNS [8, 10, 11]; it is most pronounced over the central areas of the cortex. Therefore, it is possible to study the features of MNS functioning, including in children with ASD, with the help of EEG. Authors of one of the first works in this field found that, unlike the normal group subjects, adults and children with ASD did not have their mu rhythm suppressed when watching videos of biological movements (hand movements) [12]. Based on these results, they formulated the broken mirror hypothesis.

A number of later studies that analyzed EEG of the subjects that were shown such movements did not reveal differences in mu rhythm modulation in people with ASD and normal group individuals [13–15]. However, a study that used recordings of emotionally colored social movements and movements of inanimate objects as stimuli has registered a significantly stronger reaction (mu rhythm desynchronization) thereto in typically developing children aged 7–15 years, while their peers with ASD did not react, i.e. there were no differences in desynchronization of the mu rhythm upon presentation of these stimuli [16]. Performing a task that required recognition of instruments and pantomiming actions therewith, children with ASD (ages 8–13) have shown a decrease in the mu rhythm modulation power compared with children of the normal group [17]. We have also revealed differences in reactivity of EEG-registered sensorimotor rhythms between 5–10-year old children with ASD and their normally developing peers in situations of observation, imitation and auditory perception of movements of a hand holding a computer mouse. In the control group, we registered desynchronization of mu and beta rhythms when the participants were imitating movements and perceiving shifts of the mouse by hear, while in children with ASD, such a reaction in a similar situation was either absent or the mu rhythm synchronized [18].

The analysis of such contradictions has changed the "broken mirror hypothesis" and translated into an integrated model of social modulation of MNS reactions from other areas

of the neocortex. The model suggests that mirror neurons process the visuomotor properties of the actions observed, while the medial prefrontal cortex controls the activity of the MNS depending on the social significance and context of the situation. The symptoms of the ASD manifest because of the abnormalities in the downward regulation of the MNS and not within this system. As a result, the MNS' reaction to simple movements does not differ in people with ASD and neurotypical individuals. However, complex actions, emotionally colored and social stimuli are often processed inadequately [8, 19, 20]. The model enabled development of training routines using biofeedback (BFB) by EEG, which proved effective to a degree in correcting manifestations of the ASD [21]. The routines are based on computer games and include tasks designed to trigger synchronization and desynchronization of the mu rhythm depending on the game context, which enables restructuring of connections between the core of the MNS and other areas of the neocortex.

Previous studies have shown that children with ASD can exhibit prosocial behavior in response to the needs of others, although to a lesser extent than their normally developing peers [22]. They engage in HB when situations require: instrumental helping, i.e. assisting others in executing a purposeful action; empathic help (comforting), which involves response to the emotional needs of another person and verbal or physical support of comforting nature; altruistic help, when children share resources if another person lacks them. To the best of our knowledge, the reactivity of EEG-registered mu rhythm associated with HB demonstrated by children with ASD was not measured and compared to the similar indicator in their healthy peers previously. Such a study would clarify the possible effect MNS dysfunction has on the organization of complex prosocial behavior in children with autism, and could also help develop new corrective methods involving EEG biofeedback sessions for children with ASD. Since the degree of desynchronization of the mu rhythm can be assessed incorrectly because of the partial superposition of the occipital alpha rhythm, the frequency of which is adjacent [10], it is advisable to identify individual mu rhythm range when the child makes independent movements. In this connection, the purpose of our study was to identify the features of EEG reactivity in the individual mu rhythm frequency range in preschoolers with ASD in situations requiring rendering of various types of assistance to another person.

METHODS

Sample characteristics

The study was carried out at the Scientific Equipment Shared Use Center "Experimental Physiology and Biophysics" of Vernadsky Crimean Federal University. It involved 64 right-handed children aged 4–7 years (mean age 5.7 ± 1.2 years), including 26 children with ASD (20 boys and 6 girls) and 38 typically developing children (the comparison group, 21 boys and 17 girls). Age-wise distribution of children with ASD was as follows: 4 years old — 6 people, 5 years old — 6 people, 6 years old — 8 people, 7 years old — 6 people. Similar distribution in the comparison group: 4 years old — 10, 5 years old — 8, 6 years old — 10, 7 years old — 10 people. The age distribution of children with ASD and normally developing children in these groups was similar. There were no significant differences in the mean age of all children with ASD and normally developing children (5.9 ± 1.2 and 5.5 ± 1.2 , respectively, $p = 0.17$). The ASD group included children diagnosed with "childhood autism" (F84.0 in ICD-10) or "autism spectrum disorder with

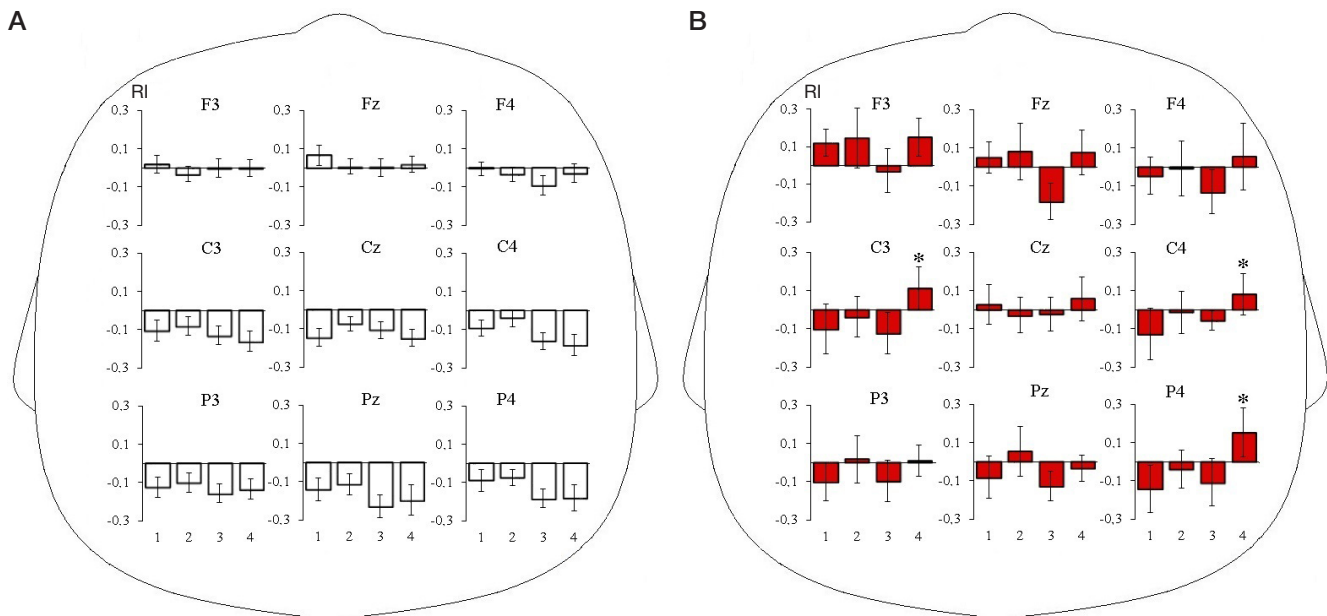


Fig. 1. Reactivity indices (RI) of the EEG-registered mu rhythm in typically developing children (**A**; white columns) and children with ASD (**B**; red columns) in situations of helping behavior. 1 — IHB, 2 — EHB, 3 — AHB, 4 — AEHB. Mean values and standard errors of means are given. Differences in reactivity indices in children of two groups: * — $p < 0.05$

intellectual disability and functional language impairment" (6A02.3 in ICD-11). The criteria for inclusion in comparison group were a sufficient level of cognitive development (IQ 90 to 120 scored in WPPSI and WISC variants of the Wechsler scale) and absence of chronic diseases of the nervous system. The inclusion criteria for both groups: normal levels of vision and hearing; preferred right-handedness.

Assessment of intensity of prosocial behavior

Four experimental situations were designed to analyze the level of HB intensity. The switch to the next situation was made when the child has completed the task or if he/she did not provide assistance within 50 seconds.

1. Instrumental helping behavior (IHB) task designed around the methods suggested by F.Warneken, M.Tomasello [23]. A box was placed on the table in front of the child; it had a small hole at the top, its side facing the child was open. Experimenter put a mug on the box, and, as if stirring tea in it, "accidentally" dropped the spoon into the hole on the top side of the box. The child was expected to help retrieve the spoon and give it to the experimenter.

2. Empathic helping behavior (EHB) task employing the clipboard [24]. Experimenter, as if by accident, pressed his finger with a paper clip, exclaimed "Oh!" and demonstrated that he was in pain (made a sad face, rubbed his finger, sighed and groaned). The analyzed result was whether the child calmed the experimenter (touched his hand, voiced concern about him, asked the parent to help the experimenter etc.).

3. Altruistic helping behavior (AHB) task based on the "unequal treat" approach [22]. Experimenter took out two transparent containers, one for himself and one for the child, and said, "Look what I have." The experimenter's container was empty, and the child's had four cookies in it. In various ways, the experimenter showed that he did not have cookies while the child did; he made a sad face, extended his hand palm up in a demanding gesture. The registered outcome was whether the child shared the cookies or not.

4. A complex task triggering altruistic and empathic helping behavior (AEHB) [25]. First, the experimenter played with the

child using two teddy bears, one of which had a paw held with a Velcro band. After several minutes of play, this paw fell off, and the experimenter made a sad face. Next, the signals that he needed help were becoming more and more obvious; for example, the experimenter said: "The paw fell off! I cannot play with my bear now!" The assessed result was the intensity of HB demonstrated by the child (simple calming, offering his toy).

The experiments were recorded with a camera. The intensity of HB was assessed on a 10-point scale based on the analysis of the recording and the criteria described earlier [22–25] (did the child offer help and how quickly, whether this required more and more insistent stimuli from the experimenter).

EEG registration and analysis

We used the Neuron-Spectrum-5 electroencephalograph (Neurosoft; Russia) monopolarly from 19 leads, using the standard 10–20% pattern (reference from combined ear electrodes), the signal bandwidth of 0.5–30.0 Hz, sampling rate of 250 Hz. EEG and video recording of experimental situations were synchronized.

For the background situation, we registered EEG (50 seconds) when the participant's eyes were open and he/she was stably paying attention to the recording of a rotating ball. For the purpose of analysis of changes in the mu rhythm associated with prosocial behavior, we selected such spans (from all four experimental situations) when the child sat motionless, observed the actions of the adult and made a decision to provide assistance of this or that nature. The duration of such recordings depended on the time after which the child provided assistance and did not exceed 50 s.

We used WinEEG software (Mizar, Russia) to process the EEG data. The independent components analysis built into the program (with additional visual recording quality control interface) enabled removal of artifacts. The EEG of one child in the comparison group and seven children with ASD contained a large number of artifacts because the children moved excessively; these were excluded from further statistical processing. The artifact-free EEG segments were divided into 2-second epochs. The segments were subjected to fast Fourier

Table. Results of ANOVA of differences in the mu rhythm reactivity, children developing normally and children with ASD

Reactivity indices	GROUP			LOCUS			GROUP × LOCUS		
	F1.54	<i>p</i>	η^2	F8.432	<i>p</i>	η^2	F8.432	<i>p</i>	η^2
RI IHB	0.1	0.74	0.002	3.64	0.0004	0.06	0.93	0.49	0.02
RI EHB	0.95	0.33	0.02	1.43	0.18	0.03	0.71	0.68	0.01
RI AHB	0.09	0.77	0.002	1.52	0.15	0.03	1.47	0.17	0.03
RI AEHB	4.24	0.04	0.08	1.9	0.06	0.04	1.16	0.32	0.02

transformation with 4 second epochs and 50% epoch overlap. The μ -rhythm amplitudes were analyzed at nine loci: frontal (F3, Fz, F4), central (C3, Cz, C4), and parietal (P3, Pz, P4). These regions were chosen as areas of interest based on the literature data, which advise analyzing the mu rhythm in children not only in the central but also in the frontal and parietal regions [26]. The amplitude of the EEG-registered mu rhythm was calculated in the frequency ranges individual to each subject; these ranges were determined based on the analysis of differences in the EEG power spectra in the C3 lead when the child was motionless and when he/she performed movements (desynchronization reaction) [27].

Statistical data processing

We used STATISTICA 12.0 software (StatSoft Inc.; USA) to perform statistical analysis of the data obtained. To assess differences in the intensity of various elements of prosocial behavior, we used the Mann–Whitney U test. The features of EEG reactivity in children with ASD were identified through calculation of the reactivity indices (RI) for the mu rhythm, which was done using the formula $RI = \ln(B / A)$ [13], where B is the amplitude of the rhythm in the experimental situation and A is the amplitude of the rhythm in the background situation. Logarithming enabled normalization of distribution. The values of $RI > 0$ mark an increase in the rhythm's amplitude in the experimental situation compared to the background level (synchronization), and $RI < 0$ indicates a decrease in the amplitude of the rhythm (desynchronization). The differences in RI of the mu rhythm were assessed with the help of repeated measures ANOVA. We have also assessed the influence of GROUP, an external participant-related factor (two levels: children with ASD and the comparison group) and LOCUS, and internal participant-related factor (nine EEG leads) by the 2×9 pattern. Linear contrasts were used to calculate significance of differences in the analyzed RI parameters relative to each of the nine EEG leads. Median and interquartile range allowed preparing description of distributions differing from the norm (prosocial behavior indicators). For the normal data distribution cases (logarithmic values of the RI), we used mean and standard error of the mean. The differences were considered statistically significant at $p < 0.05$, but because of the small sample size we also included "unshaped" differences, i.e. those already visible but not yet fully formed ($p < 0.10$).

Gender was not considered as an independent variable due to the predominance of male participants in the ASD group.

RESULTS

The features of helping behavior indicators in children with ASD

The assessment of intensity of elements of prosocial behavior in the comparison group was as follows: the IHB indicator was 7.5 (2; 10), the EHB was 1.5 (0; 3), the AHB was 6.0 (4; 10), the

AEHB was 8, 5 (4; 10) points. In children with ASD, IHB was 9.0 (1; 10), EHB — 0.0 (0; 3), AHB — 2.5 (0; 5), AEHB — 3.0 (0; 10) points. Although in most cases, HB was more intense in the group of normally developing children, the differences between the groups were significant only for AHB situation ($Z = 2.61$, $p < 0.01$), and for the AEHB it approaches significance ($Z = 1.65$, $p = 0.09$).

Features of the EEG-registered reactivity in the mu rhythm frequency range in children with ASD

The RI of the comparison group children in all experimental situations took negative values for central and parietal leads, which indicates EEG desynchronization in the mu rhythm range (Fig. 1A). In the frontal leads, the reactivity of the mu rhythm was insignificant. In children with ASD, the RI values in all analyzed leads took both positive and negative values, which indicates both desynchronization and synchronization of the EEG in the mu rhythm range (Fig. 1B).

The results of ANOVA of differences in the mu rhythm reactivity in children with ASD and the comparison group indicate a statistically significant effect the GROUP factor has on the AEHB task (Table). In this experimental situation, comparison group children had decreasing amplitudes in all leads except for Fz, and in the ASD group the individual mu rhythm amplitude was increasing except for the Pz locus (Figure). The linear contrasts method allowed concluding that the differences in the mu rhythm's RI in the two groups of children reached the level of statistical significance in the central leads of left and right hemispheres, as well as in the parietal lead of the right hemisphere (C3: $p = 0.02$; C4: $p = 0.03$; P4: $p = 0.03$). There were significant differences found between the groups for the IHB, EHB and AEHB tasks.

DISCUSSION

Same as other researchers [22, 28], we have found that despite marked social impairments, children with ASD act prosocially in response to the needs of others and may do so in situations that require different types of assistance. They have shown greater intensity of HB in an IHB situation than children of the comparison group. The possible reason behind this is the desire to restore order, which is inherent in children with ASD [29]. However, in the AHB and AEHB situations, children with ASD are less willing to help. For the participants of the study, the most difficult was the AEHB situation: while playing, the children had to evaluate what was happening, perceive the affectively colored non-verbal and verbal signals by the experimenter, provide him with emotional assistance or even share an attractive toy. In this situation, children with ASD not only exhibited less intense HB but also shown significant differences from the children of the comparison group in the EEG pattern.

In situations requiring assistance (including the AEHB situation), normally developing children have shown EEG desynchronization in the frequency range of the mu rhythm

in the central and parietal leads. In children with ASD, such desynchronization was not registered in these situations. As was already noted, desynchronization of the mu rhythm is regarded as an indicator of the MNS activation [10, 11]. Thus, the absence of mu rhythm depression in children with ASD when solving the AEHB task may indicate a lower degree of activation of the MNS, which manifests in the most difficult social situation. The results, which show that the RI in the groups differ greatest in the AEHB situation, are consistent with the so-called integrated model [8], which is based on the modulation of responses of MNS nerve cells from the prefrontal cortex and other areas of the neocortex, depending on the context of the situation.

Difficulties with switching attention in a complex social situation may also be the cause of the altered reactions of the MNS. According to some authors, children with autism have the functioning of the ventral attention module disrupted, which includes the temporo-parietal junction, the dorsal third of the superior temporal gyrus, and a number of areas of the ventral frontal cortex. This module is responsible for releasing attention and refocusing on the new, potentially important stimuli [2, 6]. In this regard, it can be assumed that the weak attention switching ability demonstrated by children with ASD (e.g., from focusing on their own game with an attractive toy to the actions and manifestations of emotions of another person) prevents

adequate activation of the MNS, since the actions of another person are simply out of the child's focus.

The results of this study indicate possible impairments in the functioning of the MNS and neocortical regions that modulate the activity of the system in children with ASD in difficult social situations that require altruistic and emotional HB. The identified features of the EEG-registered mu rhythm reactivity may be useful for the development of the new biofeedback session protocols designed to adjust the development of children with ASD. For such sessions, it seems promising to use a variety of feedback signals that have an emotional connotation and are included in the social context.

CONCLUSIONS

The results of the study indicate that preschoolers diagnosed with ASD act prosocially in response to the needs of others in situations requiring different types of assistance. However, in complex social situations, they are less inclined to provide altruistic and emotional assistance. In such cases, children with ASD, in contrast to normally developing children, exhibit no desynchronization of the EEG-registered mu rhythm in the central and parietal leads. The identified features of behavior of children with ASD can be used in corrective work, including the EEG-enabled biofeedback sessions.

References

- Eisenberg N, Fabes RA, Spinrad T. Prosocial development. In: Eisenberg N, Damon W, Lerner RM, editors. *Handbook of Child Psychology*. New York: Wiley, 2006; 646–718.
- Pereverzeva DS, Gorbachevskaya NL. Nejrobiologicheskie markery rannih stadij rasstrojstv autisticheskogo spektra. *Zhurnal vysshej nervnoj deyatel'nosti im. I. P. Pavlova*. 2016; 66 (3): 289–301. DOI: 10.7868/S0044467716030102. Russian.
- Bozhkova ED, Balandina OV, Kononov AA. Rasstrojstva autisticheskogo spektra: sovremennoe sostoyanie problemy (obzor). *Sovremennye tehnologii v medicine*. 2020; 12 (2): 111–20. DOI: 10.17691/stm2020.12.2.14. Russian.
- Salimova KR. Nejrofiziologicheskie korrelyaty narusheniya razvitiya pri rasstrojstvakh autisticheskogo spektra (RAS). *Uspehi sovremennoj biologii*. 2021; 141 (6): 557–66. DOI: 10.31857/S0042132421060065. Russian.
- Ippolito G, Bertaccini R, Tarasi L, Di Gregorio F, Trajkovic J, Battaglia S, et al. The role of alpha oscillations among the main neuropsychiatric disorders in the adult and developing human brain: evidence from the last 10 years of research. *Biomedicines*. 2022; 10 (12): 3189. DOI: 10.3390/biomedicines10123189.
- Orekhova EV, Stroganova TA. Arousal and attention re-orienting in autism spectrum disorders: evidence from auditory event-related potentials. *Front Hum Neurosci*. 2014; 8: 34. DOI: 10.3389/fnhum.2014.00034.
- Lebedeva NN, Zufman AI, Mal'cev VYu. Sistema zerkal'nyh nejronov mozga: klyuch k obucheniyu, formirovaniyu lichnosti i ponimaniyu chuzhogo soznaniya. *Uspehi fiziologicheskikh nauk*. 2017; 48 (4): 16–28. Russian.
- Yates L, Hobson H. Continuing to look in the mirror: A review of neuroscientific evidence for the broken mirror hypothesis, EP-M model and STORM model of autism spectrum conditions. *Autism*. 2020; 24 (8): 1945–59. DOI: 10.1177/1362361320936945.
- Heyes C, Catmur C. What Happened to Mirror Neurons? *Perspect Psychol Sci*. 2022; 17 (1): 153–68. DOI: 10.1177/1745691621990638.
- Hobson HM, Bishop DVM. The interpretation of mu suppression as an index of mirror neuron activity: past, present and future. *Review R Soc Open Sci*. 2017; 4 (3): 160662. DOI: 10.1098/rsos.160662.
- Larionova E. V., Garah Zh. V., Zajceva Yu. S. Myu-ritm v sovremennyh issledovaniyah: teoreticheskie i metodologicheskie aspekty. *Zhurnal vysshej nervnoj deyatel'nosti im. I. P. Pavlova*. 2022; 72 (1): 11–35. DOI: 10.31857/S0044467722010051. Russian.
- Oberman LM, Hubbard EM, McCleery JP, Altschuler EL, Ramachandran VS, Pineda JA. EEG evidence for mirror neuron dysfunction in autism spectrum disorders. *Brain Res Cogn Brain Res*. 2005; 24 (2): 190–8. DOI: 10.1016/j.cogbrainres.2005.01.014.
- Raymaekers R, Wiersema JR, Roeyers H. EEG study of the mirror neuron system in children with high functioning autism. *Brain Res*. 2009; 1304: 113–21. DOI: 10.1016/j.brainres.2009.09.068.
- Fan YT, Decety J, Yang CY, Liu JL, Cheng Y. Unbroken mirror neurons in autism spectrum disorders. *J Child Psychol Psychiatry*. 2010; 51 (9): 981–8. DOI: 10.1111/j.1469-7610.2010.02269.x.
- Sotoodeh MS, Taheri-Torbati H, Sohrabi M, Ghoshuni M. Perception of biological motions is preserved in people with autism spectrum disorder: electrophysiological and behavioural evidences. *J Intellect Disabil Res*. 2019; 63 (1): 72–84. DOI: 10.1111/jir.12565.
- Hudac CM, Kresse A, Aaronson B, DesChamps TD, Webb SJ, Bernier RA. Modulation of mu attenuation to social stimuli in children and adults with 16p11.2 deletions and duplications. *J Neurodev Disord*. 2015; 7 (1): 25. DOI: 10.1186/s11689-015-9118-5.
- Ewen JB, Lakshmanan BM, Pillai AS, McAuliffe D, Nettles C, Hallett M, et al. Decreased modulation of EEG oscillations in high-functioning autism during a motor control task. *Front Hum Neurosci*. 2016; 10: 198. DOI: 10.3389/fnhum.2016.00198.
- Kaida AI, Eismont EV, Mikhailova AA, Pavlenko VB. EEG sensorimotor rhythms in children with autism spectrum disorders. *Bulletin of RSMU*. 2020; (5): 70–6. DOI: 10.24075/brsmu.2020.055.
- Hamilton AF. Reflecting on the mirror neuron system in autism: a systematic review of current theories. *Dev Cogn Neurosci*. 2013; 3: 91–105. DOI: 10.1016/j.dcn.2012.09.008.
- Dumas G, Soussignan R, Hugueville L, Martinerie J, Nadel J. Revisiting mu suppression in autism spectrum disorder. *Brain Res*. 2014; 1585: 108–19. DOI: 10.1016/j.brainres.2014.08.035.
- Friedrich EV, Sivanathan A, Lim T, Suttie N, Louchart S, Pillen S, et al. An effective neurofeedback intervention to improve social

- interactions in children with Autism Spectrum Disorder. *J Autism Dev Disord.* 2015; 45 (12): 4084–100. DOI: 10.1007/s10803-015-2523-5.
22. Dunfield KA, Best LJ, Kelley EA, Kuhlmeier VA. Motivating moral behavior: helping, sharing, and comforting in young children with autism spectrum disorder. *Front Psychol.* 2019; 10: 25. DOI: 10.3389/fpsyg.2019.00025.
 23. Warneken F, Tomasello M. Altruistic helping in human infants and young chimpanzees. *Science.* 2006; 311 (5765): 1301–3. DOI: 10.1126/science.1121448.
 24. Paulus M, Kühn-Popp N, Licata M, Sodian B, Meinhardt J. Neural correlates of prosocial behavior in infancy: different neurophysiological mechanisms support the emergence of helping and comforting. *Neuroimage.* 2013; 66: 522–30. DOI: 10.1016/j.neuroimage.2012.10.041.
 25. Kärtner J, Schuhmacher N, Collard J. Socio-cognitive influences on the domain-specificity of prosocial behavior in the second year. *Infant Behav Dev.* 2014; 37 (4): 665–75. DOI: 10.1016/j.infbeh.2014.08.004.
 26. Marshall PJ, Young T, Meltzoff AN. Neural correlates of action observation and execution in 14-month-old infants: An event-related EEG desynchronization study. *Dev Sci.* 2011; 14 (3): 474–80. DOI: 10.1111/j.1467-7687.2010.00991.x.
 27. Mihajlova AA, Orekhova LS, Dyagileva YuO, Muhtarimova TI, Pavlenko VB. Reaktivnost' myu-ritma EhEhG pri nablyudenii i vypolnenii dejstvij u detej rannego vozrasta, imeyushih raznyj uroven' razvitiya receptivnoj rechi. *Zhurnal vyshej nervnoj deyatel'nosti im. I.P. Pavlova.* 2020; 70 (3): 422–32. DOI: 10.31857/S0044467720030077. Russian.
 28. Wang X, Auyeung B, Pan N, Lin LZ, Chen Q, Chen JJ, et al. Empathy, Theory of Mind, and prosocial behaviors in autistic children. *Front Psychiatry.* 2022; 13:844578. DOI: 10.3389/fpsy.2022.844578.
 29. Paulus M, Rosal-Grifoll B. Helping and sharing in preschool children with autism. *Exp Brain Res.* 2017; 235 (7): 2081–8. DOI: 10.1007/s00221-017-4947-y.

Литература

1. Eisenberg N, Fabes RA, Spinrad T. Prosocial development. In: Eisenberg N, Damon W, Lerner RM, editors. *Handbook of Child Psychology.* NewYork: Wiley, 2006; 646–718.
2. Переверзева Д. С., Горбачевская Н. Л. Нейробиологические маркеры ранних стадий расстройств аутистического спектра. *Журнал высшей нервной деятельности им. И. П. Павлова.* 2016; 66 (3): 289–301. DOI: 10.7868/S0044467716030102.
3. Божкова Е. Д., Баландина О. В., Коновалов А. А. Расстройства аутистического спектра: современное состояние проблемы (обзор). *Современные технологии в медицине.* 2020; 12 (2): 111–20. DOI: 10.17691/stm2020.12.2.14.
4. Салимова К. Р. Нейрофизиологические корреляты нарушения развития при расстройствах аутистического спектра (РАС). *Успехи современной биологии.* 2021; 141 (6): 557–66. DOI: 10.31857/S0042132421060065.
5. Ippolito G, Bertaccini R, Tarasi L, Di Gregorio F, Trajkovic J, Battaglia S, et al. The role of alpha oscillations among the main neuropsychiatric disorders in the adult and developing human brain: evidence from the last 10 years of research. *Biomedicine.* 2022; 10 (12): 3189. DOI: 10.3390/biomedicine10123189.
6. Orekhova EV, Stroganova TA. Arousal and attention re-orienting in autism spectrum disorders: evidence from auditory event-related potentials. *Front Hum Neurosci.* 2014; 8: 34. DOI: 10.3389/fnhum.2014.00034.
7. Лебедева Н. Н., Зуфман А. И., Мальцев В. Ю. Система зеркальных нейронов мозга: ключ к обучению, формированию личности и пониманию чужого сознания. *Успехи физиологических наук.* 2017; 48 (4): 16–28.
8. Yates L, Hobson H. Continuing to look in the mirror: A review of neuroscientific evidence for the broken mirror hypothesis, EP-M model and STORM model of autism spectrum conditions. *Autism.* 2020; 24 (8): 1945–59. DOI: 10.1177/1362361320936945.
9. Heyes C, Catmur C. What Happened to Mirror Neurons? *Perspect Psychol Sci.* 2022; 17 (1): 153–68. DOI: 10.1177/1745691621990638.
10. Hobson HM, Bishop DVM. The interpretation of mu suppression as an index of mirror neuron activity: past, present and future. *Review R Soc Open Sci.* 2017; 4 (3): 160662. DOI: 10.1098/rsos.160662.
11. Ларионова Е. В., Гарах Ж. В., Зайцева Ю. С. Мю-ритм в современных исследованиях: теоретические и методологические аспекты. *Журнал высшей нервной деятельности им. И. П. Павлова.* 2022; 72 (1): 11–35. DOI: 10.31857/S0044467722010051.
12. Oberman LM, Hubbard EM, McCleery JP, Altschuler EL, Ramachandran VS, Pineda JA. EEG evidence for mirror neuron dysfunction in autism spectrum disorders. *Brain Res Cogn Brain Res.* 2005; 24 (2): 190–8. DOI: 10.1016/j.cogbrainres.2005.01.014.
13. Raymaekers R, Wiersma JR, Roeyers H. EEG study of the mirror neuron system in children with high functioning autism. *Brain Res.* 2009; 1304: 113–21. DOI: 10.1016/j.brainres.2009.09.068.
14. Fan YT, Decety J, Yang CY, Liu JL, Cheng Y. Unbroken mirror neurons in autism spectrum disorders. *J Child Psychol Psychiatry.* 2010; 51 (9): 981–8. DOI: 10.1111/j.1469-7610.2010.02269.x.
15. Sotoodeh MS, Taheri-Torbati H, Sohrabi M, Ghoshuni M. Perception of biological motions is preserved in people with autism spectrum disorder: electrophysiological and behavioural evidences. *J Intellect Disabil Res.* 2019; 63 (1): 72–84. DOI: 10.1111/jir.12565.
16. Hudac CM, Kresse A, Aaronson B, DesChamps TD, Webb SJ, Bernier RA. Modulation of mu attenuation to social stimuli in children and adults with 16p11.2 deletions and duplications. *J Neurodev Disord.* 2015; 7 (1): 25. DOI: 10.1186/s11689-015-9118-5.
17. Ewen JB, Lakshmanan BM, Pillai AS, McAuliffe D, Nettles C, Hallett M, et al. Decreased modulation of EEG oscillations in high-functioning autism during a motor control task. *Front Hum Neurosci.* 2016; 10: 198. DOI: 10.3389/fnhum.2016.00198.
18. Кайда А. И., Эйсмонт Е. В., Михайлова А. А., Павленко В. Б. Сенсомоторные ритмы ЭЭГ у детей с расстройствами аутистического спектра. *Вестник РГМУ.* 2020; (5): 74–81. DOI: 10.24075/vrgmu.2020.055.
19. Hamilton AF. Reflecting on the mirror neuron system in autism: a systematic review of current theories. *Dev Cogn Neurosci.* 2013; 3: 91–105. DOI: 10.1016/j.dcn.2012.09.008.
20. Dumas G, Soussignan R, Hugueville L, Martinerie J, Nadel J. Revisiting mu suppression in autism spectrum disorder. *Brain Res.* 2014; 1585: 108–19. DOI: 10.1016/j.brainres.2014.08.035.
21. Friedrich EV, Sivanathan A, Lim T, Suttie N, Louchart S, Pillen S, et al. An effective neurofeedback intervention to improve social interactions in children with Autism Spectrum Disorder. *J Autism Dev Disord.* 2015; 45 (12): 4084–100. DOI: 10.1007/s10803-015-2523-5.
22. Dunfield KA, Best LJ, Kelley EA, Kuhlmeier VA. Motivating moral behavior: helping, sharing, and comforting in young children with autism spectrum disorder. *Front Psychol.* 2019; 10: 25. DOI: 10.3389/fpsyg.2019.00025.
23. Warneken F, Tomasello M. Altruistic helping in human infants and young chimpanzees. *Science.* 2006; 311 (5765): 1301–3. DOI: 10.1126/science.1121448.
24. Paulus M, Kühn-Popp N, Licata M, Sodian B, Meinhardt J. Neural correlates of prosocial behavior in infancy: different neurophysiological mechanisms support the emergence of helping and comforting. *Neuroimage.* 2013; 66: 522–30. DOI: 10.1016/j.neuroimage.2012.10.041.
25. Kärtner J, Schuhmacher N, Collard J. Socio-cognitive influences on the domain-specificity of prosocial behavior in the second year. *Infant Behav Dev.* 2014; 37 (4): 665–75. DOI: 10.1016/j.infbeh.2014.08.004.
26. Marshall PJ, Young T, Meltzoff AN. Neural correlates of action

- observation and execution in 14-month-old infants: An event-related EEG desynchronization study. *Dev Sci*. 2011; 14 (3): 474–80. DOI: 10.1111/j.1467-7687.2010.00991.x.
27. Михайлова А. А., Орехова Л. С., Дягилева Ю. О., Мухтаримова Т. И., Павленко В. Б. Реактивность мю-ритма ЭЭГ при наблюдении и выполнении действий у детей раннего возраста, имеющих разный уровень развития рецептивной речи. *Журнал высшей нервной деятельности им. И. П. Павлова*. 2020; 70 (3): 422–32. DOI: 10.31857/S0044467720030077.
 28. Wang X, Auyeung B, Pan N, Lin LZ, Chen Q, Chen JJ, et al. Empathy, Theory of Mind, and prosocial behaviors in autistic children. *Front Psychiatry*. 2022; 13:844578. DOI: 10.3389/fpsyt.2022.844578.
 29. Paulus M, Rosal-Grifoll B. Helping and sharing in preschool children with autism. *Exp Brain Res*. 2017; 235 (7): 2081–8. DOI: 10.1007/s00221-017-4947-y.

EFFECTS OF THE METAPLASTICITY-BASED THETA-BURST TRANSCRANIAL STIMULATION PROTOCOLS ON WORKING MEMORY PERFORMANCE

Bakulin IS, Zabirowa AH , Poydasheva AG, Sinitsyn DO, Lagoda DYU, Suponeva NA, Piradov MA

Research Center of Neurology, Moscow, Russia

The study of the metaplasticity-based transcranial magnetic stimulation (TMS) protocols is an extensively studied approach to increase the effectiveness of stimulation. However, the effects of protocols with different intervals between the TMS blocks on cognitive functions are poorly understood. The study was aimed to assess the effects of two theta-burst transcranial stimulation (iTBS) protocols with short and long intervals between blocks on the working memory (WM) performance in healthy volunteers. A total of 16 participants were underwent a single TMS session of each protocol, which were applied in random order (iTBS 0–15 — two iTBS blocks over the left dorsolateral prefrontal cortex (DLPFC) iTBS with an interval of 15 min between blocks followed by stimulation of the vertex area in 60 min after the first block; iTBS 0–60 — iTBS block over the left DLPFC iTBS, block of the vertex stimulation after 15 min, and the second block of iTBS over the left DLPFC iTBS 60 min after the first one; iTBS 0 — one block of iTBS over the left DLPFC iTBS and two blocks of the vertex stimulation; control protocol — three blocks of the vertex stimulation with similar intervals). WM was assessed using the n-back test before the first block and after the second and the third stimulation blocks. No significant effects of protocols on WM or differences between protocols in alterations of test results and the responder rates to TMS between protocols were observed. The trend toward statistical significance was reported for the protocol with short interval (iTBS 0–15). Furthermore, low reproducibility of individual iTBS effect was reported. The study of protocols with short intervals between blocks involving larger cohort of volunteers and taking into account the other factors potentially influencing the effect of the protocol (number of blocks and duration of a single block) seems to be promising.

Keywords: transcranial magnetic stimulation, theta-burst stimulation, non-invasive brain stimulation, metaplasticity, working memory, left dorsolateral prefrontal cortex

Funding: the study was supported by the Russian Science Foundation (RSF), grant № 21-75-00040, <https://rscf.ru/en/project/21-75-00040/>.

Author contribution: Bakulin IS, Zabirowa AH — study planning and design; Bakulin IS, Zabirowa AH, Poydasheva AG, Lagoda DYU — experimentation and data acquisition; Bakulin IS, Zabirowa AH, Sinitsyn DO — data analysis; all authors — data interpretation; Bakulin IS, Zabirowa AH — writing the draft of the manuscript; all authors — manuscript editing.

Compliance with ethical standards: the study was approved by the Ethics Committee of the Research Center of Neurology (protocol № 8-8/21 of 15 September 2021), it was conducted in accordance with the principles of the Declaration of Helsinki. The informed consent was submitted by all study participants.

✉ **Correspondence should be addressed:** Alfia H. Zabirowa
Volokolamskoye shosse, 80, Moscow, 125367, Russia; alfijasabirowa@gmail.com

Received: 24.03.2023 **Accepted:** 14.04.2023 **Published online:** 25.04.2023

DOI: 10.24075/brsmu.2023.011

ЭФФЕКТ ОСНОВАННЫХ НА МЕТАПЛАСТИЧНОСТИ ПРОТОКОЛОВ ТРАНСКРАНИАЛЬНОЙ СТИМУЛЯЦИИ ТЕТА-ВСПЫШКАМИ НА ПОКАЗАТЕЛИ РАБОЧЕЙ ПАМЯТИ

И. С. Бакулин, А. Х. Забирова , А. Г. Пойдашева, Д. О. Синицын, Д. Ю. Лагода, Н. А. Супонева, М. А. Пирадов

Научный центр неврологии, Москва, Россия

Исследование протоколов транскраниальной магнитной стимуляции (ТМС), основанных на метапластичности, является интенсивно изучаемым подходом к улучшению эффективности стимуляции. Однако эффекты протоколов с разным интервалом между блоками ТМС в отношении когнитивных функций изучены недостаточно. Целью работы было оценить эффект двух протоколов стимуляции тета-вспышками (iTBS) с коротким и длинным интервалами между блоками на показатели рабочей памяти (РП) у здоровых добровольцев. В случайном порядке 16 участникам проводили по одной сессии ТМС каждым протоколом (iTBS 0–15 — два блока iTBS левой дорсолатеральной префронтальной коры (лДЛПФК) с интервалом 15 мин между ними и последующей стимуляцией области вертекса через 60 мин после первого блока; iTBS 0–60 — блок iTBS лДЛПФК, блок стимуляции вертекса через 15 мин и второй блок iTBS лДЛПФК через 60 мин после первого, iTBS 0 — один блок iTBS лДЛПФК с двумя блоками стимуляции вертекса и контрольный протокол — три блока стимуляции вертекса с аналогичными интервалами). РП оценивали с помощью теста n-back перед первым, после второго и третьего блоков стимуляции. Статистически значимых эффектов протоколов на РП, а также различий между протоколами по изменению показателей теста или количеству участников, ответивших на ТМС, обнаружено не было. Тенденция к статистической значимости показана для протокола с коротким интервалом (iTBS 0–15). Кроме того, подтверждена низкая индивидуальная воспроизводимость эффекта iTBS. Перспективными представляются исследование протоколов с коротким интервалом между блоками на более крупных выборках добровольцев, а также учет других факторов, потенциально влияющих на эффект протокола (количество блоков и длительность одного блока).

Ключевые слова: транскраниальная магнитная стимуляция, стимуляция тета-вспышками, неинвазивная нейромодуляция, метапластичность, рабочая память, левая дорсолатеральная префронтальная кора

Финансирование: исследование выполнено за счет гранта Российского научного фонда № 21-75-00040, <https://rscf.ru/project/21-75-00040/>.

Вклад авторов: И. С. Бакулин, А. Х. Забирова — планирование и дизайн исследования; И. С. Бакулин, А. Х. Забирова, А. Г. Пойдашева, Д. Ю. Лагода — проведение исследования и сбор данных; И. С. Бакулин, А. Х. Забирова, Д. О. Синицын — анализ данных; все авторы — интерпретация данных; И. С. Бакулин, А. Х. Забирова — подготовка черновика рукописи; все авторы — редактирование рукописи.

Соблюдение этических стандартов: исследование одобрено этическим комитетом ФГБНУ «Научный центр неврологии» (протокол № 8-8/21 от 15 сентября 2021 г.), проведено в соответствии с принципами Хельсинкской декларации. Все участники подписали добровольное информированное согласие.

✉ **Для корреспонденции:** Альфия Ходжаевна Забирова
Волоколамское шоссе, д. 80, г. Москва, 125367, Россия; alfijasabirowa@gmail.com

Статья получена: 24.03.2023 **Статья принята к печати:** 14.04.2023 **Опубликована онлайн:** 25.04.2023

DOI: 10.24075/vrgmu.2023.011

Transcranial magnetic stimulation (TMS) is widely used in clinical practice and research [1, 2]. However, high variability of effects is still an important limitation of the TMS use [3]. Protocols that are based on metaplasticity mechanisms are being actively developed in order to improve the effectiveness of TMS. According to this concept, the magnitude, direction, and duration of the synaptic plasticity processes depend on the previous synaptic activity. There can be additive or homeostatic metaplasticity [4, 5]. It has been shown that metaplasticity has a significant impact on the effects of the combinations of TMS protocols [6].

The effects of combined TMS protocols depend on both the type of individual blocks of stimulation and the intervals between blocks. The effects of intervals between blocks can be seen from the protocols that include several blocks of the same type [6–9]. These data provided the basis for the hypothesis of “critical window”, according to which homeostatic metaplasticity can be induced when applying the second stimulation block within an interval representing a middle third of the expected duration of the effect of a single block, and additive metaplasticity is induced when using a shorter or longer interval [6].

The protocols with short intervals between blocks (up to 20 min) were primarily studied in healthy volunteers, and these studies yielded conflicting data [7, 10, 11]. Our study of two combined intermittent theta-burst stimulation (iTBS) protocols with short (15 min) and long (60 min) intervals between the primary motor cortex stimulation blocks revealed no significant effects of individual protocols or differences between protocols when assessing the effects on the amplitude of motor evoked potentials (MEPs) and the responder rates [12].

The authors of the majority of papers studied effects on the motor cortex excitability. Despite the fact that stimulation of motor cortex provides a convenient model, the results should be extrapolated to other cortical areas with caution. Variability of the MEP amplitude is an important limitation of the neurophysiological assessment of the motor cortex stimulation effect [13]. It is therefore reasonable to study stimulation of non-motor areas and use behavioral and other measurements for assessment of the effect.

Considering these limitations, the study was aimed to assess the effects of iTBS protocols with short and long intervals between the blocks of stimulation over the left dorsolateral prefrontal cortex (DLPFC) on the scores the n-back test for assessment of verbal working memory (WM) in healthy volunteers and to perform comparison with the standard iTBS protocol and stimulation of the control site (vertex). The combined protocols were selected based on the “critical window” hypothesis [6].

METHODS

Subjects

The study was performed in the Research Center of Neurology in 2021–2022. Participants completed a questionnaire on contraindications to TMS before inclusion in the study. Medical history of each participant was obtained and demographic data were acquired, the subjects underwent routine electroencephalography (EEG) with standard functional tests in order to exclude epileptiform activity.

Inclusion criteria: informed consent; age 18–40 years.

Non-inclusion criteria: refusal to participate; contraindications to MRI and TMS [14]; epileptiform activity on EEG; the use of medications that exert effects on the central nervous system; neurological or mental disorders; chronic somatic disease.

Exclusion criteria: severe side effects revealed during the TMS procedure (epileptic seizure, syncope, etc.); the onset of somatic, mental or neurological disorder after inclusion; pacemaker implantation, intracardiac catheter insertion or brain surgery involving placing metal objects in the cranial cavity; getting pregnant; refusal to continue participating in the study.

A total of 22 volunteers were screened, among them two people had the non-inclusion criteria, the other two were unable to continue participating in the study for logistical reasons. Two people dropped out due to poor tolerability of TMS. Thus, a total of 16 subjects completed the study (6 males; average age 28.1 years).

Stimulation protocols

To construct an individual 3D model of the brain for navigated TMS, MRI was performed in the 3D-T1-MPR mode using the MAGNETOM Verio and MAGNETOM Prisma scanners (Siemens Healthcare GmbH; Germany) (voxel size 1.0 – 0.977 – 0.977 mm³, 176 sagittal slices).

The volunteers underwent four TMS sessions with an interval of at least 72 h (Fig. 1A). Such an interval seemed to be sufficient to minimize the impact of the previous session considering the duration of the single iTBS block effect [15]. The protocol sequences were randomized according to a Latin square approach to minimize the sequence effects. All attempts were made to perform sessions at the same time interval of the day (9–13 or 14–18 h). The participants were not informed about the sequence of protocols applied.

The following protocols were studied (Fig. 1B):

- the combined protocol with a short interval between blocks (iTBS 0–15): two consecutive blocks of active stimulation with a 15 min interval between blocks and a control stimulation block 60 min after the first block;
- the combined protocol with a long interval between blocks (iTBS 0–60): a block of active stimulation followed by a control stimulation block with an interval of 15 min and a block of active stimulation 60 min after the first block;
- the standard protocol (iTBS 0): a block of active stimulation followed by the control stimulation blocks in 15 and 60 min;
- the control protocol (Control): three control stimulation blocks with intervals of 15 and 60 min.

The iTBS procedure was performed using the MagPro X100 + MagOption stimulation device (Tonica Elektronik A/S; Denmark) with a liquid-cooled figure-eight coil in combination with the Localite TMS Navigator System (Localite GmbH; Germany) and the Axillum Robotics TMS-Cobot robotic positioning system (Axillum Robotics; France). Each stimulation block consisted of 20 cycles that included 10 bursts of three stimuli with a frequency of 50 Hz, applied with a frequency of 5 Hz and divided into 2-second trains with an intertrain interval of 8 s. The number of stimuli per block was 600. The left DLPFC, defined on MRI scans as a region of superior or middle frontal gyrus located about 5 cm from the “hot spot” of the first dorsal interosseous muscle cortical representation, was used as a target for active stimulation. The vertex area defined as a zone located halfway between the glabella and the occipital protuberance in the midsagittal plane was used as a target for control stimulation. The iTBS intensity constituted 75% of the resting motor threshold (rMT) defined using the Rossini-Rothwell algorithm, an intensity, for which the most prominent effect was previously shown [16]. rMT was determined before each session of stimulation. The questionnaires on adverse events (AEs) were completed during the TMS procedure and within 24 h after TMS in order to assess tolerability.

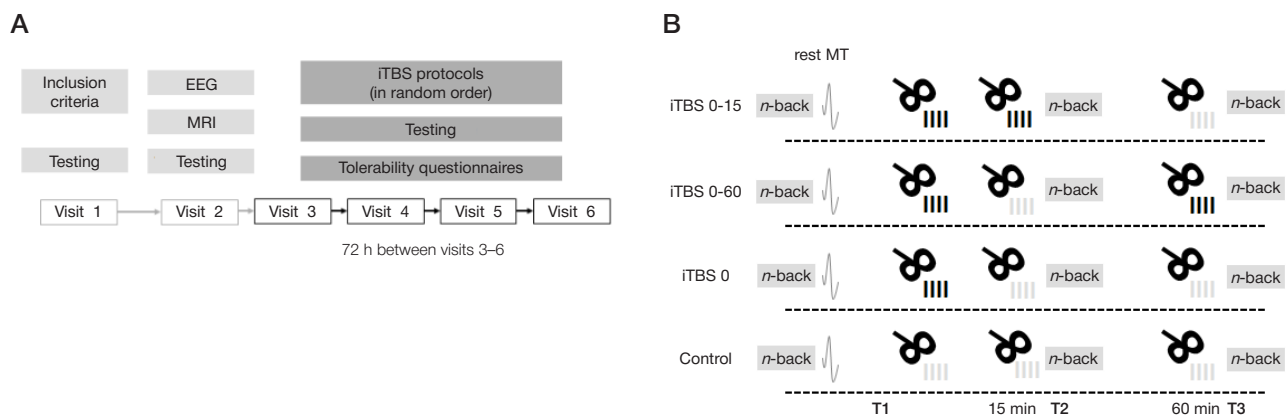


Fig. 1. A. Study design. B. Theta-burst stimulation protocols

Cognitive tests

Tests were performed using the Psychology Experiment Building Language (PEBL) open source software [17]. The *n*-back test involving presentation of verbal stimuli (Latin consonants) was performed with $n = 2, 3, 4$ (22, 23 and 24 stimuli per task, 6 matching letters per *n*). The training test was conducted twice in order to minimize the learning effect; furthermore, preliminary training test with $n = 1$ and 2 was performed prior to each session at the first testing. Performance was assessed three times: before the start of the first stimulation block (T1) and immediately after the second (T2) and the third (T3) stimulation blocks.

The *n*-back task accuracy was assessed by calculating d' -value [18].

$$d' = Z(\text{hit rate}) - Z(\text{false alarm rate}).$$

The calculation took into account the number of correct keystrokes in response to the concordant stimulus normalized to the total number of concordant stimuli (hit rate) and the number of false keystrokes in response to the discordant stimulus normalized to the total number of discordant stimuli

for each *n* (false alarm rate). Z transformation was applied to each normalized measurement.

Statistical analysis

The IBM SPSS Statistics (v.23) software package (IBM, SPSS Inc.; USA) was used for statistical analysis. Individual effects of each protocol at T2 and T3 (comparison of d' scores with T1) were assessed using the Wilcoxon's signed-rank test. The effects of the protocol at T2 and T3 were estimated as the difference between d' at this time point and the value at T1. The Friedman test was used to compare the effects of different protocols at T2 and T3.

Depending on the changes of d' at T2 and T3 the subjects were divided into responders (facilitators, when the difference was above 0, or inhibitors, when the difference was below 0) and non-responders (the difference between the values was 0). The proportions of responders were compared between the protocols using the binomial test (exact McNemar's test).

In addition, reproducibility of the effect of the combination of active stimulation block with the vertex stimulation (T2 in the iTBS 0-60 and iTBS 0 protocols) was assessed twice using Spearman's rank correlation coefficient and the

Table 1. The effects of iTBS protocols on the *n*-back test accuracy

Protocol	T2-T1	<i>p</i>	T3-T1	<i>p</i>
<i>n</i> = 2				
iTBS0-15	0	0.058	0	1
iTBS0-60	0	0.874	0.0435	0.2
iTBS0	0	0.502	0	0.866
Control	0	0.331	0	0.362
<i>n</i> = 3				
iTBS0-15	-0.003	0.363	0.555	0.054
iTBS0-60	-0.397	0.094	0.208	0.865
iTBS0	0.129	0.507	-0.106	0.851
Control	-0.268	0.495	0	0.944
<i>n</i> = 4				
iTBS0-15	0.186	0.28	0.292	0.624
iTBS0-60	0.058	0.875	-0.360	0.293
iTBS0	0.405	0.094	-0.484	0.14
Control	0	0.826	-0.405	0.078

Note: T2-T1 — median difference (d') between T2 and T1; T3-T1 — between T3 and T1; uncorrected *p*-values are provided.

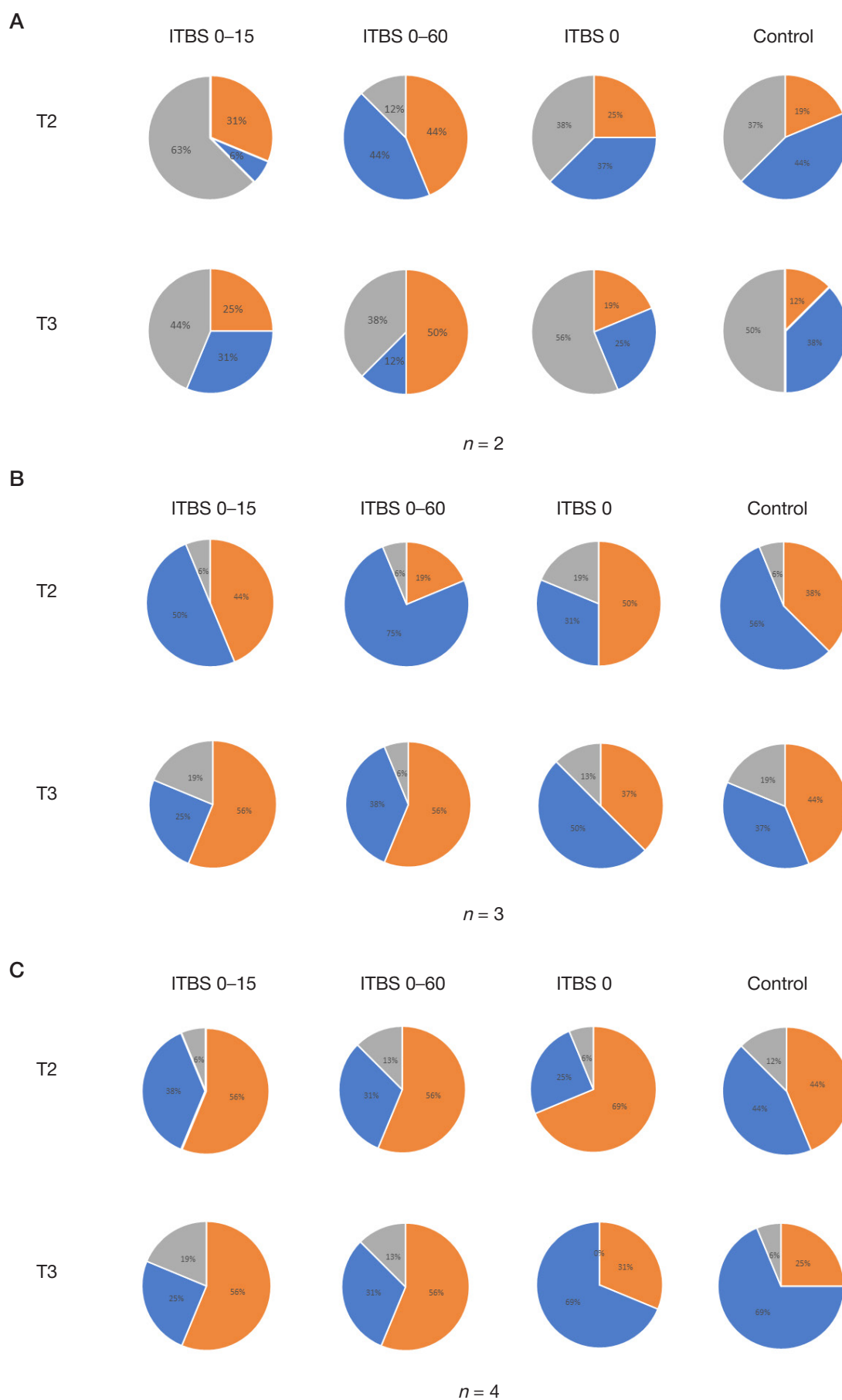


Fig. 2. Percentage of participants with various types of response to TMS protocols (A for $n = 2$, B for $n = 3$, C for $n = 4$). Facilitation is highlighted in orange, inhibition in blue, and no response in grey

Table 2. *P*-values for comparison of the number of subjects with various response types between protocols (uncorrected)

<i>n</i>	T	iTBS 0–15 vs. iTBS 0–60	iTBS 0–15 vs. iTBS 0	iTBS 0–15 vs. Control	iTBS 0–60 vs. iTBS 0	iTBS 0–60 vs. Control	iTBS 0 vs. Control
Facilitation							
<i>n</i> = 2	T2	0.726	1	0.688	0.549	0.289	1
	T3	0.289	1	0.688	0.18	0.07	1
<i>n</i> = 3	T2	0.289	1	1	0.227	0.375	0.754
	T3	1	0.508	0.754	0.508	0.688	1
<i>n</i> = 4	T2	1	0.727	0.688	0.727	0.754	0.219
	T3	0.289	0.289	0.125	1	1	1
Inhibition							
<i>n</i> = 2	T2	0.031	0.125	0.07	1	1	1
	T3	1	1	0.453	0.688	0.289	0.688
<i>n</i> = 3	T2	0.219	0.549	1	0.039	0.375	0.289
	T3	0.688	0.289	0.727	0.754	1	0.727
<i>n</i> = 4	T2	1	0.727	1	1	0.727	0.375
	T3	0.07	0.065	0.039	1	1	1

association analysis of the response type at T2 using the Fisher's exact test.

RESULTS

Assessing the effects of individual protocols

Assessment of the effects of protocols on the *n*-back accuracy at T2 and T3 revealed no significant differences (Table 1). The lowest *p*-values were obtained for the accuracy of *n*-back test with *n* = 2 after the second stimulation block of the iTBS 0–15 protocol (*p* = 0.058), and for *n* = 3 after the third stimulation block of the same protocol (*p* = 0.054); the Bonferroni adjusted *p*-value were 1.

The percentage of subjects showing different response to TMS at T2 and T3 was calculated for each protocol (Fig. 2)

Comparing the effects of protocols

No significant differences in the effects between protocols for any of *n*-values were revealed when performing comparison at T2 (Friedman test; uncorrected *p* = 0.6, 0.62 and 0.428 for *n* = 2, 3, 4, respectively) and T3 (*p* = 0.283, 0.294 and 0.13). No differences were found when comparing the effects immediately after two blocks of active stimulation, i.e. between iTBS 0–15 at T2 and iTBS 0–60 at T3 (Wilcoxon's signed-rank test; uncorrected *p* = 0.372; *p* = 0.535; *p* = 0.211 for *n* = 2, 3 and 4).

Assessing the differences in the direction of the TMS protocol effects

As for the rate of participants showing facilitation, no significant differences were revealed (Table 2). Uncorrected

p-values lower than 0.05 were obtained when comparing the percentage of subjects showing inhibition in the iTBS 0–15 and iTBS 0–60 protocols at T2 for *n* = 2 and the iTBS 0–15 and Control protocols at T3 for *n* = 4. Furthermore, comparison of inhibition in the iTBS 0–15 and iTBS 0–60 protocols at T2 yielded a *p*-value lower than 0.05. The Bonferroni adjusted *p*-values for these tests were 1.

Assessing reproducibility of the effect

A *p*-value of 0.02 was obtained for *n* = 2 (negative Spearman's sample correlation coefficient), the Bonferroni adjusted *p*-value was 0.06 (Table 3).

Association analysis of both facilitation and inhibition revealed no significant correlation between the iTBS 0–60 and iTBS 0 protocols (Table 4). Furthermore, only 6 subjects out of 16 (37.5%) showed facilitation at T2 for *n* = 4 in both protocols, iTBS 0–60 and iTBS 0, while the lower complexity tests revealed no subjects showing similar facilitatory response to both protocols.

Tolerability of protocols

The studied TMS protocols were characterized by favorable safety profile. No serious AEs were reported. Two volunteers discontinued participation in the study due to poor tolerance (one case of severe pain during stimulation of the left DLPFC and one case of headache during stimulation of the vertex persisting for a few hours after stimulation and resolving after taking ibuprofen). The AEs reported during the 67.2% of session and within 24 h after 8% of the assessed sessions were mild and had no impact on the desire to continue participation in the study. Pain and sleepiness were most often reported during stimulation (28.3% each), along with the contraction of

Table 3. Correlation of the effects of two iterations of the combination of active stimulation block with the vertex stimulation (T2 in the iTBS 0–60 and iTBS 0 protocols) with the *n*-back test accuracy

<i>n</i>	<i>n</i> = 2		<i>n</i> = 3		<i>n</i> = 4	
Parameter	<i>ρ</i>	<i>p</i>	<i>ρ</i>	<i>p</i>	<i>ρ</i>	<i>p</i>
iTBS 0–60 vs. iTBS 0 (T2)	–0.573	0.02	–0.157	0.563	0.274	0.304

Note: *ρ* — Spearman's rank correlation coefficient, *p* — uncorrected *p*-value.

Table 4. Association analysis of the direction of responses to two iterations of the combination of active stimulation block with the vertex stimulation (T2 in the iTBS 0–60 and iTBS 0 protocols)

Facilitation				
$n = 2$		Facilitation in iTBS 0	No facilitation in iTBS 0	$p = 0.088$
	Facilitation in iTBS 0–60	0/16	7/16	
	No facilitation in iTBS 0–60	4/16	5/16	
$n = 3$		Facilitation in iTBS 0	No facilitation in iTBS 0	$p = 0.200$
	Facilitation in iTBS 0–60	0/16	3/16	
	No facilitation in iTBS 0–60	8/16	5/16	
$n = 4$		Facilitation in iTBS 0	No facilitation in iTBS 0	$p = 1$
	Facilitation in iTBS 0–60	6/16	3/16	
	No facilitation in iTBS 0–60	5/16	2/16	
Inhibition				
$n = 2$		Inhibition in iTBS 0	No inhibition in iTBS 0	$p = 0.633$
	Inhibition in iTBS 0–60	2/16	5/16	
	No inhibition in iTBS 0–60	4/16	5/16	
$n = 3$		Inhibition in iTBS 0	No inhibition in iTBS 0	$p = 1$
	Inhibition in iTBS 0–60	4/16	8/16	
	No inhibition in iTBS 0–60	1/16	3/16	
$n = 4$		Inhibition in iTBS 0	No inhibition in iTBS 0	$p = 0.546$
	Inhibition in iTBS 0–60	2/16	3/16	
	No inhibition in iTBS 0–60	2/16	9/16	

Note: uncorrected p -values are provided (Fisher's exact test).

facial muscles in the vicinity of the left DLPFC (9%); within 24 h headache was the only AE reported (8%).

DISCUSSION

The aim of the study was to assess the effects of two metaplasticity-based theta-burst stimulation protocols of the left DLPFC with short and long intervals between blocks on the WM performance in healthy individuals. The effects were also compared with that of the standard and control protocols. We estimated the differences in the number of participants with the same direction of stimulation effects in various protocols as well. The protocols applied were safe and well tolerated. No convincing data to confirm the effectiveness of individual protocols on the WM or variability of the response to stimulation were obtained. Low reproducibility of individual iTBS effects was reported.

The effect of a single iTBS block on the WM performance in healthy individuals was explored in a number of projects, however, these studies yielded inconsistent results [16, 19–21]. Variability of response to stimulation confirmed for the effect on the motor cortex excitability can be one of the sources of differences [22, 23]. At the same time, variability of the iTBS effects in terms of WM is still poorly understood.

The use of metaplasticity-based protocols is a method to potentially increase the effectiveness of TMS, however, the problem of optimal interval between blocks of stimulation is not resolved. We compared the effects of protocols with short and long intervals between active stimulation blocks on the WM performance. No significant differences between the test results for individual protocols were reported. Furthermore, comparison of metaplasticity-based protocols with the standard and control protocols revealed no significant differences in alterations of the n -back test accuracy at both time points. There were also no significant differences in the number of subjects who showed better (facilitation) or worse (inhibition) performance during testing between protocols. Such results are consistent with our

previously reported data obtained for the effects on the motor cortex excitability [12].

At the same time, a possible trend toward statistical significance of the effects of the protocol with short interval between blocks (iTBS 0–15) on the n -back test with $n = 2$, when performing measurement after the second block, and $n = 3$, when performing measurement after the third block, is noteworthy. In the studied sample, a lower number of participants, who showed inhibitory response after the second stimulation block in this protocol, compared to the iTBS 0–60 protocol for $n = 2$, and after the control protocol for $n = 4$, was also observed. It is interesting to note that the stimulation protocol consisting of three blocks with an interval of 15 min between blocks significantly improved the visuospatial WM, executive functions [24], and decision-making in healthy individuals [25]. Furthermore, it was shown that 14 sessions of stimulation using this protocol improved cognitive functions in patients with Alzheimer's disease [26]. In our opinion, it seems appropriate to continue studying the effects of protocols with short intervals between blocks (15 min) on cognitive functions.

In addition, we assessed reproducibility of the iTBS 0–60 and iTBS 0 protocol effects after the second stimulation block. No significant correlation of the effect or association of the response direction between two protocols was reported. Assessment of the tests with $n = 2$ and 3 yielded 0% of participants showing facilitation, while the percentage for $n = 4$ was 37.5%. The findings are consistent with the results of earlier studies focused on assessing variability of the response to a single block of the motor cortex theta-burst stimulation [7, 22, 23]. We can conclude that the response to iTBS has low intra-individual variability in terms of both motor cortex excitability and cognitive performance. In our study, the sources of variability associated with anatomical features and the changes in the coil position were minimized by MRI navigation and the use of robotic coil positioning system, therefore, it can be assumed that intra-individual variability of the response to iTBS is the cause of insufficient stimulation effect reproducibility.

The lack of stimulation effect reported in our study may result from insufficient number of active stimulation blocks. The earlier reported study also showed no significant effect of two blocks of the left DLPFC iTBS with an interval of 15 min between blocks on the *n*-back test results [21]. The assumption of the higher effectiveness of protocols consisting of three blocks is in line with the results of the earlier study showing a significant effect of three, not two, blocks of motor cortex stimulation with an interval of 15 min between blocks [27], and with the earlier reported data on the effectiveness of the DLPFC stimulation protocol consisting of three blocks with an interval of 15 min [24]. It should be noted that the metaplasticity-based stimulation protocols than have shown some clinical efficacy, for example in drug-resistant depression [28, 29] or spasticity associated with multiple sclerosis [30], consist of 10 and three stimulation blocks, respectively.

Furthermore, the duration of a single block may have an impact on its effect. The protocols that have shown clinical efficacy comprise prolonged stimulation blocks (1800 stimuli compared to 600 in the standard one) [28–30]. However, to date, the effects of prolonged iTBS blocks on cognitive functions are poorly understood.

Small cohort size can be considered one of the limitations of the study, however, in the current pilot study the sample size may be enough for detection of large effects and selection of the most effective protocols to be studied in the larger cohorts. Furthermore, the crossover study design can affect the test results due to learning effect. On the other hand, the impact of this effect seems to be minimal: first, when performing re-tests within the protocol the effect is controlled by comparison with the protocol comprising the same number of the vertex stimulation blocks. Second, the average effect values reported

during sessions do not depend on possible effects of the session sequence number due to Latin square randomization, i.e. possible learning effect between sessions does not cause bias in estimates of the differences between protocols.

The use of only one *n*-back test with verbal stimuli can be considered one more limitation of the study. However, it is widely used in neuropsychological research for assessment of WM. It is also necessary to bear in mind the ceiling effect observed when performing the lowest complexity test (*n* = 2). Such an effect can explain a high non-responder rate observed at this *n*. A small number of stimuli per task can be considered one more limitation that should be taken into account when performing further research. Furthermore, we assessed the effects of stimulation immediately after the second and the third block. This does not exclude possible delayed effects [19].

It should be noted that the lack of effects of metaplasticity-based protocols on both cognitive test results and neurophysiological parameters in healthy volunteers does not mean a lack of clinical efficacy. It is important to consider that metaplasticity patterns observed in patients and healthy volunteers may be different, that is why the findings should be translated into clinical practice with caution.

CONCLUSIONS

The study yielded no convincing data to support the effectiveness of the metaplasticity-based protocols on the WM performance and direction of the response to stimulation in healthy individuals. Considering the findings and limitations, further study of the effects of protocols with short intervals between blocks consisting of the larger number of stimulation blocks and comprising prolonged iTBS blocks seems to be promising.

References

1. Beynel L, Appelbaum LG, Luber B, Crowell CA, Hilbig SA, Lim W, et al. Effects of online repetitive transcranial magnetic stimulation (rTMS) on cognitive processing: A meta-analysis and recommendations for future studies. *Neurosci Biobehav Rev*. 2019; 107: 47–58. DOI: 10.1016/j.neubiorev.2019.08.018. PMID: 31473301; PMCID: PMC7654714.
2. Lefaucheur JP, Aleman A, Baeken C, Benninger DH, Brunelin J, Di Lazzaro V, et al. Evidence-based guidelines on the therapeutic use of repetitive transcranial magnetic stimulation (rTMS): An update (2014–2018). *Clin Neurophysiol*. 2020; 131 (2): 474–528. DOI: 10.1016/j.clinph.2019.11.002. PMID: 31901449.
3. Goldsworthy MR, Hordacre B, Rothwell JC, Ridding MC. Effects of rTMS on the brain: is there value in variability? *Cortex*. 2021; 139: 43–59. DOI: 10.1016/j.cortex.2021.02.024. PMID: 33827037.
4. Abraham WC, Bear MF. Metaplasticity: the plasticity of synaptic plasticity. *Trends Neurosci*. 1996; 19 (4): 126–30. DOI: 10.1016/S0166-2236(96)80018-X. PMID: 8658594.
5. Bakulin IS, Poydasheva AG, Zabirowa AH, Suponeva NA, Piradov MA. Metaplasticity and non-invasive brain stimulation: the search for new biomarkers and directions for therapeutic neuromodulation. *Annals of clinical and experimental neurology*. 2022; 16(3): 74–82. Russian. DOI: 10.54101/ACEN.2022.3.9.
6. Hassanzahraee M, Zoghi M, Jaberzadeh S. How different priming stimulations affect the corticospinal excitability induced by noninvasive brain stimulation techniques: a systematic review and meta-analysis. *Rev Neurosci*. 2018; 29 (8): 883–99. DOI: 10.1515/revneuro-2017-0111. PMID: 29604209.
7. Tse NY, Goldsworthy MR, Ridding MC, Coxon JP, Fitzgerald PB, Fornito A, et al. The effect of stimulation interval on plasticity following repeated blocks of intermittent theta burst stimulation. *Sci Rep*. 2018; 8 (1): 8526. DOI: 10.1038/s41598-018-26791-w. PMID: 29867191.
8. Thomson AC, Sack AT. How to Design Optimal Accelerated rTMS Protocols Capable of Promoting Therapeutically Beneficial Metaplasticity. *Front Neurol*. 2020; 11: 599918. DOI: 10.3389/fneur.2020.599918. PMID: 33224103.
9. Yu F, Tang X, Hu R, Liang S, Wang W, Tian S, et al. The After-Effect of Accelerated Intermittent Theta Burst Stimulation at Different Session Intervals. *Front Neurosci*. 2020; 14: 576. DOI: 10.3389/fnins.2020.00576. Erratum in: *Front Neurosci*. 2021; 15: 687972. PMID: 32670006.
10. Gamboa OL, Antal A, Laczó B, Molácz V, Nitsche MA, Paulus W. Impact of repetitive theta burst stimulation on motor cortex excitability. *Brain Stimul*. 2011; 4 (3): 145–51. DOI: 10.1016/j.brs.2010.09.008. PMID: 21777874.
11. Murakami T, Müller-Dahlhaus F, Lu MK, Ziemann U. Homeostatic metaplasticity of corticospinal excitatory and intracortical inhibitory neural circuits in human motor cortex. *J Physiol*. 2012; 590 (22): 5765–81. DOI: 10.1113/jphysiol.2012.238519. PMID: 22930265.
12. Bakulin I, Zabirowa A, Sinitsyn D, Poydasheva A, Lagoda D, Suponeva N, et al. Adding a Second iTBS Block in 15 or 60 Min Time Interval Does Not Increase iTBS Effects on Motor Cortex Excitability and the Responder Rates. *Brain Sci*. 2022; 12 (8): 1064. DOI: 10.3390/brainsci12081064. PMID: 36009127.
13. Vallence AM, Goldsworthy MR, Hodyl NA, Semmler JG, Pitcher JB, Ridding MC. Inter- and intra-subject variability of motor cortex plasticity following continuous theta-burst stimulation. *Neuroscience*. 2015; 304: 266–78. DOI: 10.1016/j.neuroscience.2015.07.043. PMID: 26208843.
14. Rossi S, Hallett M, Rossini PM, Pascual-Leone A, Safety of TMS Consensus Group. Safety, ethical considerations, and application guidelines for the use of transcranial magnetic stimulation in

- clinical practice and research. *Clin Neurophysiol.* 2009; 120 (12): 2008–39. DOI: 10.1016/j.clinph.2009.08.016. PMID: 19833552.
15. Rounis E, Huang YZ. Theta burst stimulation in humans: a need for better understanding effects of brain stimulation in health and disease. *Exp Brain Res.* 2020; 238 (7–8): 1707–14. DOI: 10.1007/s00221-020-05880-1. PMID: 32671422.
 16. Chung SW, Rogasch NC, Hoy KE, Sullivan CM, Cash RFH, Fitzgerald PB. Impact of different intensities of intermittent theta burst stimulation on the cortical properties during TMS-EEG and working memory performance. *Hum Brain Mapp.* 2018; 39 (2): 783–802. DOI: 10.1002/hbm.23882. PMID: 29124791.
 17. Mueller ST, Piper BJ. The Psychology Experiment Building Language (PEBL) and PEBL Test Battery. *J Neurosci Methods.* 2014; 222: 250–9. DOI: 10.1016/j.jneumeth.2013.10.024. PMID: 24269254.
 18. Haatveit BC, Sundet K, Hugdahl K, Ueland T, Melle I, Andreassen OA. The validity of d prime as a working memory index: results from the "Bergen n-back task". *J Clin Exp Neuropsychol.* 2010; 32 (8): 871–80. DOI: 10.1080/13803391003596421. PMID: 20383801.
 19. Hoy KE, Bailey N, Michael M, Fitzgibbon B, Rogasch NC, Saeki T, et al. Enhancement of Working Memory and Task-Related Oscillatory Activity Following Intermittent Theta Burst Stimulation in Healthy Controls. *Cereb Cortex.* 2016; 26 (12): 4563–73. DOI: 10.1093/cercor/bhv193. PMID: 26400923.
 20. Viejo-Sobera R, Redolar-Ripoll D, Boixadós M, Palaus M, Valero-Cabré A, Marron EM. Impact of Prefrontal Theta Burst Stimulation on Clinical Neuropsychological Tasks. *Front Neurosci.* 2017; 11: 462. DOI: 10.3389/fnins.2017.00462. PMID: 28867993.
 21. Chung SW, Rogasch NC, Hoy KE, Fitzgerald PB. The effect of single and repeated prefrontal intermittent theta burst stimulation on cortical reactivity and working memory. *Brain Stimul.* 2018; 11 (3): 566–74. DOI: 10.1016/j.brs.2018.01.002. PMID: 29352668.
 22. Perellón-Alfonso R, Kralik M, Pilecky I, Princic M, Bon J, Matzhold C, et al. Similar effect of intermittent theta burst and sham stimulation on corticospinal excitability: A 5-day repeated sessions study. *Eur J Neurosci.* 2018; 48 (4): 1990–2000. DOI: 10.1111/ejn.14077. PMID: 30022548.
 23. Boucher PO, Ozdemir RA, Momi D, Burke MJ, Jannati A, Fried PJ, et al. Sham-derived effects and the minimal reliability of theta burst stimulation. *Sci Rep.* 2021; 11 (1): 21170. DOI: 10.1038/s41598-021-98751-w. PMID: 34707206.
 24. Wu X, Wang L, Geng Z, Wei L, Yan Y, Xie C, et al. Improved Cognitive Promotion through Accelerated Magnetic Stimulation. *eNeuro.* 2021; 8 (1): ENEURO.0392-20.2020. DOI: 10.1523/ENEURO.0392-20.2020. PMID: 33452108.
 25. Wang L, Wu X, Ji GJ, Xiao G, Xu F, Yan Y, et al. Better modulation for risk decision-making after optimized magnetic stimulation. *J Neurosci Res.* 2021; 99 (3): 858–71. DOI: 10.1002/jnr.24772. PMID: 33617027.
 26. Wu X, Ji GJ, Geng Z, Wang L, Yan Y, Wu Y, et al. Accelerated intermittent theta-burst stimulation broadly ameliorates symptoms and cognition in Alzheimer's disease: A randomized controlled trial. *Brain Stimul.* 2022; 15 (1): 35–45. DOI: 10.1016/j.brs.2021.11.007. PMID: 34752934.
 27. Nettekoven C, Volz LJ, Kutscha M, Pool EM, Rehme AK, Eickhoff SB, et al. Dose-dependent effects of theta burst rTMS on cortical excitability and resting-state connectivity of the human motor system. *J Neurosci.* 2014; 34 (20): 6849–59. DOI: 10.1523/JNEUROSCI.4993-13.2014. PMID: 24828639.
 28. Poydasheva AG, Bakulin IS, Sinitsyn DO, Zabirowa AH, Suponeva NA, Maslenikov NV, et al. Experience of Stanford neuromodulation therapy in patients with treatment-resistant depression. *Bulletin of RSMU.* 2022; (4): 31–7. Russian. DOI: 10.24075/brsmu.2022.044.
 29. Cole EJ, Phillips AL, Bentzley BS, Stimpson KH, Nejad R, Barnak F, et al. Stanford Neuromodulation Therapy (SNT): A Double-Blind Randomized Controlled Trial. *Am J Psychiatry.* 2022; 179 (2): 132–41. DOI: 10.1176/appi.ajp.2021.20101429. PMID: 34711062.
 30. Bakulin IS, Poydasheva AG, Zabirowa AH, Lagoda DY, Rimkevichus AA, Zakharova MN, et al. Use of a metaplasticity-based protocol of therapeutic transcranial magnetic stimulation in patients with progressive multiple sclerosis and spasticity: first experience. *Neuromuscular Diseases.* 2022; 12 (3): 26–35. DOI: 10.17650/2222-8721-2022-12-3-26-35. Russian.

Литература

1. Beynel L, Appelbaum LG, Lubner B, Crowell CA, Hilbig SA, Lim W, et al. Effects of online repetitive transcranial magnetic stimulation (rTMS) on cognitive processing: A meta-analysis and recommendations for future studies. *Neurosci Biobehav Rev.* 2019; 107: 47–58. DOI: 10.1016/j.neubiorev.2019.08.018. PMID: 31473301; PMCID: PMC7654714.
2. Lefaucheur JP, Aleman A, Baeken C, Benninger DH, Brunelin J, Di Lazzaro V, et al. Evidence-based guidelines on the therapeutic use of repetitive transcranial magnetic stimulation (rTMS): An update (2014–2018). *Clin Neurophysiol.* 2020; 131 (2): 474–528. DOI: 10.1016/j.clinph.2019.11.002. PMID: 31901449.
3. Goldsworthy MR, Hordacre B, Rothwell JC, Ridding MC. Effects of rTMS on the brain: is there value in variability? *Cortex.* 2021; 139: 43–59. DOI: 10.1016/j.cortex.2021.02.024. PMID: 33827037.
4. Abraham WC, Bear MF. Metaplasticity: the plasticity of synaptic plasticity. *Trends Neurosci.* 1996; 19 (4): 126–30. DOI: 10.1016/s0166-2236(96)80018-x. PMID: 8658594.
5. Бакулин И. С., Пойдашева А. Г., Забиrowa А. Х., Супонева Н. А., Пирадов М. А. Метапластичность и неинвазивная стимуляция мозга: поиск новых биомаркеров и направлений терапевтической нейромодуляции. *Анналы клинической и экспериментальной неврологии.* 2022; 16 (3): 74–82. DOI: 10.54101/ACEN.2022.3.9.
6. Hassanzahraee M, Zoghi M, Jaberzadeh S. How different priming stimulations affect the corticospinal excitability induced by noninvasive brain stimulation techniques: a systematic review and meta-analysis. *Rev Neurosci.* 2018; 29 (8): 883–99. DOI: 10.1515/revneuro-2017-0111. PMID: 29604209.
7. Tse NY, Goldsworthy MR, Ridding MC, Coxon JP, Fitzgerald PB, Fornito A, et al. The effect of stimulation interval on plasticity following repeated blocks of intermittent theta burst stimulation. *Sci Rep.* 2018; 8 (1): 8526. DOI: 10.1038/s41598-018-26791-w. PMID: 29867191.
8. Thomson AC, Sack AT. How to Design Optimal Accelerated rTMS Protocols Capable of Promoting Therapeutically Beneficial Metaplasticity. *Front Neurol.* 2020; 11: 599918. DOI: 10.3389/fneur.2020.599918. PMID: 33224103.
9. Yu F, Tang X, Hu R, Liang S, Wang W, Tian S, et al. The After-Effect of Accelerated Intermittent Theta Burst Stimulation at Different Session Intervals. *Front Neurosci.* 2020; 14: 576. DOI: 10.3389/fnins.2020.00576. Erratum in: *Front Neurosci.* 2021; 15: 687972. PMID: 32670006.
10. Gamboa OL, Antal A, Laczó B, Moliadze V, Nitsche MA, Paulus W. Impact of repetitive theta burst stimulation on motor cortex excitability. *Brain Stimul.* 2011; 4 (3): 145–51. DOI: 10.1016/j.brs.2010.09.008. PMID: 21777874.
11. Murakami T, Müller-Dahlhaus F, Lu MK, Ziemann U. Homeostatic metaplasticity of corticospinal excitatory and intracortical inhibitory neural circuits in human motor cortex. *J Physiol.* 2012; 590 (22): 5765–81. DOI: 10.1113/jphysiol.2012.238519. PMID: 22930265.
12. Bakulin I, Zabirowa A, Sinitsyn D, Poydasheva A, Lagoda D, Suponeva N, et al. Adding a Second iTBS Block in 15 or 60 Min Time Interval Does Not Increase iTBS Effects on Motor Cortex Excitability and the Responder Rates. *Brain Sci.* 2022; 12 (8): 1064. DOI: 10.3390/brainsci12081064. PMID: 36009127.
13. Vallence AM, Goldsworthy MR, Hodyl NA, Semmler JG, Pitcher JB, Ridding MC. Inter- and intra-subject variability of motor cortex plasticity following continuous theta-burst stimulation. *Neuroscience.* 2015; 304: 266–78. DOI: 10.1016/j.neuroscience.2015.07.043. PMID: 26208843.
14. Rossi S, Hallett M, Rossini PM, Pascual-Leone A, Safety of TMS Consensus Group. Safety, ethical considerations, and application

- guidelines for the use of transcranial magnetic stimulation in clinical practice and research. *Clin Neurophysiol.* 2009; 120 (12): 2008–39. DOI: 10.1016/j.clinph.2009.08.016. PMID: 19833552.
15. Rounis E, Huang YZ. Theta burst stimulation in humans: a need for better understanding effects of brain stimulation in health and disease. *Exp Brain Res.* 2020; 238 (7–8): 1707–14. DOI: 10.1007/s00221-020-05880-1. PMID: 32671422.
 16. Chung SW, Rogasch NC, Hoy KE, Sullivan CM, Cash RFH, Fitzgerald PB. Impact of different intensities of intermittent theta burst stimulation on the cortical properties during TMS-EEG and working memory performance. *Hum Brain Mapp.* 2018; 39 (2): 783–802. DOI: 10.1002/hbm.23882. PMID: 29124791.
 17. Mueller ST, Piper BJ. The Psychology Experiment Building Language (PEBL) and PEBL Test Battery. *J Neurosci Methods.* 2014; 222: 250–9. DOI: 10.1016/j.jneumeth.2013.10.024. PMID: 24269254.
 18. Haatveit BC, Sundet K, Hugdahl K, Ueland T, Melle I, Andreassen OA. The validity of d prime as a working memory index: results from the "Bergen n-back task". *J Clin Exp Neuropsychol.* 2010; 32 (8): 871–80. DOI: 10.1080/13803391003596421. PMID: 20383801.
 19. Hoy KE, Bailey N, Michael M, Fitzgibbon B, Rogasch NC, Saeki T, et al. Enhancement of Working Memory and Task-Related Oscillatory Activity Following Intermittent Theta Burst Stimulation in Healthy Controls. *Cereb Cortex.* 2016; 26 (12): 4563–73. DOI: 10.1093/cercor/bhv193. PMID: 26400923.
 20. Viejo-Sobera R, Redolar-Ripoll D, Boixadós M, Palau M, Valero-Cabré A, Marron EM. Impact of Prefrontal Theta Burst Stimulation on Clinical Neuropsychological Tasks. *Front Neurosci.* 2017; 11: 462. DOI: 10.3389/fnins.2017.00462. PMID: 28867993.
 21. Chung SW, Rogasch NC, Hoy KE, Fitzgerald PB. The effect of single and repeated prefrontal intermittent theta burst stimulation on cortical reactivity and working memory. *Brain Stimul.* 2018; 11 (3): 566–74. DOI: 10.1016/j.brs.2018.01.002. PMID: 29352668.
 22. Perellón-Alfonso R, Kralik M, Pileckyte I, Princic M, Bon J, Matzhöld C, et al. Similar effect of intermittent theta burst and sham stimulation on corticospinal excitability: A 5-day repeated sessions study. *Eur J Neurosci.* 2018; 48 (4): 1990–2000. DOI: 10.1111/ejn.14077. PMID: 30022548.
 23. Boucher PO, Ozdemir RA, Momi D, Burke MJ, Jannati A, Fried PJ, et al. Sham-derived effects and the minimal reliability of theta burst stimulation. *Sci Rep.* 2021; 11 (1): 21170. DOI: 10.1038/s41598-021-98751-w. PMID: 34707206.
 24. Wu X, Wang L, Geng Z, Wei L, Yan Y, Xie C, et al. Improved Cognitive Promotion through Accelerated Magnetic Stimulation. *eNeuro.* 2021; 8 (1): ENEURO.0392-20.2020. DOI: 10.1523/ENEURO.0392-20.2020. PMID: 33452108.
 25. Wang L, Wu X, Ji GJ, Xiao G, Xu F, Yan Y, et al. Better modulation for risk decision-making after optimized magnetic stimulation. *J Neurosci Res.* 2021; 99 (3): 858–71. DOI: 10.1002/jnr.24772. PMID: 33617027.
 26. Wu X, Ji GJ, Geng Z, Wang L, Yan Y, Wu Y, et al. Accelerated intermittent theta-burst stimulation broadly ameliorates symptoms and cognition in Alzheimer's disease: A randomized controlled trial. *Brain Stimul.* 2022; 15 (1): 35–45. DOI: 10.1016/j.brs.2021.11.007. PMID: 34752934.
 27. Nettekoven C, Volz LJ, Kutscha M, Pool EM, Rehme AK, Eickhoff SB, et al. Dose-dependent effects of theta burst rTMS on cortical excitability and resting-state connectivity of the human motor system. *J Neurosci.* 2014; 34 (20): 6849–59. DOI: 10.1523/JNEUROSCI.4993-13.2014. PMID: 24828639.
 28. Пойдашева А. Г., Бакулин И. С., Силицын Д. О., Забиров А. Х., Супонева Н. А., Маслеников Н. В. и др. Опыт применения Стэнфордской нейромодулирующей терапии у пациентов с терапевтически резистентной депрессией. *Вестник РГМУ.* 2022; (4): 35–42. DOI: 10.24075/vrgmu.2022.044
 29. Cole EJ, Phillips AL, Bentzley BS, Stimpson KH, Nejad R, Barmak F, et al. Stanford Neuromodulation Therapy (SNT): A Double-Blind Randomized Controlled Trial. *Am J Psychiatry.* 2022; 179 (2): 132–41. DOI: 10.1176/appi.ajp.2021.20101429. PMID: 34711062.
 30. Бакулин И. С., Пойдашева А. Г., Забиров А. Х., Лагода Д. Ю., Римкевичус А. А., Захарова М. Н. и др. Первый опыт терапевтической транскраниальной магнитной стимуляции при прогрессирующем рассеянном склерозе и спастичности по протоколу, основанному на метапластичности. *Нервно-мышечные болезни.* 2022; 12 (3): 26–35. DOI: 10.17650/2222-8721-2022-12-3-26-35.

SOURCES AND IMPACT OF HUMAN BRAIN POTENTIAL VARIABILITY IN THE BRAIN-COMPUTER INTERFACE

Ganin IP¹✉, Vasilyev AN^{1,2}, Glazova TD¹, Kaplan AY¹

¹ Lomonosov Moscow State University, Moscow, Russia

² Neurocognitive Research Center (MEG Center), Moscow State University of Psychology and Education, Moscow, Russia

In the brain-computer interface based on the P300 wave (P300 BCI), the selection of the command by the user becomes possible due to focusing the user's attention on the external stimulus/command and extraction of the response to this stimulus in the form of the event-related potential (ERP) components from EEG. To obtain the ERP signal, stimuli should be repeated many times, however, in view of the existing variability in latency of the response to certain stimuli, the averaged ERPs may give a distorted view of the nature of such responses and reduce accuracy of the interface. The study was aimed to develop an effective method for identification of the effects of the ERP components' latency variability and for accounting these effects in the P300 BCI, as well as to identify the possible impact of psychophysiological factors on the nature of ERP variability. We have conducted a BCI-based study of 19 healthy subjects involving extraction and adjustment of latency in the N1 and P300 spatial components, which play a key role in the command classification in the P300 BCI, to explore the mechanisms underlying variability. Such an approach ensured higher accuracy compared to the use of conventional EEG leads, and the highest increase of 10% was observed when using the minimum number of the stimulus repetitions. Furthermore, modifications of the interface allowing one to ensure a higher level of the user's focus on the task and a more accurate visual fixation on the target objects contributed to the increase in the amplitude of the ERP components by reducing variability of the responses to single stimuli. The findings emphasize the important role of the processes underlying the ERP components' variability and provide an effective tool for scientific exploration of such processes and the development of advanced BCI systems.

Keywords: brain-computer interface, BCI, electroencephalogram, EEG, event-related potentials, ERP, N1, P300, ERP variability

Funding: the study was supported by the Russian Science Foundation Grant № 21-75-00021, <https://rscf.ru/project/21-75-00021/>

Acknowledgements: the authors would like to thank Yu. Nuzhdin (Kurchatov Institute) for developing and supporting software for EEG recording used to perform the study

Author contribution: Ganin IP — conducting research, data analysis and interpretation, literature review, manuscript writing; Vasilyev AN — data analysis and interpretation, literature review, manuscript writing; Glazova TD — conducting research, literature review; Kaplan AY — data interpretation.

Compliance with ethical standards: the study was approved by the Ethics Committee of the Lomonosov Moscow State University (protocol № 113-d of 19 June 2020); the informed consent was submitted by all study participants.

✉ **Correspondence should be addressed:** Ilya P. Ganin
Leninskiye Gory, 1, str. 12, k. 246, Moscow, 119234, Russia; ipganin@mail.ru

Received: 14.04.2023 **Accepted:** 27.04.2023 **Published online:** 28.04.2023

DOI: 10.24075/brsmu.2023.013

ИСТОЧНИКИ И ЗНАЧИМОСТЬ ВАРИАТИВНОСТИ ПОТЕНЦИАЛОВ МОЗГА ЧЕЛОВЕКА В ИНТЕРФЕЙСЕ МОЗГ–КОМПЬЮТЕР

И. П. Ганин¹✉, А. Н. Васильев^{1,2}, Т. Д. Глазова¹, А. Я. Каплан¹

¹ Московский государственный университет имени М. В. Ломоносова, Москва, Россия

² Центр нейроркогнитивных исследований (МЭГ-центр), Московский государственный психолого-педагогический университет, Москва, Россия

В интерфейсе мозг–компьютер на волне P300 (ИМК-P300) выбор команд пользователя возможен за счет фокусирования им внимания на внешнем стимуле-команде и выделении из ЭЭГ реакции к этому стимулу — в виде компонентов потенциалов, связанных с событиями (ПСС). Для получения сигнала ПСС стимулы необходимо многократно повторять, однако ввиду существующей вариативности латентности реакций на отдельные стимулы усредненные ПСС могут давать искаженное представление о характере таких реакций, а также снижать точность работы интерфейса. Целью работы было разработать эффективный способ выявления эффектов вариативности латентности компонентов ПСС и учета этих эффектов в ИМК-P300, и выявить возможное влияние психофизиологических факторов на характер вариативности ПСС. Для изучения механизмов вариативности мы провели ИМК-исследование на 19 здоровых испытуемых, где использовали выделение и коррекцию латентности в пространственных компонентах N1 и P300, играющих ключевую роль в классификации команд в ИМК-P300. Этот подход обеспечил более высокую точность по сравнению с использованием обычных отведений ЭЭГ, при этом наибольший рост в 10% наблюдался при минимальном числе повторов стимулов. Также модификации интерфейса, позволяющие обеспечить более высокий уровень внимания пользователя к задаче и более четкую фиксацию взгляда на целевых объектах, способствовали повышению амплитуд компонентов ПСС посредством снижения вариативности реакций на единичные стимулы. Полученные результаты подчеркивают важную роль процессов вариативности компонентов ПСС и дают эффективный инструмент для их научного изучения, а также для разработки перспективных систем ИМК.

Ключевые слова: интерфейс мозг–компьютер (ИМК), электроэнцефалограмма (ЭЭГ), потенциалы, связанные с событиями, ПСС, N1, P300, вариативность ПСС

Финансирование: исследование выполнено за счет гранта Российского научного фонда № 21-75-00021, <https://rscf.ru/project/21-75-00021/>

Благодарности: авторы благодарят Ю. Нуждина из НИЦ «Курчатовский институт» за разработку и поддержку программного обеспечения для регистрации ЭЭГ, при помощи которого проведено исследование.

Вклад авторов: И. П. Ганин — проведение исследования, анализ и интерпретация данных, анализ литературы, подготовка текста рукописи; А. Н. Васильев — анализ и интерпретация данных, анализ литературы, подготовка текста рукописи; Т. Д. Глазова — проведение исследования, анализ литературы; А. Я. Каплан — интерпретация данных.

Соблюдение этических стандартов: исследование одобрено этическим комитетом МГУ имени М. В. Ломоносова (протокол № 113-д от 19 июня 2020 г.); все участники подписали добровольное информированное согласие на участие в исследовании.

✉ **Для корреспонденции:** Илья Петрович Ганин
Ленинские горы, д. 1, стр. 12, к. 246, Москва, 119234, Россия; ipganin@mail.ru

Статья получена: 14.04.2023 **Статья принята к печати:** 27.04.2023 **Опубликована онлайн:** 28.04.2023

DOI: 10.24075/vrgmu.2023.013

Brain-computer interfaces (BCI) make it possible to directly translate brain activity into commands to control computer or any other device without involving muscles and nerves, only via analysis of the user's electroencephalogram (EEG) [1]. The concept of BCI, proposed and developed many years ago, has become an interdisciplinary technology, the primary purpose of which is supporting people with severe speech and movement disorders [2], along with the use as a tool for instrumental diagnosis or cognitive training [3–5].

BCI technologies often involve the use of event-related potentials (ERPs) [6]. One of the most widely used and well-proven systems is referred to as P300 BCI, since it is based on the analysis of the P300 component related to attention [7, 8]. The user of such interface usually mentally counts the number of flashes of the character or other command symbol of interest. The ERPs elicited to flashing of this (target) object are distinguished from ERPs elicited to flashing of all other (non-target) symbols by the presence of the P300 component [9]. The BCI algorithm recognizes the target symbol (command) by this feature and the presence of other components (primarily N1) in the ERP [10, 11].

The P300 BCI systems are in demand for communication: during typewriting or step-by-step control of certain device [12]. However, the main disadvantages of those include the need for repetition of stimuli aimed at accumulating ERP responses with the least error when the BCI user has to focus on the task for a long time. Furthermore, despite the assumption of similarity of the brain responses to the repeated stimuli, there is some temporal variability of certain responses relative to stimuli [13, 14]. This is a well-known neurophysiological phenomenon that generally reflects a number of natural brain processes at different levels, from cellular to the neural network level, and is also determined by fluctuation in the processes underlying perception of external stimuli [15].

It is known that such variability can affect the shape of the resulting averaged ERPs, including reducing the peak amplitude of certain components [16]. Lack of accounting of the variability effects may negatively affect the effectiveness of the P300 BCI based on the ERP extraction method, thereby reducing accuracy of the target command recognition [17, 18].

In general, changes in the ERP variability are considered to be associated with fatigue, increased cognitive load, complication of the user's task [15, 19], as well as conditions characterized by reduced attention, such as ADHD and autism [20, 21]. However, the factors affecting ERP variability in terms of P300 BCI were never systematically studied. Meanwhile, identification of the BCI operation modes having a beneficial or negative effect on ERPs and the command classification accuracy would make it possible to develop more effective systems capable of ensuring more reliable control, especially when it comes to potential users with reduced attention.

It also seems appropriate to consider ERP variability in the P300 BCI by modifying the command classification algorithms. This can be particularly important when a relatively small number of stimuli is accumulated in the interface, and the effects of variability may not be compensated by the number of averaging procedures. Given the ERP components' different contributions to classification along with variation in their topography among various users [22], extracting independent spatial components to analyze and consider their variability separately can be a more effective approach.

The study was aimed to identify possible factors of the stimulus environment and P300 BCI operation modes affecting ERP variability, as well as to develop and test more effective

methods for independent detection of variability of individual ERP components during classification.

METHODS

The study involved 19 healthy subjects (5 males and 14 females) aged 18–23. Inclusion criteria: healthy male and female volunteers aged 18–35. Exclusion criteria: diagnosed neurological/mental disorder, episodes of seizures or diagnosed status epilepticus.

During the experiment the subject sat in a chair in front of the monitor on which a standard P300 BCI matrix sized 6×6 with letters of Russian alphabet and numbers was presented. The angular dimensions of the matrix were $18^\circ \times 18^\circ$, the cell size was 1.7° , and the cell spacing was 1.1° . The background of the screen and cells was black (RGB 0,0,0), while cell frames and characters within the cells were grey (RGB 89,90,97). Stimuli were represented by random flashes (the background color changed from black to grey, and the color of characters changed from grey to black) of rows and columns in the matrix. The duration of stimulus and the interstimulus interval were 97 and 48.5 ms, respectively (16 and 8 frames for the refresh rate of 165 Hz). Stimulation involved using the stimulus sequences, each sequence included presentation of all 12 stimuli available in the matrix (six rows and six columns).

A separate experimental mode included 15 blocks, one cell of the matrix per block was designated as a target cell (it was marked by repeated wink at the start of the block). Five stimulus sequences per block were presented, which corresponded to 60 stimuli (10 target stimuli and 50 non-target ones). Thus, each mode included 150 target stimuli and 750 non-target ones.

Several modes distinguished by parameters of the stimulus environment and the subject's task were used to study the impact of various factors on the ERP variability. In the passive attention mode the subject was not supposed to count flashes of the target stimulus as in the P300 BCI, he/she simply fixed his/her gaze on the target cell. The task was complicated by using the mode involving mixing-up letters: the characters in all cells of the matrix randomly changed their places with each target flash. The subjects were asked to count not only all target flashes, but the number of consonants in the target cell when the character changed. To make it easier to fix gaze on the cell and reduce the effects of distractor in the modes involving the use of half-empty matrix, the characters were not made permanently visible, these appeared only with flashes (Fig. 1).

The modes and brief instructions for the subject were as follows:

- 1) ordinary matrix, passive attention ("just look at the target cell");
- 2) ordinary matrix, active attention ("count the number of flashes of the target cell");
- 3) half-empty matrix, active attention ("count the number of flashes of the target cell");
- 4) half-empty matrix, mixing up, active attention ("count the number of flashes of the target cell");
- 5) half-empty matrix, mixing up, cognitive load ("count the number of consonants in the target cell");
- 6) ordinary matrix, mixing up, active attention: ("count the number of flashes of the target cell");
- 7) ordinary matrix, mixing up, cognitive load ("count the number of consonants in the target cell").

All modes alternated to generate a pseudo-random sequence, except for the passive attention mode that was always the first due to special instruction.

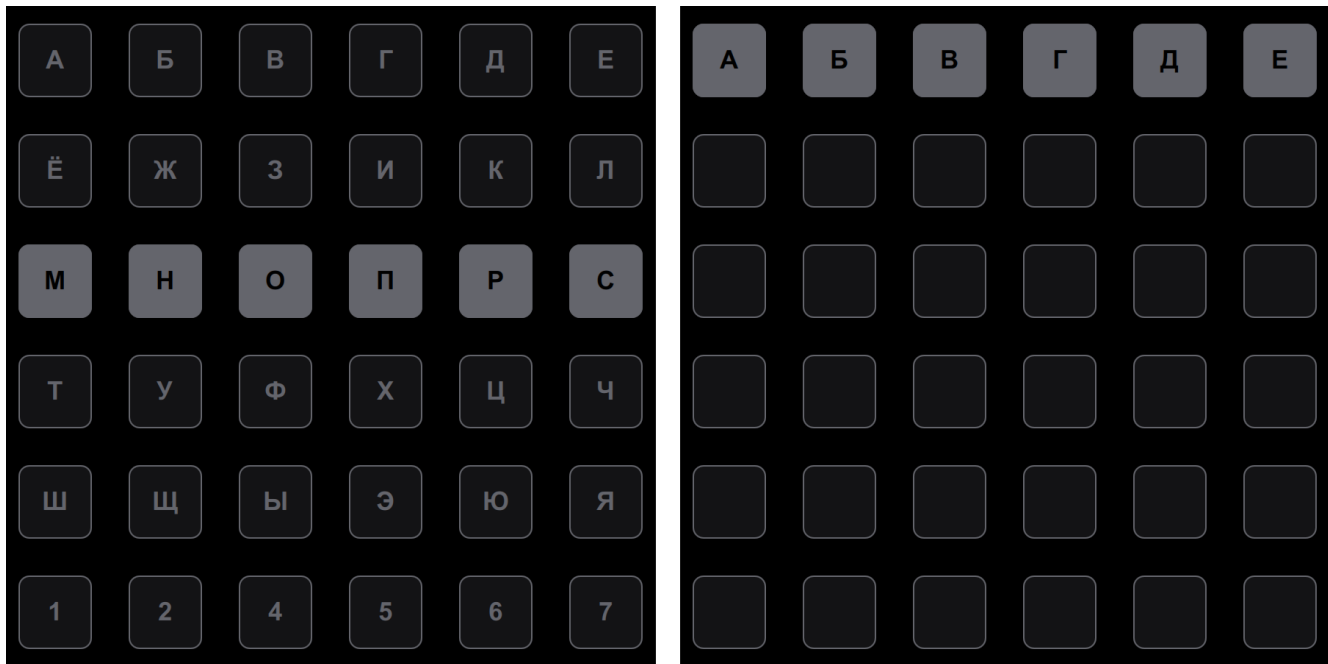


Fig. 1. The stimulus matrix P300 BCI used in the study. The matrix was located in the center of the screen on the black background. "Ordinary matrix" is on the left, "half-empty matrix" is on the right

EEG was recorded with 30 scalp electrodes (Fp1, Fp2, F7, F3, Fz, F4, F8, FC5, FC1, FC2, FC6, T7, C3, Cz, C4, T8, CP5, CP1, CP2, CP6, P7, P3, Pz, P4, P8, PO7, POz, PO8, O1, O2) and a common reference electrode TP9 + TP10 using the NVX52 amplifier (MCS, Zelenograd; Russia). The sampling frequency was 1000 Hz. A miniature photosensor mounted in the upper left corner of the screen was used to ensure EEG synchronization with the flashes. Signal recording and management of experimental procedure were implemented in the original Resonance programming environment written in C++ (<http://resonance.bci-lab.net/documentation>).

EEG signal processing and classification were performed in MATLAB 9.13 (R2022b) (MathWorks; USA). The EEG signal was band-pass filtered within the 1–10 Hz range using a FIR filter without a phase shift. Then ocular artifacts were removed by independent component analysis (ICA). After that the continuous signal was split into epochs from –400 to 1200 ms relative to the stimulus onset.

The next phase of analysis involved acquisition of spatial filters to extract the components of interest (N1 and P300) from the multichannel EEG signal. For that the epochs in the vicinity of individual ERP peaks were extracted in each subject, after that

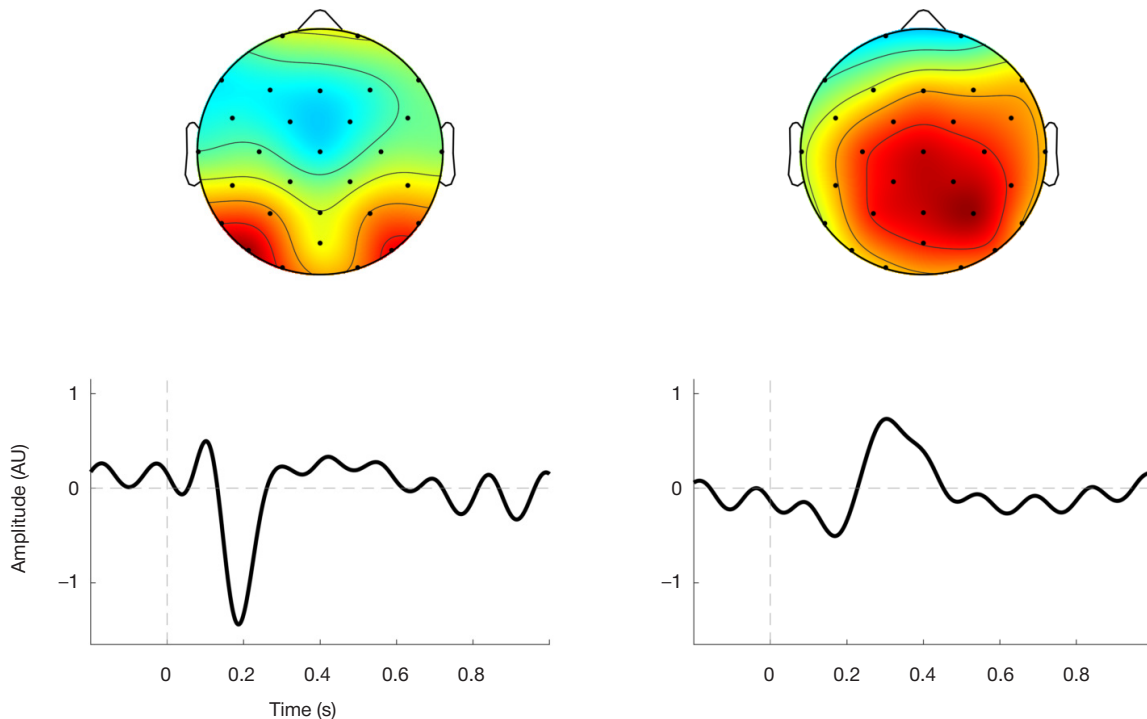


Fig. 2. The extracted spatial components N1 and P300. The figure above shows topography of the spatial filter patterns. The figure below shows components N1 and P300 averaged across all subjects. Vertical axis — normalized amplitude in arbitrary units; horizontal axis — time (s). The vertical dotted line (0 s) corresponds to the stimulus onset. N = 19 subjects

Table 1. The average amplitudes of the N1 and P300 components in all modes when using the standard averaging method (no latency correction) and when averaging the epochs adjusted to latency of the appropriate component. The mean and standard error of the mean are provided. N = 19 subjects

Component	Mode 1	Mode 2	Mode 3	Mode 4	Mode 5	Mode 6	Mode 7
Amplitude with no latency correction, AU							
N1	-1.17 ± 0.11	-1.38 ± 0.08	-1.53 ± 0.09	-1.50 ± 0.08	-1.81 ± 0.09	-1.29 ± 0.09	-1.67 ± 0.11
P300	0.92 ± 0.07	1 ± 0.06	0.94 ± 0.07	0.86 ± 0.06	1.07 ± 0.08	0.89 ± 0.06	1.05 ± 0.05
Amplitude with latency correction, AU							
N1	-1.50 ± 0.09	-1.67 ± 0.08	-1.81 ± 0.07	-1.77 ± 0.07	-2.05 ± 0.09	-1.59 ± 0.07	-1.93 ± 0.09
P300	1.47 ± 0.06	1.59 ± 0.04	1.52 ± 0.06	1.46 ± 0.04	1.62 ± 0.07	1.53 ± 0.04	1.67 ± 0.04

optimal spatial projections (spatial filters) were calculated based on the Fisher's criterion [23]. Such method made it possible to reduce the EEG signal dimension, increase the signal-to-noise ratios of the studied components, and largely isolate two components from each other for independent study [23]. The further analysis was performed for these two extracted spatial components (once for N1 and once for P300). Signals of the components were normalized to the standard deviation of all non-target epochs within each subject (hereinafter, AU instead of μV).

A set of target and non-target epochs was formed within each subject, component (N1 and P300), and mode. To acquire ERPs averaged by conventional method, all the epochs of the same subject were averaged individually for each mode, for the class of the target and non-target epochs of the N1 and P300 sets. The amplitude of these components was defined as the minimum/maximum signal value within the 100–350 and 200–500 ms windows, respectively, and the peak latencies were defined as the time after the stimulus onset when the signal reached its maximum or minimum.

Furthermore, to analyze the ERP variability, the N1 and P300 component latencies were calculated within certain non-averaged target epochs as local minima or maxima in the same windows as for ERP. The component's amplitude was determined by the signal values for the latencies found within this epoch. To assess variability of the ERP peak latencies, the mean absolute deviation (MAD) was calculated in each mode for each subject. To estimate the effect of variability on the ERP amplitude, the epochs were shifted along the time axis by the difference between the average latency and the component latency within certain epoch prior to averaging.

To estimate the effects of ERP variability on the effectiveness of command recognition in the BCI, classification accuracy was calculated for ordinary EEG channels (standard approach) and for the extracted spatial components N1 and P300. It is important to note that classification scores of two types were calculated for the latter: without equalization of latency peaks and with equalization (correction for N1 or P300 only and correction for both peaks, N1 and P300). The signal amplitude values within the 0–600 ms window (every 10th point) in 11 channels of EEG leads Cz, CP1, CP2, P3, Pz, P4, PO7, POz, PO8, O1, O2 or two channels obtained for N1 and P300 of

appropriate spatial components were used as the Fisher's linear discriminant features. The classification accuracy was assessed by cross-validation with sequential testing of the data of a single block (all epochs of the same target cell) of the classifier trained using the other 14 blocks. The classification accuracy was determined as a proportion of the correctly recognized letters (out of 15). When performing testing, accuracy was calculated for different number of the stimulus sequences (one to five). The accuracy was calculated for each mode, subject, and signal feature extraction method.

Statistical analysis was performed in MATLAB using the generalized linear mixed effects models. A single constant coefficient was used as a random factor for the "subject" variable, while experimental conditions ("active attention", "cognitive load", "half-empty matrix", "mixing up elements") and latency correction modes were considered as fixed effects. The fixed effect significance was assessed using F-test. The following dependent variables were assessed: amplitude, latency, MAD of the N1 and P300 latencies, and classification accuracy. We used binomial regression to assess classification accuracy and linear regression to assess other parameters.

RESULTS

Fig. 2 shows the extracted spatial components N1 and P300 and the corresponding patterns (topographic distribution of weighting coefficients). The N1 component with the average latency of 187 ms had typical lateral occipital localization, while P300 with the latency of 315 ms had medial parietal localization.

Table 1 provides the group-averaged amplitudes of the N1 and P300 components obtained in each mode, before and after correction of latencies within individual epochs. The N1 and P300 amplitudes of the averaged ERPs increased after applying correction: $F(1,258) = 581.24$; $p = 0.00000$. The factor of active attention turned out to be significant for the N1 amplitude that increased relative to passive attention to the stimulus (mode 1): $F(1,36) = 17.87$; $p = 0.00015$. The increase in the N1 amplitude was reported for such factors, as "half-empty matrix" ($F(1,110) = 16.10$; $p = 0.00011$) and "cognitive load" ($F(1,110) = 48.49$; $p = 0.00000$). The increase in the P300 amplitude was reported for the "cognitive load" factor ($F(1,110) = 18.01$; $p = 0.00005$), while the decrease

Table 2. The average absolute latencies and the average indicators of their variability (MAD) for the N1 and P300 components in all modes. The mean and standard error of the mean are provided. N = 19 subjects

Component	Mode 1	Mode 2	Mode 3	Mode 4	Mode 5	Mode 6	Mode 7
Latency, ms							
N1	187 ± 3.25	187 ± 2.6	184 ± 2.3	185 ± 2.2	185 ± 2.1	191 ± 2.6	191 ± 2.7
P300	323 ± 10.5	320 ± 9.3	303 ± 10.6	302 ± 10.4	305 ± 11.6	316 ± 10.3	325 ± 10.8
Mean absolute deviation (MAD) of latency, ms							
N1	21.1 ± 1.5	18.9 ± 1.4	16.3 ± 1.2	18.0 ± 1.1	15.1 ± 0.8	19.2 ± 1.6	17.5 ± 1.5
P300	42.5 ± 2.2	41.3 ± 2.2	43.2 ± 2.7	44.9 ± 2.6	43.0 ± 2.4	44.0 ± 2.5	44.9 ± 2.7

Table 3. The average classification accuracy obtained in all modes for one or two stimulus sequences that has been calculated for various signal feature sets used by the classifier — usual 11 EEG electrodes and the extracted spatial components N1 and P300 with or without peak latency correction. The mean and standard error of the mean are provided. N = 19 subjects

Method of the signal feature extraction	Mode 1	Mode 2	Mode 3	Mode 4	Mode 5	Mode 6	Mode 7
Accuracy when using one stimulus sequence, %							
EEG leads	66.7 ± 5.4	75.3 ± 4.6	77.29 ± 3.7	74.4 ± 4.0	84.2 ± 3.0	68.4 ± 4.6	80.7 ± 3.1
Spatial components	56.4 ± 5.8	63.5 ± 4.2	68.8 ± 3.7	62.8 ± 3.2	76.8 ± 2.8	59.7 ± 3.7	73.0 ± 3.3
Spatial components + correction of N1 + P300	76.8 ± 3.4	81.8 ± 2.9	86.3 ± 3.0	85.3 ± 2.6	86.7 ± 2.9	76.1 ± 2.5	84.9 ± 2.2
Accuracy when using two stimulus sequences, %							
EEG leads	83.9 ± 4.1	90.0 ± 2.1	94.7 ± 1.4	94.0 ± 1.7	96.8 ± 1.3	88.8 ± 4.1	92.3 ± 2.1
Spatial components	75.8 ± 4.9	86.6 ± 3.3	86.3 ± 2.8	88.8 ± 2.0	93.3 ± 1.9	82.8 ± 4.0	93.0 ± 1.2
Spatial components + correction of N1 + P300	94.0 ± 1.2	97.1 ± 1.0	97.5 ± 1.6	93.3 ± 1.8	97.9 ± 1.0	95.4 ± 1.5	96.8 ± 1.5

was reported for the factor of “mixing up elements” ($F(1.110) = 4.72$; $p = 0.032$).

The average latencies of the N1 and P300 components together with the indicator of the latency variability (MAD) are provided in Table 2. The decrease in the N1 and P300 latencies were reported for the factor of “half-empty matrix”: $F(1.110) = 45.87$, $p = 0.00000$ and $F(1.110) = 24.51$, $p = 0.00000$, respectively. The increase in the N1 latency was also reported for the factor of “mixing up elements”: $F(1.110) = 5.17$; $p = 0.025$. Active attention resulted in the decrease of the N1 component MAD relative to the passive attention mode: $F(1.36) = 1.60$; $p = 0.0016$. The decrease in the N1 MAD was reported for the factors of “half-empty matrix” ($F(1.110) = 12.43$; $p = 0.00061$) and “cognitive load” ($F(1.110) = 11.56$; $p = 0.00094$). As for P300, the increase in MAD was reported for the factor of “mixing up elements”: $F(1.110) = 4.80$; $p = 0.03056$.

Table 3 provides assessment of the average classification accuracy in all modes using different signal feature extraction methods: EEG channels and the channels for N1 and P300 of the corresponding spatial components, to which the latency correction was applied or not applied. The table provides data for the minimum number (1 or 2) of the stimulus sequences per letter, when accuracy is still low, and the differences between the modes are larger. The trend towards an increase in accuracy is reported for the “cognitive load” factor: $F(1.108) = 3.39$; $p = 0.068$.

Fig. 3 presents the average classification accuracy for different signal feature extraction methods and different number of the stimulus sequences. When using spatial filters (only two data vectors, for N1 and P300) without latency correction, the accuracy was the lowest and was even lower than when using the usual 11 EEG electrodes: $F(1.3284) = 5.99$, $p = 0.014$. Applying latency correction to the spatial component N1 only yielded higher accuracy, however, this option did not differ significantly from the option involving the use of usual EEG electrodes: $F(1.3284) = 1.1771$, $p = 0.28$. However, applying latency correction to the spatial component P300 only resulted in higher accuracy compared to the use of usual EEG electrodes: $F(1.3284) = 24.51$, $p = 0.00000$. The highest classification accuracy values were obtained when applying latency correction to both N1 and P300 (in each of the two appropriate spatial components). In this case, the accuracy was higher compared to the use of usual EEG electrodes ($F(1.3284) = 24.29$, $p = 0.00000$) and higher than when applying latency correction to P300 only ($F(1.3284) = 4.34$, $p = 0.037$) (as for the latter, the differences were reported for the 2nd and 3rd stimulus sequences: $p < 0.05$).

DISCUSSION

In our study we proposed an effective approach to assessing the ERP variability in the P300 BCI that allowed us to identify a number of factors affecting the ERP characteristics and explore the contribution of the variability effects to the command recognition accuracy in this interface.

To analyze the effects of the ERP latency variability, it is necessary to detect the components in individual (non-averaged) epochs. This process is very complicated due to both technogenic and physiological noise, that is why it is extremely important to make the most of valuable information contained in the EEG signal. Despite the fact that in some trials the effects of variability were studied in terms of the P300 BCI, the impact of these effects was estimated in usual EEG channels for the P300 component only [17, 24]. In our previous study, we applied latency correction to two components, N1 and P300, however, each component was analyzed in its own channel set [18]. The use of the combined information from all channels with simultaneous analysis of several components

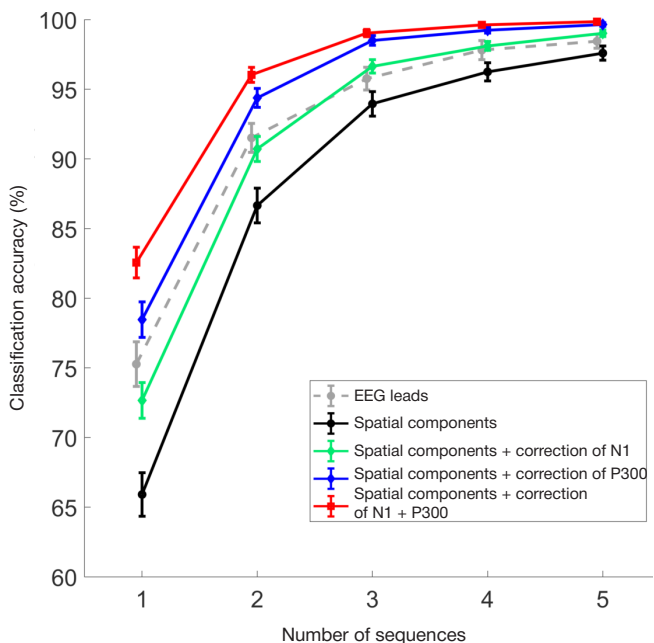


Fig. 3. The average classification accuracy with different number of the stimulus sequences calculated for various signal feature sets used by the classifier — usual 11 EEG electrodes, extracted spatial components N1 and P300 (no latency correction, latency correction applied to N1 only, to P300 only, or to both components, N1 and P300). The mean and standard error of the mean are provided. N = 19 subjects

in each of these channels can be a more effective approach. For example, the independent components extracted by ICA have been already used by the authors of papers on assessing variability (not related to BCI), however, these researchers have analyzed only one early component of ERP [21, 25]. Furthermore, the ICA method does not guarantee extraction of the components of interest for analysis. In this study we have proposed the use of spatial filters for extraction of two components, N1 and P300, that are functionally significant for the P300 BCI, with subsequent analysis of variability in these components instead of individual EEG channels. This method was used earlier [23], but in that study it was an additional step of preprocessing and extraction of the signal features for classification in the BCI, it had nothing to do with assessment of the ERP variability effects. The extraction of spatial components aimed at independent correction of these components has never been applied previously. Moreover, the use of the approach involving spatial components reduces the likelihood of erroneous peak detection within individual epochs compared to the use of signal in certain EEG leads, thereby making the variability analysis more objective.

An essential aspect of the work was to reveal the possible factors affecting the ERP characteristics in the P300 BCI. Active attention (the directive to emotionally count flashes) resulted in the increase in the N1 component amplitude, and the mechanism underlying such an increase was likely to include the decrease in the latency variability of responses to individual stimuli, since a simultaneous decrease in MAD was observed. The increase in the ERP components' amplitude relative to passive attention to stimuli in the P300 BCI has been earlier reported for such construct in this group [26]. Presumably, the directive to actively count the stimuli improves fixation of gaze on the target position within the matrix, which is important for the N1 component [27]. Lack of characters in all cells of the matrix is also likely to improve fixation of gaze on the target cell, since the N1 amplitude increase in the "half-empty matrix" mode has been reported along with the decrease in its variability. This is consistent with opposite effects on the N1 component in the environment, where tracing the target objects is complicated by their mobility [18], and supports the relationship between the features of oculomotor system function and the ERP components' variability [28].

The constant changing of characters in the matrix cells is likely to adversely affect attention to the target stimulus, as evidenced by the decrease in the P300 amplitude and the increase in its variability, along with the increase in the N1 latency. The negative impact of such manipulations with the stimulus environment on the P300 BCI is also confirmed by the fact that the subjects have reported trouble following instructions in the modes involving mixing-up characters. At the same time, an interesting and not entirely obvious result is that additional cognitive load applied in the modes involving mixing-up characters (counting consonants with the change of letters), in contrast, resulted in the increase in the N1 and P300 amplitudes. Furthermore, the effect reported for N1 at least

partially resulted from the reduced variability. It is well-known that the effects of individual responses' variability are enhanced when the subject's attention flits between two competing tasks [29]. Perhaps, the cognitive load integrated into a task of tracing the target events, that was used in our study, on the contrary, caused the increase in attention, that is why such modification of the stimulus environment may be prospective for the P300 BCI.

The potential effectiveness of using the factors that have a beneficial effect on attention in the BCI is also confirmed by the trend towards the increased target stimuli classification accuracy in the modes with cognitive load (Table 3). The method of applying variability correction not to usual EEG leads, but to the extracted spatial components N1 and P300, that has been proposed in our study, has ensured the best classification accuracy (Fig. 2). Furthermore, the largest increase in accuracy is observed when using the least number of the stimulus sequences (94% vs. 84%). This emphasizes the value of this method for the P300 BCI operation modes and provides superior results compared to that yielded by the studies also involving extraction of spatial components, but not taking into account the effects of variability [23, 30]. The fact, that the N1 and P300 components' contributions to the effectiveness of classification are unequal, attracts attention: the contribution of uncorrected N1 is larger than that of uncorrected P300. However, given the higher P300 variability, correction of its latency resulted in the significantly increased accuracy, thereby overperforming both correction of N1 only and the use of standard EEG electrodes.

To date, the fact, that in this study we have not adjusted latency in the non-target epochs, is considered to be a limitation of the approach. In the future, it would be necessary to develop an algorithm, which, for example, would allow us to avoid correction of low-amplitude peaks in the non-target epochs, for implementation of the online BCI.

CONCLUSIONS

The paper proposes an approach to analysis of the ERP latency variability in the extracted EEG spatial components. The use of this method in the P300 BCI has made it possible to achieve better results in terms of the command classification accuracy compared to the existing methods. Furthermore, the use of such an approach has revealed some factors of the stimulus environment and the P300 BCI operation modes having an impact on the ERP variability effects. Specifically, modifications of the interface affecting the user's attention, including the cognitive load applied in addition to the main task, and making it easier to fix gaze on the target objects have a beneficial effect on the ERP amplitude and the decrease in variability of individual responses to stimuli. The findings complement the existing knowledge of the mechanisms underlying the ERP latency variability and provide new reasons for the development of more effective BCI systems.

References

1. Mridha MF, Das SC, Kabir MM, Lima AA, Islam MR, Watanobe Y. Brain-Computer Interface: Advancement and Challenges. *Sensors* (Basel). 2021; 21 (17): 5746.
2. Orban M, Elsamanty M, Guo K, Zhang S, Yang H. A Review of Brain Activity and EEG-Based Brain-Computer Interfaces for Rehabilitation Application. *Bioengineering* (Basel). 2022; 9 (12): 768.
3. Carelli L, Solca F, Faini A, Meriggi P, Sangalli D, Cipresso P, Riva G, Ticozzi N, Ciammola A, Silani V, Poletti B. Brain-Computer Interface for Clinical Purposes: Cognitive Assessment and

- Rehabilitation. *Biomed Res Int.* 2017; 2017: 1695290.
4. Ganin IP, Kosichenko EA, Sokolov AV, Ioannisyanc OM, Arefev IM, Basova AY, Kaplan AY. Adaptation of the p300-based brain-computer interface for anorexia nervosa patients state evaluation. *Bulletin of RSMU.* 2019; 2: 32-38.
5. Eldeeb S, Susam BT, Akcakaya M, Conner CM, White SW, Mazefsky CA. Trial by trial EEG based BCI for distress versus non distress classification in individuals with ASD. *Sci Rep.* 2021; 11 (1): 6000.
6. Abiri R, Borhani S, Sellers EW, Jiang Y, Zhao X. A comprehensive review of EEG-based brain-computer interface paradigms. *J Neural Eng.* 2019; 16 (1): 011001.
7. Luck SJ. An introduction to the event related potential technique. MIT Press, Cambridge, MA; 2005.
8. Pan J, Chen X, Ban N, He J, Chen J, Huang H. Advances in P300 brain-computer interface spellers: toward paradigm design and performance evaluation. *Front Hum Neurosci.* 2022; 16: 1077717.
9. Farwell LA, Donchin E. Talking off the top of your head: toward a mental prosthesis utilizing event-related brain potentials. *Electroencephalography and Clinical Neurophysiology.* 1988; 70: 510-523.
10. Krusienski DJ, Sellers EW, McFarland DJ, Vaughan TM, Wolpaw JR. Toward enhanced P300 speller performance. *J Neurosci Methods.* 2008; 167 (1): 15-21.
11. Rezeika A, Benda M, Stawicki P, Gembler F, Saboor A, Volosyak I. Brain-Computer Interface Spellers: A Review. *Brain Sciences.* 2018; 8 (4): 57.
12. Allison BZ, Kübler A, Jin J. 30+ years of P300 brain-computer interfaces. *Psychophysiology.* 2020; 57 (7): e13569.
13. Makeig S, Onton J. ERP features and EEG dynamics: an ICA perspective. *Oxford handbook of event-related potential components.* Oxford University Press, New York; 2011.
14. Dowdall JR, Luczak A, Tata MS. Temporal variability of the N2pc during efficient and inefficient visual search. *Neuropsychologia.* 2012; 50 (10): 2442-53.
15. Dinstein I, Heeger DJ, Behrmann M. Neural variability: friend or foe? *Trends Cogn. Sci.* 2015; 19 (6): 322-328.
16. Ouyang G, Hildebrandt A, Sommer W, Zhou C. Exploiting the intra-subject latency variability from single-trial event-related potentials in the P3 time range: A review and comparative evaluation of methods. *Neurosci. Biobehav. Rev.* 2017; 75: 1-21.
17. Aricò P, Aloise F, Schettini F, Salinari S, Mattia D, Cincotti F. Influence of P300 latency jitter on event related potential-based brain-computer interface performance. *Journal of neural engineering.* 2014; 11 (3): 035008.
18. Ganin IP, Kaplan AY. Study of the human brain potentials variability effects in P300 based brain-computer interface. *Bulletin of RSMU.* 2022; 3: 78-85.
19. Yagi Y, Coburn KL, Estes KM, Arruda JE. Effects of aerobic exercise and gender on visual and auditory P300, reaction time, and accuracy. *Eur J Appl Physiol Occup Physiol.* 1999; 80 (5): 402-8.
20. Kovarski K, Malvy J, Khanna RK, Arsène S, Batty M, Latinus M. Reduced visual evoked potential amplitude in autism spectrum disorder, a variability effect? *Translational Psychiatry.* 2019; 9 (1): 1-9.
21. Gonen-Yaacovi G, Arazi A, Shahar N, Karmo A, Haar S, Meiran N, Dinstein I. Increased ongoing neural variability in ADHD. *Cortex.* 2016; 81: 50-63.
22. Tou SLJ, Warschausky SA, Karlsson P, Huggins JE. Individualized Electrode Subset Improves the Calibration Accuracy of an EEG P300-design Brain-Computer Interface for People with Severe Cerebral Palsy. *bioRxiv.* 2023: 533775.
23. Pires G, Nunes U, Castelo-Branco M. Statistical spatial filtering for a P300-based BCI: tests in able-bodied, and patients with cerebral palsy and amyotrophic lateral sclerosis. *Journal of neuroscience methods.* 2011; 195 (2): 270-281.
24. Thompson DE, Warschausky S, Huggins JE. Classifier-based latency estimation: a novel way to estimate and predict BCI accuracy. *Journal of neural engineering.* 2013; 10 (1): 016006.
25. Milne E. Increased intra-participant variability in children with autistic spectrum disorders: evidence from single-trial analysis of evoked EEG. *Front Psychol.* 2011; 2: 51.
26. Basyul IA, Kaplan AY. Izmeneniya N200 i P300 komponentov potencialov, svyazannykh s sobytiyami, pri var'irovaniy usloviy vnimaniya v sisteme Brain Computer Interface. *Zhurnal vysshej nervnoj deyatel'nosti im. IP Pavlova.* 2014; 64 (2): 159-65. Russia.
27. Hillyard SA, Vogel EK, Luck SJ. Sensory gain control (amplification) as a mechanism of selective attention: electrophysiological and neuroimaging evidence. *Philos Trans R Soc L. B Biol Sci.* 1998; 353 (1373): 1257-70.
28. Zhang B, Stevenson SS, Cheng H, Laron M, Kumar G, Tong J, et al. Effects of fixation instability on multifocal VEP (mfVEP) responses in amblyopes. *Journal of Vision.* 2008; 8 (3): 16.
29. Polich J. Updating P300: an integrative theory of P3a and P3b. *Clin. Neurophysiol.* 2007; 118 (10): 2128-48.
30. Zhang Y, Zhou G, Zhao Q, Jin J, Wang X, Cichocki A. Spatial-Temporal Discriminant Analysis for ERP-Based Brain-Computer Interface. *IEEE Transactions on Neural Systems and Rehabilitation Engineering.* 2013; 21 (2): 233-43.

Литература

1. Mridha MF, Das SC, Kabir MM, Lima AA, Islam MR, Watanobe Y. Brain-Computer Interface: Advancement and Challenges. *Sensors (Basel).* 2021; 21 (17): 5746.
2. Orban M, Elsamanty M, Guo K, Zhang S, Yang H. A Review of Brain Activity and EEG-Based Brain-Computer Interfaces for Rehabilitation Application. *Bioengineering (Basel).* 2022; 9 (12): 768.
3. Carelli L, Solca F, Faini A, Meriggi P, Sangalli D, Cipresso P, Riva G, Ticozzi N, Ciammola A, Silani V, Poletti B. Brain-Computer Interface for Clinical Purposes: Cognitive Assessment and Rehabilitation. *Biomed Res Int.* 2017; 2017: 1695290.
4. Ганин И. П., Косиченко Е. А., Соколов А. В., Иоаннисянц О. М., Арефьев И. М., Басова А. Я., и др. Адаптация технологии интерфейсов мозг-компьютер на волне P300 для оценивания состояния больных нервной анорексией. *Вестник Российского государственного медицинского университета.* 2019; 2: 36-43.
5. Eldeeb S, Susam BT, Akcakaya M, Conner CM, White SW, Mazefsky CA. Trial by trial EEG based BCI for distress versus non distress classification in individuals with ASD. *Sci Rep.* 2021; 11 (1): 6000.
6. Abiri R, Borhani S, Sellers EW, Jiang Y, Zhao X. A comprehensive review of EEG-based brain-computer interface paradigms. *J Neural Eng.* 2019; 16 (1): 011001.
7. Luck SJ. An introduction to the event related potential technique. MIT Press, Cambridge, MA; 2005.
8. Pan J, Chen X, Ban N, He J, Chen J, Huang H. Advances in P300 brain-computer interface spellers: toward paradigm design and performance evaluation. *Front Hum Neurosci.* 2022; 16: 1077717.
9. Farwell LA, Donchin E. Talking off the top of your head: toward a mental prosthesis utilizing event-related brain potentials. *Electroencephalography and Clinical Neurophysiology.* 1988; 70: 510-523.
10. Krusienski DJ, Sellers EW, McFarland DJ, Vaughan TM, Wolpaw JR. Toward enhanced P300 speller performance. *J Neurosci Methods.* 2008; 167 (1): 15-21.
11. Rezeika A, Benda M, Stawicki P, Gembler F, Saboor A, Volosyak I. Brain-Computer Interface Spellers: A Review. *Brain Sciences.* 2018; 8 (4): 57.
12. Allison BZ, Kübler A, Jin J. 30+ years of P300 brain-computer interfaces. *Psychophysiology.* 2020; 57 (7): e13569.
13. Makeig S, Onton J. ERP features and EEG dynamics: an ICA perspective. *Oxford handbook of event-related potential components.* Oxford University Press, New York; 2011.
14. Dowdall JR, Luczak A, Tata MS. Temporal variability of the N2pc during efficient and inefficient visual search. *Neuropsychologia.* 2012; 50 (10): 2442-53.
15. Dinstein I, Heeger DJ, Behrmann M. Neural variability: friend or

- foe? *Trends Cogn. Sci.* 2015; 19 (6): 322–328.
16. Ouyang G, Hildebrandt A, Sommer, W, Zhou C. Exploiting the intra-subject latency variability from single-trial event-related potentials in the P3 time range: A review and comparative evaluation of methods. *Neurosci. Biobehav. Rev.* 2017; 75: 1–21.
 17. Aricò P, Aloise F, Schettini F, Salinari S, Mattia D, Cincotti F. Influence of P300 latency jitter on event related potential-based brain-computer interface performance. *Journal of neural engineering.* 2014; 11 (3): 035008.
 18. Ганин И. П., Каплан А. Я. Изучение эффектов вариативности потенциалов мозга человека в интерфейсе мозг-компьютер на волне P300. *Вестник Российского государственного медицинского университета.* 2022; 3: 78–85.
 19. Yagi Y, Coburn KL, Estes KM, Arruda JE. Effects of aerobic exercise and gender on visual and auditory P300, reaction time, and accuracy. *Eur J Appl Physiol Occup Physiol.* 1999; 80 (5): 402–8.
 20. Kovarski K, Malvy J, Khanna RK, Arsène S, Batty M, Latinus M. Reduced visual evoked potential amplitude in autism spectrum disorder, a variability effect? *Translational Psychiatry.* 2019; 9 (1): 1–9.
 21. Gonen-Yaacovi G, Arazi A, Shahar N, Karmo A, Haar S, Meiran N, Dinstein I. Increased ongoing neural variability in ADHD. *Cortex.* 2016; 81: 50–63.
 22. Tou SLJ, Warschausky SA, Karlsson P, Huggins JE. Individualized Electrode Subset Improves the Calibration Accuracy of an EEG P300-design Brain-Computer Interface for People with Severe Cerebral Palsy. *bioRxiv.* 2023: 533775.
 23. Pires G, Nunes U, Castelo-Branco M. Statistical spatial filtering for a P300-based BCI: tests in able-bodied, and patients with cerebral palsy and amyotrophic lateral sclerosis. *Journal of neuroscience methods.* 2011; 195 (2): 270–281.
 24. Thompson DE, Warschausky S, Huggins JE. Classifier-based latency estimation: a novel way to estimate and predict BCI accuracy. *Journal of neural engineering.* 2013; 10 (1): 016006.
 25. Milne E. Increased intra-participant variability in children with autistic spectrum disorders: evidence from single-trial analysis of evoked EEG. *Front Psychol.* 2011; 2: 51.
 26. Басюл И. А., Каплан А. Я. Изменения N200 и P300 компонентов потенциалов, связанных с событиями, при варьировании условий внимания в системе Brain Computer Interface. *Журнал высшей нервной деятельности им. ИП Павлова.* 2014; 64 (2): 159–65.
 27. Hillyard SA, Vogel EK, Luck SJ. Sensory gain control (amplification) as a mechanism of selective attention: electrophysiological and neuroimaging evidence. *Philos Trans R Soc L. B Biol Sci.* 1998; 353 (1373): 1257–70.
 28. Zhang B, Stevenson SS, Cheng H, Laron M, Kumar G, Tong J, et al. Effects of fixation instability on multifocal VEP (mfVEP) responses in amblyopes. *Journal of Vision.* 2008; 8 (3): 16.
 29. Polich J. Updating P300: an integrative theory of P3a and P3b. *Clin. Neurophysiol.* 2007; 118 (10): 2128–48.
 30. Zhang Y, Zhou G, Zhao Q, Jin J, Wang X, Cichocki A. Spatial-Temporal Discriminant Analysis for ERP-Based Brain-Computer Interface. *IEEE Transactions on Neural Systems and Rehabilitation Engineering.* 2013; 21 (2): 233–43.

SINGLE-STAGE ENDOVITREAL SURGERY OF RETINAL DETACHMENT COMPLICATED BY MACULAR HOLE INVOLVING THE SHORT-TERM PERFLUOROCARBON TAMPONADE

Takhchidi KhP, Takhchidi NKh, Mahno NA ✉

Pirogov Russian National Research Medical University, Moscow, Russia

Rhegmatogenous retinal detachment complicated by macular hole is a rare disorder that is the most challenging in terms of vitreoretinal surgery, and good anatomical outcome is not always associated with high visual functions. Today, vitrectomy, involving macular hole closure with autologous platelet-rich plasma, sealing peripheral retinal tears, and subsequent vitreal cavity tamponade with vitreous substitutes, is considered to be the most effective method for surgical treatment of this disorder. Despite variability of surgical approaches to treatment of rhegmatogenous retinal detachment complicated by macular holes, the search for safe and effective surgical technique, allowing one to achieve beneficial morphological and functional outcome with minimal damage to the retinal structures and to minimize the patient's rehabilitation period, is still relevant. The clinical case reported demonstrates the possibility of performing single-stage endovitreals treatment of retinal detachment complicated by macular hole using the autologous conditioned plasma in combination with the short-term perfluorocarbon tamponade. The results of using this technique show its reliability and superior efficiency and ensure good morphological and functional outcome in the postoperative period: restored macular architectonics, macular hole closure, anatomic retinal adhesion, and improved visual functions.

Keywords: rhegmatogenous retinal detachment, macular hole, autologous conditioned plasma, vitreoretinal surgery, perfluorocarbon

Author contribution: Takhchidi KhP — study concept and design, surgical treatment of the patient, manuscript editing; Takhchidi NKh — literature review; Mahno NA — data acquisition and processing, manuscript writing.

Compliance with ethical standards: the patient submitted the informed consent to surgery and personal data processing.

✉ **Correspondence should be addressed:** Nadezhda A. Mahno
Volokolamskoe shosse, 30/2, Moscow, 123182, Russia; nadezda.mahno7@gmail.com

Received: 27.03.2023 **Accepted:** 21.04.2023 **Published online:** 28.04.2023

DOI: 10.24075/brsmu.2023.016

ОДНОМОМЕНТНОЕ ЭНДОВИТРЕАЛЬНОЕ ЛЕЧЕНИЕ ОТСЛОЙКИ СЕТЧАТКИ, ОСЛОЖНЕННОЙ МАКУЛЯРНЫМ РАЗРЫВОМ С КРАТКОВРЕМЕННОЙ ТАМПОНАДОЙ ПЕРФТОРОРГАНИЧЕСКИМ СОЕДИНЕНИЕМ

Х. П. Тахчиди, Н. Х. Тахчиди, Н. А. Махно ✉

Российский национальный исследовательский медицинский университет имени Н. И. Пирогова, Москва, Россия

Регматогенная отслойка сетчатки, осложненная макулярным разрывом, является редкой и наиболее трудной патологией в плане витреоретинальной хирургии, а успешный анатомический результат не всегда сопровождается высокими зрительными функциями. На сегодняшний день наиболее эффективным методом хирургического лечения данной патологии принято считать витрэктомия с закрытием макулярного разрыва аутоплазмой крови с повышенным содержанием тромбоцитов, блокированием периферических разрывов и последующей тампонадой витреальной полости заместителями стекловидного тела. При всей вариативности хирургических подходов к лечению регматогенной отслойки сетчатки, осложненной сквозным макулярным разрывом, остается актуальным поиск безопасной и эффективной хирургической технологии, позволяющей при минимальном повреждении ретинальных структур достичь высоких морфо-функциональных результатов и минимизировать при этом срок реабилитации пациента. Представленный клинический случай демонстрирует возможность одномоментного микрохирургического лечения регматогенной отслойки сетчатки, осложненной сквозным макулярным разрывом с применением аутологичной кондиционированной плазмы в комбинации с кратковременной тампонадой перфторорганическим соединением. Результаты использования данной технологии показали ее надежность и высокую эффективность, а также обеспечили высокий морфо-функциональный результат в послеоперационном периоде — восстановление макулярной архитектоники, закрытие макулярного разрыва, анатомическое прилегание сетчатки и улучшение зрительных функций.

Ключевые слова: регматогенная отслойка сетчатки, макулярный разрыв, аутологичная кондиционированная плазма, витреоретинальная хирургия, перфторорганическое соединение

Вклад авторов: Х. П. Тахчиди — концепция и дизайн исследования, хирургическое лечение пациента, редактирование текста; Н. Х. Тахчиди — анализ литературных данных; Н. А. Махно — сбор и обработка материала, написание текста.

Соблюдение этических стандартов: от пациента получено добровольное информированное согласие на хирургическое лечение и обработку персональных данных.

✉ **Для корреспонденции:** Надежда Александровна Махно
Волоколамское шоссе, д. 30/2, г. Москва, 123182, Россия; nadezda.mahno7@gmail.com

Статья получена: 27.03.2023 **Статья принята к печати:** 21.04.2023 **Опубликована онлайн:** 28.04.2023

DOI: 10.24075/vrgmu.2023.016

Rhegmatogenous retinal detachment complicated by macular hole is a rare disorder that is currently one of the most challenging in terms of vitreoretinal surgery, the good anatomical outcome of which not always ensure high visual functions.

According to the literature, the prevalence of rhegmatogenous retinal detachment complicated by macular hole is 2.3–4% of cases. The disorder occurs predominantly in individuals with high myopia and peripheral retinal tears [1]. Macular holes less often occur secondary to retinal detachment

as a result of vitreoretinal traction due to posterior vitreous detachment, eye injury, tangential traction caused by epiretinal fibrosis, or proliferative vitreoretinopathy [1, 2].

The main goal of treatment of rhegmatogenous retinal detachment complicated by macular hole until the end of the 20th century was to achieve anatomic retinal adhesion by sealing peripheral tears without any attempts of the macular defect closure. This resulted in poor functional outcomes and the development of central scotoma [3, 4].

The literature describes clinical cases of two-stage surgical treatment of the combination of these disorders. The second stage surgery aimed at sealing the macular hole is performed some time after restoration of anatomic retinal adhesion. However, such an approach not always ensures restoration of macular architectonics, requires high material costs, and not always guarantees good visual and morphological outcome [5, 6].

Today, three port pars plana vitrectomy involving removal of posterior layers of the vitreous, macular hole closure, sealing peripheral tears followed by the vitreal cavity tamponade with vitreous substitutes (silicone oils of varying viscosity, air-gas tamponade with long resorption period, sterile air) is considered the only effective method for surgical treatment of rhegmatogenous retinal detachment complicated by macular hole allowing one to achieve good anatomic and functional outcome [1, 5, 7–9].

Various surgical methods of macular defect closure have been proposed in order to improve the effectiveness of the macular hole surgical treatment, i.e. to increase the anatomic closure rate and the rate of visual function improvement: mechanical approximation of the hole edges, internal limiting membrane (ILM) peeling, sealing of the hole with various modifications of the inverted ILM flap, amniotic membrane plug, transplantation of the anterior lens capsule, ILM preservation [1, 7–11].

In recent years, there is growing interest in the methods associated with sealing the macular hole with autologous platelet-rich plasma. Currently, two methods of plasma collection are extensively used in treatment of retinal disorders: PRP, platelet-rich plasma with the platelet levels 3–4 times higher compared to baseline blood levels, and ACP, autologous conditioned plasma with almost no white blood cells and elevated platelet levels (2–3 times higher compared to baseline blood levels). Local application of autologous factors during macular surgery makes it possible to achieve good anatomic and functional outcome and minimize retinal tissue injury during the operation [12–15].

Despite variability of surgical approaches to treatment of rhegmatogenous retinal detachment complicated by macular holes, the search for safe and effective surgical technique, allowing one to achieve anatomic retinal adhesion and restoration of macular architectonics with minimal damage to the retinal structures and to minimize the patient's rehabilitation period, is still relevant.

The clinical case reported demonstrates a single-stage approach to treatment of rhegmatogenous retinal detachment complicated by macular hole.

The aim was to assess the effectiveness and safety of the single-stage approach to endovitreous treatment of rhegmatogenous retinal detachment complicated by macular hole involving sealing a peripheral tear by endolaser photocoagulation, macular hole closure with autologous conditioned plasma, and short-term perfluorocarbon tamponade of the vitreous cavity.

Clinical case

In July 2022, female patient A. aged 60 presented to the Research Center of Ophthalmology of the Pirogov Russian National Research Medical University complaining of the rapid decrease in visual acuity of her left eye and the emergence of dark curtain falling across the left eye peripheral visual field from the top on the nasal and temporal sides. The above developed suddenly five days before the visit. According to medical history, the patient underwent surgery, phacoemulsification of

cataract with intraocular lens (IOL) implantation, on both eyes (OU) in 2015.

The patient underwent preoperative comprehensive eye examination involving the use of standard (visometry to determine uncorrected visual acuity (UCVA) and best-corrected visual acuity (BCVA), pneumatonometry, biomicrophthalmoscopy with a MaxField indirect lens MaxField (Ocular Inc.; USA)) and specific assessment methods (B-mode sonography of the eye with the Compact Touch NEW scanner (Quantel Medical; France) and spectral-domain optical coherence tomography (SD-OCT) with the Spectralis HRA+OCT module (Spectralis HRA+OCT, Heidelberg Engineering, Module, OCT-2 85,000 Hz Inc., Germany)).

Initial assessment showed that visual acuity of the left eye (OS) was 0.01 (incurable, eccentric viewing), and intraocular pressure (IOP) was 15 mmHg. Ophthalmoscopy OS showed that the anterior segment was intact, and the well-centered IOL was in the capsular bag. Retinal detachment involving the macular zone was found between the 12 and 8 clock h, a flap tear extending for 1 clock h was visible in the peripheral retina, a roundish red-colored defect was found in the macular zone. Ultrasonography revealed subtotal retinal detachment with a height of 9.13 mm and a flap tear in the superior outer quadrant. Macular SD-OCT revealed retinal detachment in the center of the retina and a defect with a diameter of 380 μ m penetrating through all retinal layers in the foveal zone (Fig. 1).

The following diagnosis was established based on the patient's comprehensive eye examination, complaints, and medical history: OS Subtotal rhegmatogenous retinal detachment. Macular hole. Pseudophakia.

The patient underwent three port pars plana vitrectomy performed using a disposable 27G tool kit according to standard method with the cut rate of up to 5,500 cpm and vacuums of up to 650 mmHg (Fig. 2). Initial application of the triamcinolone acetate contrast agent was followed by induction and subsequent removal of the posterior hyaloid membrane and adjacent posterior layers of the vitreous. A flap retinal tear extending for 1 clock h was found when examining the peripheral retina. A perfluoroorganic compound was injected in small increments into the vitreous cavity in order to reduce retinal mobility and ensure smoothing of the detached retina. As a result, adaptation of the detached retina to subadjacent layers was achieved along with the subretinal fluid drainage into the vitreous cavity through the hole. Partial aspiration of the perfluoroorganic compound was performed using active extrusion. The macular zone of the retina was stained with the Membrane Blue-Dual dye injected intravitreally in order to identify ILM, while the zone of macular hole was covered with the perfluoroorganic compound drop allowing us to prevent the dye penetration under the retina. Aspiration of intravitreal dye and the remaining perfluoroorganic compound was followed by the ILM removal with endovitreous forceps 360 degrees around the foveola within the limits of vascular arcades.

The vitreous cavity was once again plugged with the perfluoroorganic compound, the remaining subretinal fluid was aspirated above the zone of the hole. Endolaser photocoagulation of the flap tear extending for 1 clock h was performed.

The perfluoroorganic compound was partially aspirated by active extrusion to a volume of 3–4 diameters of the optic disc over the zone of the macular hole and substituted with the balanced salt solution (BSS). The macular hole edges were approximated to the center using the extrusion cannula until these were in full contact (the cannula tip did not touch the retinal tissue), and the remaining subretinal fluid was aspirated.



Fig. 1. Spectral domain optical coherence tomography scan of the macular zone (before surgery). Retinal detachment. Macular hole (red arrow) with a diameter of 380 μ m

Autologous conditioned plasma (ACP) was prepared during surgery using the proprietary Arthrex ACP double syringe (RU № FZN 2012/12123 of 08.11.2016) by drawing 15 mL of the patient's venous blood using a 18–20 G butterfly needle with no anticoagulant into the Arthrex ACP syringe. Blood collection was followed by the syringe installation in the ROTOFIX 32A centrifuge (Hettich; Germany) and subsequent centrifugation for 5 min at 1700 rpm.

After aspiration of the remaining perfluoroorganic compound, a syringe with a blunt needle was used to sequentially apply the 0.1 mL ACP drops with the exposure time of up to 1 min to form multiple layers in the zone of the macular hole until a faint translucent film was formed within the limits of vascular arcades. The surgical procedure ended with short-term perfluorocarbon tamponade of the vitreous cavity (8 days) aimed at the chorioretinal adhesion formation in the area of peripheral tear and retaining the applied ACP in the macular zone for the macular hole sealing and subsequent regeneration.

Standard drug therapy (antibacterial and anti-inflammatory) was used during the postoperative period.

On day one after surgery the patient reported improvement in visual acuity of her left eye along with no dark curtain in the left eye peripheral visual field; she complained of metamorphopsia. Examination revealed UCVA of 0.05, BCVA of 0.16, and IOP of 18 mmHg. Ophthalmoscopy revealed the translucent fibrin film in the macular zone within the limits of vascular arcades, the tear in the peripheral retina extending for 1 clock h was sealed by edematous coagula, the entire retina was adapted. According to macular SD-OCT, the macular hole edges were closed, and the fibrin film on the retinal surface was visible (Fig. 3).

Based on the SD-OCT findings, lysis of the fibrin film, macular profile shaping, and complete closure of the macular hole were revealed within 7 days during the postoperative period.

On day eight, the second stage surgery was performed using a disposable 27G tool kit. Perfluoroorganic compound was removed by active aspiration. Similarly to the above technology, ACP was prepared during surgery, and the 0.1 mL ACP drops were sequentially applied to the retinal region in the macular zone with the exposure time of up to 1 min to form multiple layers until a faint translucent film was formed within the limits of vascular arcades. The surgical procedure ended with substitution of the previously injected BSS with air, first by active aspiration of the solution, and then by passive aspiration of the remaining layer of fluid corresponding to 2–3 diameters of the macula using the cannula. Sclerostomies were sutured after removal of the ports.

One month after surgery the patient reported the improvement in visual acuity OS, the complaints of

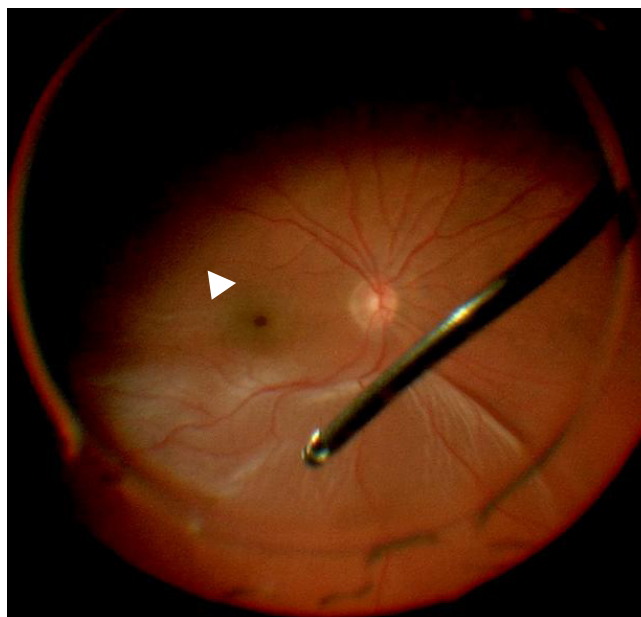


Fig. 2. Intraoperative fundus image: macular hole in the center of the retina (white arrow). Retinal detachment in the superior, temporal and inferior quadrants

metamorphopsia declined. Ophthalmic examination showed that UCVA was 0.16, BCVA was 0.3, and IOP was 16 mmHg. Ophthalmoscopy revealed no retinal defect in the macular zone, the tear in the peripheral retina extending for 1 clock h was sealed by pigmented coagula, the entire retina was adherent. According to micropirometry (MAIA, CenterVue Inc.; Italy), the average central retinal sensitivity (CRS) OS was 24.7 dB, fixation was stable. According to macular SD-OCT, the normal foveal profile was formed, the macular hole was closed, and retinal segmentation was partially restored (Fig. 4).

On the follow-up examination three months after treatment the patient reported improvement in visual acuity of her left eye and no metamorphopsia. Examination revealed improved visual acuity: UCVA was 0.2, BCVA was 0.5, and IOP was 17 mmHg. Ophthalmoscopy revealed a blunted reflex in the macular zone, the tear in the peripheral retina extending for 1 clock h was sealed by pigmented coagula, the entire retina was adherent. The average CRS OS improved to 25.3 dB, and fixation remained stable. SD-OCT revealed a normal macular profile together with partially restored external retinal layers.

The patient had no complaints on the follow-up examination six months after surgery. Examination showed that her visual acuity was stable: UCVA was 0.2, BCVA was 0.5, and IOP was 15 mmHg. Ophthalmoscopy revealed a blunted reflex in the macular zone, the entire retina was adherent, and the tear in the peripheral retina extending for 1 clock h was sealed by pigmented coagula. According to micropirometry, the average CRS OS improved to 26.1 dB, and fixation was stable. SD-OCT revealed a preserved macular profile together with partially restored segmentation of the external retinal layers (Fig. 5).

Clinical case discussion

Rhegmatogenous retinal detachment coexisting with macular hole is associated with poorer prognosis of beneficial outcome in terms of morphological and functional parameters. The surgeon has to execute a number of additional intraoperative manipulations increasing the risk of intra- and postoperative complications during surgery. Today, the issue of choosing the effective and safe method for surgical treatment of

rhegmatogenous retinal detachment complicated by macular hole is still relevant.

According to the literature, the majority of reported surgical techniques for treatment of this combination of disorders end with the silicone oil tamponade of the vitreous cavity followed by the silicone oil removal after 3–6 months [1, 7, 8, 11, 16] or with the air-gas tamponade [5, 17]. However, silicone oil is unable to tightly press the retina at the posterior pole. It is well known that there is a layer of intraocular fluid between silicone oil and the retina, that is why the conditions are not optimal for the macular hole sealing and regeneration (compared to the perfluorocarbon tamponade). Furthermore, the long-term presence of silicone oil in the vitreous cavity may result in such complications, as secondary ocular hypertension, lens opacity, contact keratopathy, perisilicone proliferation, cystoid macular edema. Moreover, silicone oil induces high hypermetropia and irregular astigmatism, thereby significantly reducing visual acuity throughout the period of tamponade [18]. Air-gas tamponade of the vitreous cavity forces the patient to stay in prone position for a long time, reduces his/her quality of life during the period of tamponade, limits the possibility of ophthalmoscopy-based control over the retinal adaptation and the macular hole closure during the postoperative period, promotes the development of cataract, retinal folds, and peripheral retinal tears.

The reported use of short-term perfluorocarbon tamponade of the vitreous cavity ensures reliable adaptation of the retina to subadjacent tissues, contributes to formation of strong chorioretinal adhesion and prevents displacement of the retina relative to subadjacent layers. Perfluorocarbon tamponade ensures stable fibrin film retention and tight adhesion of fibrin to the retinal defect, thereby reducing the risk of the fibrin film displacement relative to the macular hole and contributing to the macular defect strong sealing and effective regeneration. The use of this vitreous substitute does not require staying in certain forced position and does not reduce the patient's mobility in the early postoperative period. No complications develop during the short period of perfluorocarbon tamponade of the vitreous cavity.

The possibility of using ACP (under protection of perfluorocarbon tamponade) allows maximum use of its reparative and regenerative potential. This ensures optimal restoration of the macular zone morphology and makes it possible to achieve high visual functions.

The use of proposed microsurgical approach for treatment of rhegmatogenous retinal detachment complicated by macular hole resulted in complete anatomic adhesion of the retina, restored macular architectonics of the retina, and visual function improvement.

References

1. Stappler T, Montesel A, Konstantinidis L, Wolfensberger TJ, Eandi CM. Inverted internal limiting membrane flap technique for macular hole coexistent with rhegmatogenous retinal detachment. *Retina*. 2022; 42 (8): 1491–7.
2. Cunningham MA, Tarantola RM, Folk JC, Sohn EH, Boldt HC, Graff JA et al. Proliferative vitreoretinopathy may be a risk factor in combined macular hole retinal detachment cases. *Retina*. 2013; 33 (3): 579–85.
3. Chignell AH, Billington B. The treatment of macular holes by pars plana vitrectomy and internal air/SF6 exchange. *Graefes Arch Clin Exp Ophthalmol*. 1986; 224 (1): 67–68.
4. Gonvers M, Machemer R. A new approach to treating retinal detachment with macular hole. *Am J Ophthalmol*. 1982; 94 (4): 468–72.
5. Singh AJ. Combined or sequential surgery for management of rhegmatogenous retinal detachment with macular holes. *Retina*. 2009; 29 (8): 1106–10.
6. Balashevich LI, Platov EA, Nigmatov BF. Sluchaj xirurgicheskogo lecheniya regmatogennoj otstojki setchatki s makulyarnym razryvom. V sbornike: Problemy sovremennoj mediciny: aktual'nye voprosy. Sbornik nauchnyx trudov po itogam mezhdunarodnoj nauchno-prakticheskoy konferencii; 6 noyabrya 2014 g; Krasnoyarsk; 37–39. Russian.
7. Zhao PP, Wang S, Liu N, Shu ZM, Zhao JS. A review of surgical outcomes and advances for macular holes. *J Ophthalmol*. 2018; 1–10.
8. Abouhusein MA, Elbaha SM, Aboushousha M. Human amniotic membrane plug for macular holes coexisting with rhegmatogenous

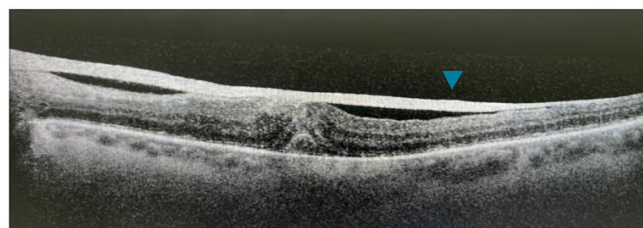


Fig. 3. Spectral domain optical coherence tomography scan of the macular region (24 h after surgery). The macular hole is closed, there is a hyperreflective structure represented by the fibrin film on the retinal surface (blue arrow)

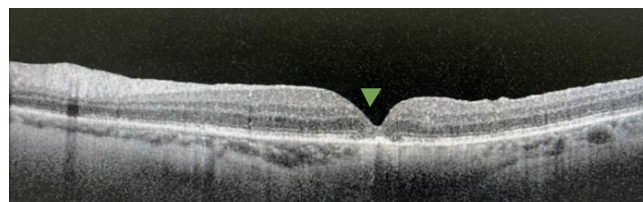


Fig. 4. Spectral domain optical coherence tomography scan of the macular region (one month after surgery). Apparent macular profile (green arrow). The "retinal pigment epithelium — Bruch's membrane" complex and discontinuous external limiting membrane are visible

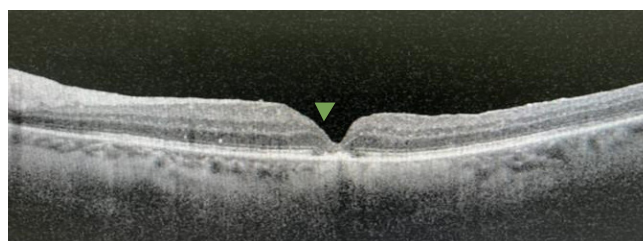


Fig. 5. Spectral domain optical coherence tomography scan of the macular region (six months after surgery). Apparent macular profile (green arrow). The "retinal pigment epithelium — Bruch's membrane" complex is visible. Partially restored segmentation of the external retinal layers (discontinuous external limiting membrane), partially restored photoreceptor zone of the retina

CONCLUSION

The proposed technique for endovitreous microsurgery of rhegmatogenous retinal detachment complicated by macular hole involving the use of endolaser photocoagulation, autologous conditioned plasma, and short-term perfluorocarbon tamponade of the vitreous cavity proved to be reliable and highly effective and ensured good morphological and functional results, i.e. restoration of macular architectonics, macular hole closure, anatomic retinal adhesion, and visual function improvement, in the postoperative period. The deeper analysis requires further testing of the proposed technology.

- retinal detachment. Clin Ophthalmol. 2020; 14: 2411–6.
9. Shukla D, Kalliath J, Srinivasan K, Neelakantan N, Rajendran A, Naresh KB, et al. Management of rhegmatogenous retinal detachment with coexisting macular hole: a comparison of vitrectomy with and without internal limiting membrane peeling. Retina. 2013; 33 (3): 571–78.
 10. Ryan EH Jr, Bramante CT, Mittra RA, Dev S, Bennett SR, Williams DF, et al. Management of rhegmatogenous retinal detachment with coexistent macular hole in the era of internal limiting membrane peeling. Am J Ophthalmol. 2011; 152 (5): 815–9.
 11. Liu X, Huang J, Zhou R, Jiang Z, Chen H, Chen W, et al. Comparison of internal limiting membrane peeling with the inverted internal limiting membrane flap technique for rhegmatogenous retinal detachment coexisting with macular hole. Retina. 2022; 42 (4): 697–703.
 12. Krupina EA. Xirurgicheskoe lechenie idiopaticeskogo makulyarnogo razryva s primeneniem bogatoj trombocitami plazmy krovi [dissertaciya]. M., 2019. Russian.
 13. Popov EM, Kulikov AN, Churashov SV, Gavriljuk IO, Egorova EN, Abbasova AI. Sravnenie pokazatelej poluchaemoj raznymi sposobami autoplazmy, ispol'zuemoj dlya lecheniya pacientov s makulyarnym razryvom. Oftal'mologicheskie vedomosti. 2021; 14 (4): 27–34. Russian.
 14. Arsyutov DG. Ispol'zovanie autologichnoj kondicionirovannoj plazmy, obogashhennoj trombocitami, v xirurgii regmatogennoj otsojki setchatki s central'nym i perifericheskimi razryvami. Acta biomedica scientifica. 2019; 4 (4): 61–65. DOI: 10.29413/ABS.2019-4.4.8. Russian.
 15. Bajborodov YaV, Zhogolev KS. Autologichnaya kondicionirovannaya plazma — inducirovannaya fibrinnaya plenka v xirurgicheskom lechenii makulyarnyx razryvov. Sovremennye tekhnologii v oftal'mologii. 2020. 4: 283. Russian.
 16. Xurdaeva AG, Zaxarov VD, Shkvorchenko DO, Krupina EA, Norman KS, Yuxananova AV. Xirurgicheskoe lechenie regmatogennoj otsojki setchatki, oslozhennoj makulyarnym razryvom, s primeneniem bogatoj trombocitami plazmy krovi i lokal'nym okrashivaniem vnutrennej pograničnoj membrany. Sovremennye tekhnologii v oftal'mologii. 2019; 4 (29): 267–70. Russian.
 17. O'Driscoll AM, Goble RR, Kirkby GR. Vitrectomy for retinal detachments with both peripheral retinal breaks and macular holes. An assessment of outcome and the status of the macular hole. Retina. 2001; 21 (3): 221–5.
 18. Taxchidi XP, Metaev SA, Glinchuk NYa, Gazal NA. Obosnovanie rannego udaleniya silikonovogo masla pri lechenii tyazhelyx otsolek setchatki razlichnogo geneza. Vestnik Orenburgskogo gosudarstvennogo universiteta, 2004; 5: 60–65. Russian.

Литература

1. Stappler T, Montesel A, Konstantinidis L, Wolfensberger TJ, Eandi CM. Inverted internal limiting membrane flap technique for macular hole coexistent with rhegmatogenous retinal detachment. Retina. 2022; 42 (8): 1491–7.
2. Cunningham MA, Tarantola RM, Folk JC, Sohn EH, Boldt HC, Graff JA et al. Proliferative vitreoretinopathy may be a risk factor in combined macular hole retinal detachment cases. Retina. 2013; 33 (3): 579–85.
3. Chignell AH, Billington B. The treatment of macular holes by pars plana vitrectomy and internal air/SF6 exchange. Graefes Arch Clin Exp Ophthalmol. 1986; 224 (1): 67–68.
4. Gonvers M, Macherer R. A new approach to treating retinal detachment with macular hole. Am J Ophthalmol. 1982; 94 (4): 468–72.
5. Singh AJ. Combined or sequential surgery for management of rhegmatogenous retinal detachment with macular holes. Retina. 2009; 29 (8): 1106–10.
6. Балашевич Л. И., Платов Е. А., Нигматов Б. Ф. Случай хирургического лечения регматогенной отслойки сетчатки с макулярным разрывом. В сборнике: Проблемы современной медицины: актуальные вопросы. Сборник научных трудов по итогам международной научно-практической конференции; 6 ноября 2014 г.; Красноярск; 37–39.
7. Zhao PP, Wang S, Liu N, Shu ZM, Zhao JS. A review of surgical outcomes and advances for macular holes. J Ophthalmol. 2018; 1–10.
8. Abouhusein MA, Elbaha SM, Aboushousha M. Human amniotic membrane plug for macular holes coexisting with rhegmatogenous retinal detachment. Clin Ophthalmol. 2020; 14: 2411–6.
9. Shukla D, Kalliath J, Srinivasan K, Neelakantan N, Rajendran A, Naresh KB, et al. Management of rhegmatogenous retinal detachment with coexisting macular hole: a comparison of vitrectomy with and without internal limiting membrane peeling. Retina. 2013; 33 (3): 571–78.
10. Ryan EH Jr, Bramante CT, Mittra RA, Dev S, Bennett SR, Williams DF, et al. Management of rhegmatogenous retinal detachment with coexistent macular hole in the era of internal limiting membrane peeling. Am J Ophthalmol. 2011; 152 (5): 815–9.
11. Liu X, Huang J, Zhou R, Jiang Z, Chen H, Chen W, et al. Comparison of internal limiting membrane peeling with the inverted internal limiting membrane flap technique for rhegmatogenous retinal detachment coexisting with macular hole. Retina. 2022; 42 (4): 697–703.
12. Крупина Е. А. Хирургическое лечение идиопатического макулярного разрыва с применением богатой тромбоцитами плазмы крови [диссертация]. М., 2019.
13. Попов Е. М., Куликов А. Н., Чурашов С. В., Гаврилюк И. О., Егорова Е. Н., Аббасова А. И. Сравнение показателей получаемой разными способами аутоплазмы, используемой для лечения пациентов с макулярным разрывом. Офтальмологические ведомости. 2021; 14 (4): 27–34.
14. Арсютков Д. Г. Использование аутологичной кондиционированной плазмы, обогащенной тромбоцитами, в хирургии регматогенной отслойки сетчатки с центральным и периферическими разрывами. Acta biomedica scientifica. 2019; 4 (4): 61–65. DOI: 10.29413/ABS.2019-4.4.8.
15. Байбородов Я. В., Жоголев К. С. Аутологичная кондиционированная плазма — индуцированная фибриновая пленка в хирургическом лечении макулярных разрывов. Современные технологии в офтальмологии. 2020. 4: 283.
16. Хурдаева А. Г., Захаров В. Д., Шкворченко Д. О., Крупина Е. А., Норман К. С., Юхананова А. В. Хирургическое лечение регматогенной отслойки сетчатки, осложненной макулярным разрывом, с применением богатой тромбоцитами плазмы крови и локальным окрашиванием внутренней пограничной мембраны. Современные технологии в офтальмологии. 2019; 4 (29): 267–70.
17. O'Driscoll AM, Goble RR, Kirkby GR. Vitrectomy for retinal detachments with both peripheral retinal breaks and macular holes. An assessment of outcome and the status of the macular hole. Retina. 2001; 21 (3): 221–5.
18. Тахчиди Х. П., Метаев С. А., Глинчук Н. Я., Газаль Н. А. Обоснование раннего удаления силиконового масла при лечении тяжелых отслоек сетчатки различного генеза. Вестник Оренбургского государственного университета, 2004; 5: 60–65.

METABOLIC ENGINEERING IS A PROMISING WAY TO GENERATE HIGHLY EFFECTIVE PRODUCERS OF BIOACTIVE SUBSTANCES

Blokhina AE^{1,2}, Palkina KA¹, Shakhova ES¹, Malyshevskaya AK^{1,2}, Osipova ZM^{1,3}, Myshkina NM¹ ✉

¹ Shemyakin–Ovchinnikov Institute of Bioorganic Chemistry, Moscow, Russia

² Lomonosov Moscow State University, Moscow, Russia

³ Pirogov Russian National Research Medical University, Moscow, Russia

Medicines play an indisputable role in life extension and improvement of the quality of life. To obtain medicinal compounds, researchers traditionally rely on natural sources and chemical synthesis, however, currently developing biotechnological methods allow one to introduce the group of genes encoding new metabolic pathways into the genomes of heterologous hosts and regulate activity of the hosts' intrinsic metabolic pathways. Such an approach makes it possible to reproduce biosynthesis of bioactive substances in heterologous hosts, the approach combines the benefits of conventional methods and works around the shortcomings of those. In our view, the use of metabolic engineering to obtain medicinal compounds is becoming increasingly important for their production.

Keywords: heterologous gene expression, metabolic pathways, metabolic engineering, biosynthesis of medicinal compounds

Funding: the study was supported by the Russian Science Foundation Grant № 21-74-00075, <https://rscf.ru/project/21-74-00075/>

Acknowledgements: the authors would like to thank A.S. Sheglov, research fellow at the Laboratory of Chemistry of Metabolic Pathways, for valuable criticisms.

Author contribution: Blokhina AE, Palkina KA, Shakhova ES, Malyshevskaya AK, Osipova ZM — literature review, data processing; Myshkina NM — literature review, data processing, project management, manuscript writing.

✉ **Correspondence should be addressed:** Nadezhda M. Myshkina
Miklukho-Maklaya, 16/10, Moscow, 117997, Russia; markina.nadya@gmail.com

Received: 05.04.2023 **Accepted:** 19.04.2023 **Published online:** 26.04.2023

DOI: 10.24075/brsmu.2023.014

МЕТАБОЛИЧЕСКАЯ ИНЖЕНЕРИЯ — ПЕРСПЕКТИВНЫЙ ПУТЬ ПОЛУЧЕНИЯ ВЫСОКОЭФФЕКТИВНЫХ ПРОДУЦЕНТОВ БИОЛОГИЧЕСКИ АКТИВНЫХ ВЕЩЕСТВ

А. Е. Блохина^{1,2}, К. А. Палкина¹, Е. С. Шахова¹, А. К. Малышевская^{1,2}, З. М. Осипова^{1,3}, Н. М. Мышкина¹ ✉

¹ Институт биоорганической химии имени М. М. Шемякина и Ю. А. Овчинникова, Москва, Россия

² Московский государственный университет имени М. В. Ломоносова, Москва, Россия

³ Российский национальный исследовательский медицинский университет имени Н. И. Пирогова, Москва, Россия

Лекарственные препараты играют неоспоримую роль в продлении жизни и повышении ее качества. Для получения лекарственных соединений исследователи традиционно обращаются к природным источникам и химическому синтезу, однако в настоящее время активно развиваются биотехнологические методы, позволяющие внедрять группы генов, кодирующие новые метаболические пути, в геномы гетерологических хозяев и регулировать активность их собственных метаболических путей. Такой подход дает возможность воспроизводить биосинтез биологически активных соединений в гетерологических хозяевах, сочетает достоинства традиционных методов их получения и обходит недостатки этих методов. С нашей точки зрения, применение метаболической инженерии для получения лекарственных соединений приобретает все большее значение в производстве.

Ключевые слова: гетерологическая экспрессия генов, метаболические пути, метаболическая инженерия, биосинтез лекарственных соединений

Финансирование: исследование выполнено за счет гранта Российского научного фонда № 21-74-00075, <https://rscf.ru/project/21-74-00075/>

Благодарности: научному сотруднику лаборатории химии метаболических путей А. С. Щеглову за ценные критические замечания.

Вклад авторов: А. Е. Блохина, К. А. Палкина, Е. С. Шахова, А. К. Малышевская, З. М. Осипова — анализ литературы, обработка данных, Н. М. Мышкина — анализ литературы, обработка данных, руководство проектом, написание статьи.

✉ **Для корреспонденции:** Надежда Михайловна Мышкина
ул. Миклухо-Маклая, 16/10, г. Москва, 117997, Россия; markina.nadya@gmail.com

Статья получена: 05.04.2023 **Статья принята к печати:** 19.04.2023 **Опубликована онлайн:** 26.04.2023

DOI: 10.24075/vrgmu.2023.014

Living organisms, especially fungi and plants, are conventional sources of bioactive compounds and medicines. However, extraction of these compounds from natural sources can be a complex and costly process due to low content of compounds. Development of the organic synthesis techniques has provided a breakthrough in drug manufacturing [1], however, it is not rational to obtain all natural compounds chemically due to multistage synthetic pathways, requirements for optical activity, and low yield of pure substance [2, 3]. Biotechnology offers an alternative approach that allows to produce medicinal compounds in heterologous hosts [4], such as bacteria, yeast, plants, algae, and mold fungi, many of which combine the features of rapid growth, simplicity and low cost of cultivation.

Heterologous gene expression provides opportunities to program new properties of the host at the cellular and organism levels, including the large-scale production of atypical substances [5]. Since bioactive compounds cannot usually be encoded by single genes, the projects of metabolic engineering of entire biochemical pathways are becoming increasingly popular. Integration of long multigene constructs into the host genome is supported by the development of methods for DNA assembly [6] and delivery [7]. Regulation of the host's intrinsic metabolic pathways has a significant impact on the success of such projects, since it allows the host cell to produce appropriate amounts of essential intermediate metabolites. Engineering of autotrophic yeast, *Pichia pastoris*, is one such example [8].

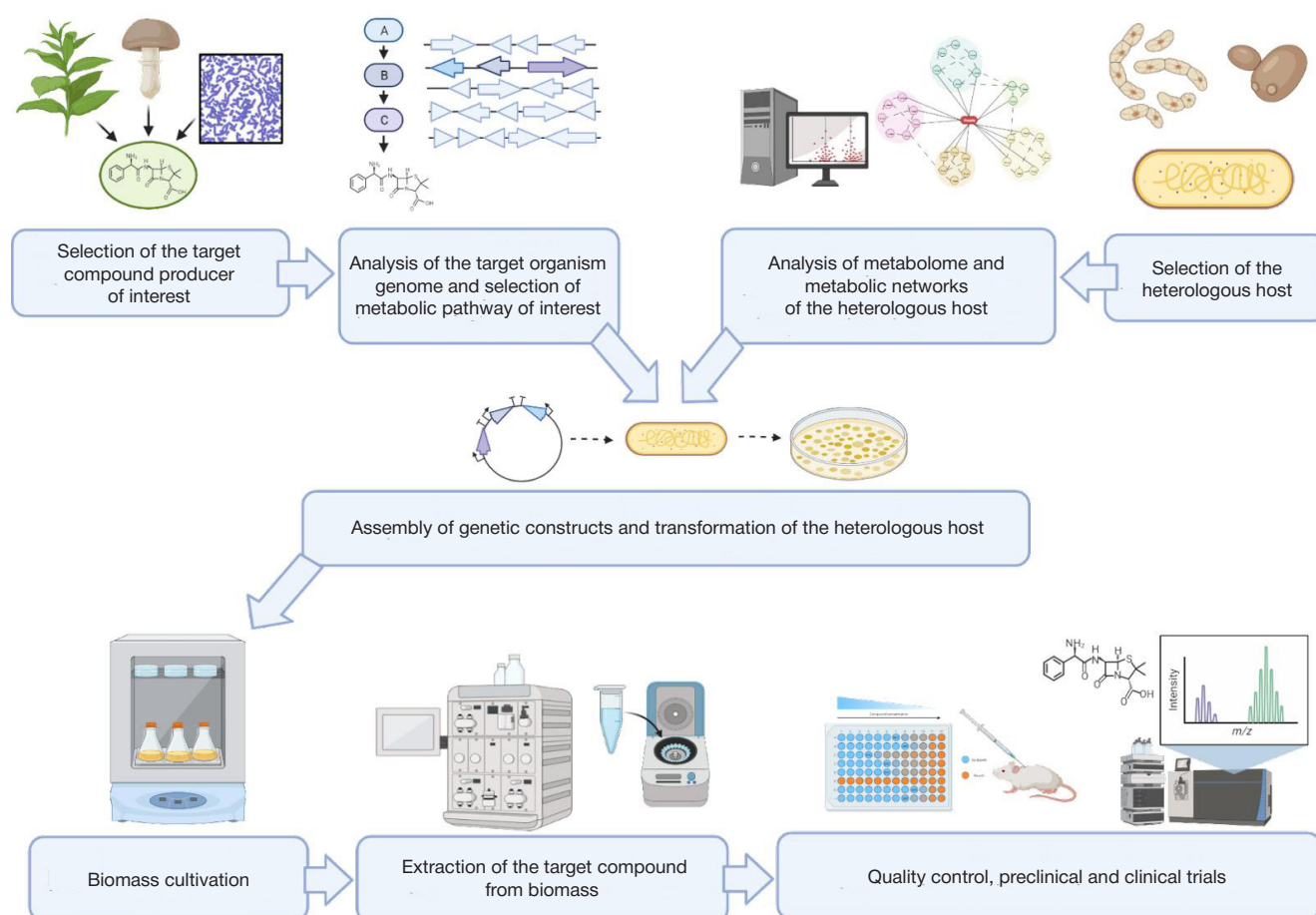


Fig. Scheme of contemporary approach of generating bioactive compounds in heterologous hosts

Metabolic pathways of any organism form complex metabolic networks, that is why it is extremely important to have a detailed picture of the enzyme components of certain biosynthetic pathways and their products to select the points of metabolic regulation in the heterologous host. For this purpose, various databases, such as KEGG (Kyoto Encyclopedia of Genes and Genomes) [9], BRENDA (BRaunschweig ENzyme DAtabase) [10], and PathBank [11] can be used, along with the gene co-expression databases, such as ATTED-II (Arabidopsis thaliana trans-factor and cis-element prediction database) that has been designed for Arabidopsis [12]. However, the built-in algorithms of these databases may not be informative enough when dealing with the understudied genes or organisms; the bioinformatics tools based on the machine learning algorithms, the predictive power of which improves with time, are used in such cases [13].

After defining the points of metabolic regulation, biochemical pathways can be tuned by site-specific genome editing and/or epigenetic regulation. Considering the general trends of switching from omnidirectional effects to more specific ones, fine tuning of the host gene expression levels is becoming increasingly popular and accessible. In particular, the guide RNAs and artificial Cas9-based transcription factors can be used for gene activation [14, 15].

The combined approach involving implementation of heterologous metabolic pathways and rerouting of the host's intrinsic metabolic pathways (see Figure) yields spectacular results of the target bioactive compound biosynthesis in the heterologous host [4].

CONCLUSION

The success of the medicinal compound biosynthesis is based on the combination of several orthogonal approaches. Successful implementation requires determining the shortest metabolic path to the desired substance or property using databases, defining the limiting stages using conventional biochemical models or machine learning algorithms, selecting the optimal method for host genome transformation, constructing genetic constructs that are compatible with the selected host, characterizing the host's metabolic landscape, and regulating the activity of the host's intrinsic metabolic pathways aimed at directing metabolic flows towards heterologous pathway. The development of modern technology makes it possible to increase the efficiency of each stage and eventually results in production of the new source of medicinal compound.

References

1. Liebig J. Ueber die Zersetzung des Alkohols durch Chlor. *Ann Pharmacother.* 1832; 1: 31–32.
2. Campos KR, Coleman PJ, Alvarez JC, Dreher SD, Garbaccio RM, Terrett NK, et al. The importance of synthetic chemistry in the pharmaceutical industry. *Science.* 2019; 363. DOI: 10.1126/science.aat0805.
3. Blakemore DC, Castro L, Churcher I, Rees DC, Thomas AW, Wilson DM, et al. Organic synthesis provides opportunities to transform drug discovery. *Nat Chem.* 2018; 10: 383–94.
4. Dhakal D, Kim E-S, Koffas M. Editorial: Engineering the Microbial Platform for the Production of Biologics and Small-Molecule Medicines. *Frontiers in Microbiology.* 2019. DOI: 10.3389/fmicb.2019.02307.
5. Damos AG, Hunter JGL, Pardhe MD, Rosenthal SH, Sun H, Foster BC, et al. High Level Production of Monoclonal Antibodies Using an Optimized Plant Expression System. *Front Bioeng Biotechnol.* 2019; 7: 472.
6. Weber E, Engler C, Gruetzner R, Werner S, Marillonnet S. A modular cloning system for standardized assembly of multigene constructs. *PLoS One.* 2011; 6: e16765.
7. Demirel GS, Zhang H, Goh NS, González-Grandío E, Landry MP. Carbon nanotube-mediated DNA delivery without transgene integration in intact plants. *Nat Protoc.* 2019; 14: 2954–71.
8. Gassler T, Sauer M, Gasser B, Egermeier M, Troyer C, Causon T, et al. The industrial yeast *Pichia pastoris* is converted from a heterotroph into an autotroph capable of growth on CO₂. *Nat Biotechnol.* 2020; 38: 210–16.
9. Ogata H, Goto S, Sato K, Fujibuchi W, Bono H, Kanehisa M. KEGG: Kyoto Encyclopedia of Genes and Genomes. *Nucleic Acids Res.* 1999; 27: 29–34.
10. Schomburg I, Chang A, Hofmann O, Ebeling C, Ehrentreich F, Schomburg D. BRENDA: a resource for enzyme data and metabolic information. *Trends Biochem Sci.* 2002; 27: 54–56.
11. Wishart DS, Li C, Marcu A, Badran H, Pon A, Budinski Z, et al. PathBank: a comprehensive pathway database for model organisms. *Nucleic Acids Res.* 2020; 48: D470–8.
12. Obayashi T, Kinoshita K, Nakai K, Shibaoka M, Hayashi S, Saeki M, et al. ATTED-II: a database of co-expressed genes and cis elements for identifying co-regulated gene groups in Arabidopsis. *Nucleic Acids Res.* 2007; 35: D863–9.
13. Costello Z, Martin HG. A machine learning approach to predict metabolic pathway dynamics from time-series multiomics data. *NPJ Syst Biol Appl.* 2018; 4: 19.
14. Selma S, Sanmartín N, Espinosa-Ruiz A, Gianoglio S, Lopez-Gresa MP, Vázquez-Vilar M, et al. Custom-made design of metabolite composition in *N. benthamiana* leaves using CRISPR activators. *Plant Biotechnol J.* 2022; 20: 1578–90.
15. Garcia-Perez E, Diego-Martin B, Quijano-Rubio A, Moreno-Giménez E, Selma S, Orzaez D, et al. A copper switch for inducing CRISPR/Cas9-based transcriptional activation tightly regulates gene expression in *Nicotiana benthamiana*. *BMC Biotechnol.* 2022; 22: 12.

Литература

1. Liebig J. Ueber die Zersetzung des Alkohols durch Chlor. *Ann Pharmacother.* 1832; 1: 31–32.
2. Campos KR, Coleman PJ, Alvarez JC, Dreher SD, Garbaccio RM, Terrett NK, et al. The importance of synthetic chemistry in the pharmaceutical industry. *Science.* 2019; 363. DOI: 10.1126/science.aat0805.
3. Blakemore DC, Castro L, Churcher I, Rees DC, Thomas AW, Wilson DM, et al. Organic synthesis provides opportunities to transform drug discovery. *Nat Chem.* 2018; 10: 383–94.
4. Dhakal D, Kim E-S, Koffas M. Editorial: Engineering the Microbial Platform for the Production of Biologics and Small-Molecule Medicines. *Frontiers in Microbiology.* 2019. DOI: 10.3389/fmicb.2019.02307.
5. Damos AG, Hunter JGL, Pardhe MD, Rosenthal SH, Sun H, Foster BC, et al. High Level Production of Monoclonal Antibodies Using an Optimized Plant Expression System. *Front Bioeng Biotechnol.* 2019; 7: 472.
6. Weber E, Engler C, Gruetzner R, Werner S, Marillonnet S. A modular cloning system for standardized assembly of multigene constructs. *PLoS One.* 2011; 6: e16765.
7. Demirel GS, Zhang H, Goh NS, González-Grandío E, Landry MP. Carbon nanotube-mediated DNA delivery without transgene integration in intact plants. *Nat Protoc.* 2019; 14: 2954–71.
8. Gassler T, Sauer M, Gasser B, Egermeier M, Troyer C, Causon T, et al. The industrial yeast *Pichia pastoris* is converted from a heterotroph into an autotroph capable of growth on CO₂. *Nat Biotechnol.* 2020; 38: 210–16.
9. Ogata H, Goto S, Sato K, Fujibuchi W, Bono H, Kanehisa M. KEGG: Kyoto Encyclopedia of Genes and Genomes. *Nucleic Acids Res.* 1999; 27: 29–34.
10. Schomburg I, Chang A, Hofmann O, Ebeling C, Ehrentreich F, Schomburg D. BRENDA: a resource for enzyme data and metabolic information. *Trends Biochem Sci.* 2002; 27: 54–56.
11. Wishart DS, Li C, Marcu A, Badran H, Pon A, Budinski Z, et al. PathBank: a comprehensive pathway database for model organisms. *Nucleic Acids Res.* 2020; 48: D470–8.
12. Obayashi T, Kinoshita K, Nakai K, Shibaoka M, Hayashi S, Saeki M, et al. ATTED-II: a database of co-expressed genes and cis elements for identifying co-regulated gene groups in Arabidopsis. *Nucleic Acids Res.* 2007; 35: D863–9.
13. Costello Z, Martin HG. A machine learning approach to predict metabolic pathway dynamics from time-series multiomics data. *NPJ Syst Biol Appl.* 2018; 4: 19.
14. Selma S, Sanmartín N, Espinosa-Ruiz A, Gianoglio S, Lopez-Gresa MP, Vázquez-Vilar M, et al. Custom-made design of metabolite composition in *N. benthamiana* leaves using CRISPR activators. *Plant Biotechnol J.* 2022; 20: 1578–90.
15. Garcia-Perez E, Diego-Martin B, Quijano-Rubio A, Moreno-Giménez E, Selma S, Orzaez D, et al. A copper switch for inducing CRISPR/Cas9-based transcriptional activation tightly regulates gene expression in *Nicotiana benthamiana*. *BMC Biotechnol.* 2022; 22: 12.